INVESTIGATION INTO THE ROLE OF TFIID AS A COACTIVATOR FOR THE CELL-CYCLE REGULATED TRANSCRIPTION FACTOR, SWI6P

By

Sadia Sadaff Khan

Thesis

Submitted to the Faculty of the

Graduate School of Vanderbilt University

in partial fulfillment of the requirements for

the degree of

MASTER of SCIENCE

in

Molecular Physiology and Biophysics

May, 2007

Nashville, Tennessee

Approved:

Professor Roland Stein

Professor Linda Sealy

Professor P.A. Weil

TABLE OF CONTENTS

LIST OF TABLES

LIST OF FIGURES

LIST OF ABBREVIATIONS

A_{260}	absorbance at 260 nm
bp	base pair
BSA	bovine serum albumin
C. elegans	*Caenorhabditis elegans*
CNBr	cyanogen bromide
D. melanogaster	*Drosophila melanogaster*
dATP	2'-deoxyadenosine-5' triphosphate
dCTP	2'-deoxycytidine-5' triphosphate
dGTP	2'-deoxyguanosine-5' triphosphate
DNA	deoxyribonucleic acid
dNTP	deoxynucleotide triphosphate
DTT	dithiothreitol
dTTP	2'-deoxythymidine-5' triphosphate
E. coli	*Escherichia coli*
EDTA	ethylenediamine tetraacetic acid
EGTA	ethylene glycol tetraacetic acid
EM	electron microscopy
EthBr	ethidium bromide
g	gram
G418	G418 sulfate
g/mL	gram per milliliter
GTF	general transcription factor

H. sapiens	*Homo sapiens*
HA_3	tag of three hemagglutinin epitopes in tandem
His_6	tag of six histidines in tandem
His_{10}	tag of ten histidines in tandem
HRP	horseradish peroxidase
IgG	immunoglobulin, isotype G
IP	immunoprecipitate
KAN	kanamycin
KAN^R	kanamycin resistant
kDa	kilodalton
kg	kilogram
krpm	kilorevolutions per minute
L	liter
LDS	lithium dodecyl sulfate
M	molar
M. musculus	*Mus musculus*
MBF	heteromer of Swi6p and Mbp1p
MCB	DNA element recognized by MBF and, to some extent, by SBF
$MgCl_2$	magnesium chloride
mL	milliliter
mM	millimolar
mmol	millimole

MOPS	3-*N*-[morphilino] propane sulfonic acid
mRNA	messenger RNA
MW	molecular weight
Na	sodium
NaCl	sodium chloride
NaH_2PO_4	sodium phosphate, dibasic
NDSB 201	non-detergent sulfobetaine 201
nm	nanometer
NP-40	Nonidet P-40
OD	optical density
OD_{600}	optical density at 600 nm
PBS	phosphate buffered saline
PCR	polymerase chain reaction
pg/μL	picogram per microliter
PIC	preinitiation complex
pmol	picomole
PMSF	phenylmethyl sulfonyl fluroide
PVDF	polyvinylidene difluoride
R. norvegicus	*Rattus norvegicus*
RNA	ribonucleic acid
RNA Pol	RNA polymerase
rRNA	ribosomal RNA
S. cerevisiae	*Saccharomyes cerevisiae*

S. pombe	*Schizosaccharomyces pombe*
SAGA	Spt-Ada-GCN5 acetyltransferase
SBF	heteromer of Swi6p and Swi4p
SCB	DNA element recognized by SBF and, to some extent, MBF
SDS	sodium dodecyl sulfate
SDS-PAGE	sodium dodecyl sulfate -polyacrylamide gel electrophoresis
SSPE	sodium chloride, sodium phosphate, EDTA
Taf_{II}	TBP associated factor
TBP	TATA box binding protein
TBS	Tris buffered saline
TBS-T	Tris buffered saline with Tween-20
TE	Tris EDTA buffer, with EDTA at 1 mM
T0.1E	Tris EDTA buffer, with EDTA at 0.1 mM
TF	transcription factor
TFIIA, TFIIB, TFIID…	general transcription factors associated with RNA polymerase II
TLCK	Nα-tosyl-L-lysine chloromethyl ketone hydrochloride
TPCK	N-ρ-tosyl-L-phenylalanine cholormethyl ketone
tRNA	transfer RNA
ts	temperature sensitive
UV	ultraviolet light
WCE	whole cell extract

YPAD	yeast extract, peptone, adenine, dextrose
YPD	yeast extract, peptone, dextrose
µg	microgram
µg/mL	microgram per milliliter
µL	microliter
µM	micromolar
µg/µL	microgram per microliter

CHAPTER I

INTRODUCTION

Overview of transcription initiation

RNA polymerase is a large, multisubunit protein complex that catalyzes transcription or, the synthesis of RNA from a DNA template. There are three major classes of RNA. The first class consists of ribosomal RNAs (rRNAs); these RNAs are involved in the formation and function of ribosomes, which are large, multisubunit complexes of RNA and protein that catalyze translation or, the synthesis of protein from an RNA template. The second type of RNA is transfer RNAs (tRNAs); these RNAs deliver amino acids to the ribosome and, thus, are critical for translation as well. The third class of RNAs is messenger RNAs (mRNAs); these RNAs serve as the templates from which all proteins in the cell are synthesized from.

Each of these classes of RNA is transcribed by a distinct RNA polymerase. RNA polymerase I transcribes rRNAs, RNA polymerase II transcribes mRNAs, and RNA polymerase III transcribes tRNAs as well as a range of other small RNA molecules (Figure I-1). Out of these three polymerases, RNA polymerase II (RNA Pol II) has been the most intensively studied.

Proteins are the essential workhorses of the cell, providing both cellular structure and function. The three dimensional structure of proteins is critical for protein function. The three dimensional structure of a protein is dictated by that protein's amino acid sequence. In many cases, mutations in a protein's amino acid sequence can disrupt

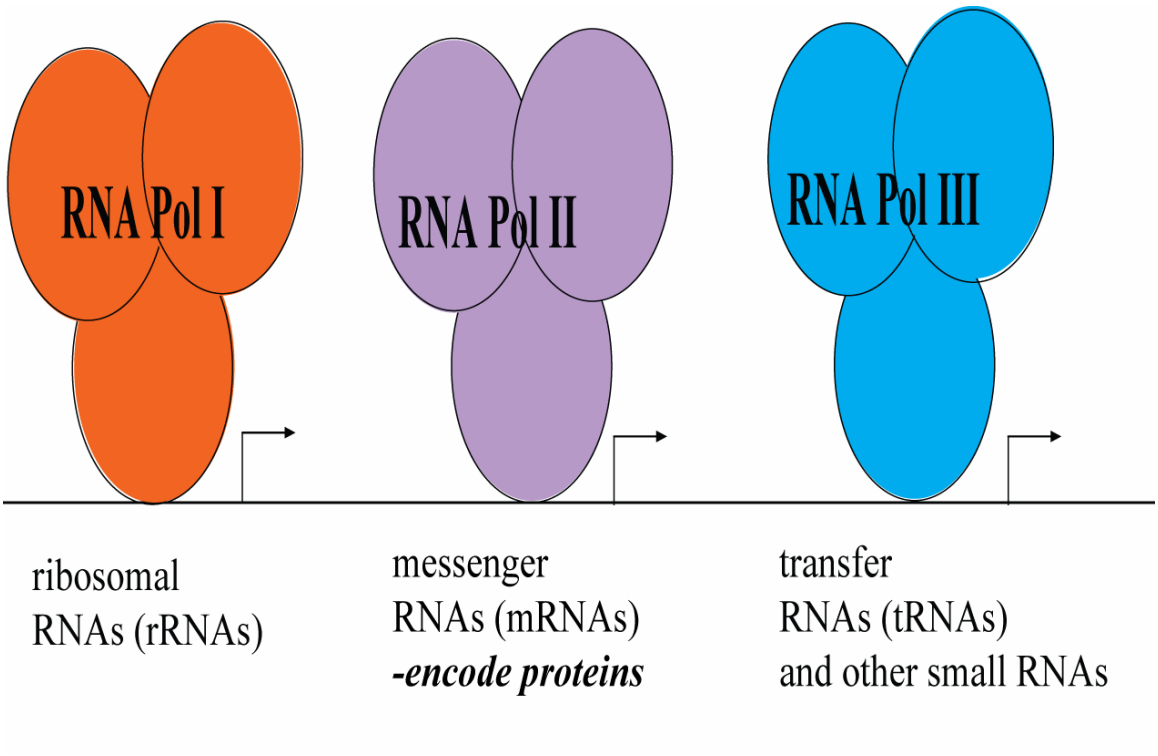

Figure I-1. A distinct RNA polymerase transcribes each class of RNA. The arrows in the figure denote transcription initiation sites. RNA Pol = RNA polymerase.

or alter the three dimensional structure of a protein such that the function of a protein is disrupted or altered in undesirable ways. Changes in the function of individual proteins can impair cellular structure and function. Such mutations in the amino acid sequence can result from mutations in the mRNAs from which proteins are translated from or in the DNA from which mRNAs are transcribed. Therefore, it is important that the cell transcribe mRNAs accurately, and that DNA is replicated correctly during each cell division. The cell has evolved elaborate mechanisms to ensure proper mRNA transcription and proper DNA replication. In this thesis, I will focus on the regulation of mRNA transcription.

mRNA is transcribed from a DNA template known as a gene. The process of mRNA transcription from individual genes can be divided into three stages: initiation, elongation, and termination. During initiation, RNA Pol II binds upstream of the start codon at a location known as the promoter. During elongation, RNA Pol II traverses the gene and synthesizes RNA in response to the template base sequence. During termination, RNA Pol II dissociates from the gene at a specific termination site, and releases the finished mRNA transcript (Figure I-2).

The process thus described appears to be deceptively simple, but in reality, RNA Pol II faces two formidable barriers to accurate transcription. First, the enzyme itself is unable to identify the promoter selectively; therefore, RNA Pol II requires assistance in locating the correct initiation site on a gene. Second, DNA is not found naked in the nucleus; DNA is packaged with large complexes of histone proteins known as nucleosomes to form chromatin. Nucleosomes can effectively mask the

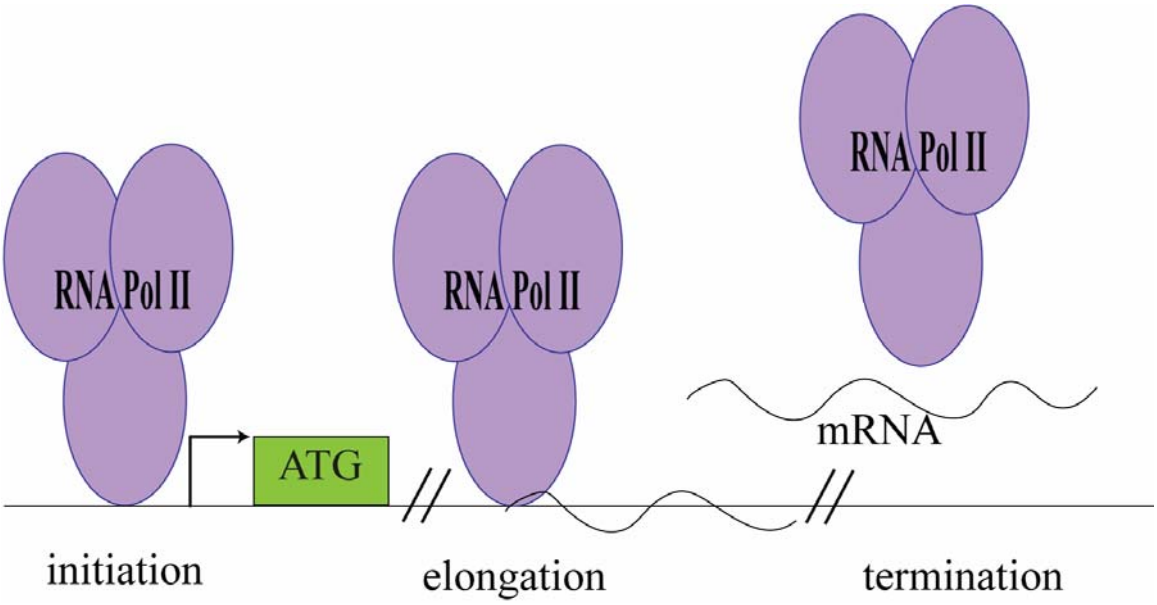

Figure I-2. Transcription can be divided into three stages: initiation, elongation, and termination. First, during initiation, RNA Pol II binds near the transcription initiation site of a gene, which is marked with an arrow. Second, during elongation, RNA Pol II synthesizes RNA from DNA as it travels along the gene. Third, during termination, RNA Pol II dissociates from the gene at a specific termination site, releasing a complete RNA transcript.

initiation sites on genes as well as impose a steric barrier to elongation and, therefore, are generally repressive to transcription.

To help RNA Pol II overcome each of these barriers, the enzyme utilizes accessory protein factors. Protein factors known as general transcription factors (GTFs) locate and bind near the transcription initiation site on a gene (Figure I-3). GTFs, in turn, recruit RNA Pol II to the transcription initiation site through direct interactions with the enzyme. Additional protein factors disrupt the structure of the nucleosomes such that the initiation sites on genes are exposed and available for interaction with GTFs and RNA Pol II. These protein factors often function as large multisubunit complexes known as chromatin remodeling complexes (Figure I-3).

In this thesis I will focus on the mechanisms by which GTFs regulate the accurate initiation of gene transcription. In order to understand how GTFs function, however, it is important to understand the structure of a gene itself. A typical gene is composed of several different types of elements. The actual portion of the gene from which mRNA is transcribed from is known as the coding region. The transcription initiation site is located upstream of the start codon, and downstream of the coding region is the transcription termination site. DNA upstream of the transcription initiation site is defined broadly as the promoter. The portion that is immediately upstream (up to ~100-200 base pairs) and flanking the transcription initiation site is known as the core promoter. DNA further upstream but directly adjacent to the core promoter is known as the proximal promoter. Finally, especially in complex organisms, there are specific DNA elements known as enhancers that can exist at long distances and are not immediately contiguous with the gene itself (Figure I-4).

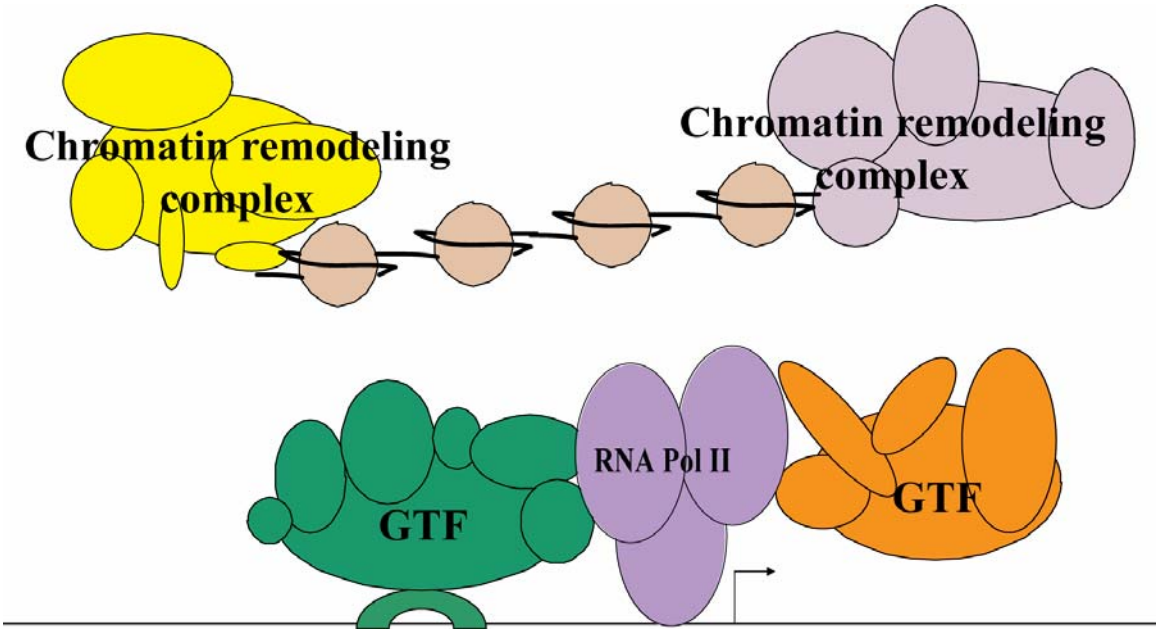

Figure I-3. Accessory protein factors assist RNA Pol II in mediating transcription. (Top) Chromatin remodeling complexes alter the structure of chromatin to render the transcription initiation sites of genes accessible to RNA Pol II. In the figure, the black line depicts DNA whereas the light brown spheres depict complexes of histone proteins around which DNA is wrapped.
(Bottom) General transcription factors, or GTFs, assist in recruiting RNA Pol II to the correct transcription initiation site of a gene. The arrow denotes the transcription initiation site.

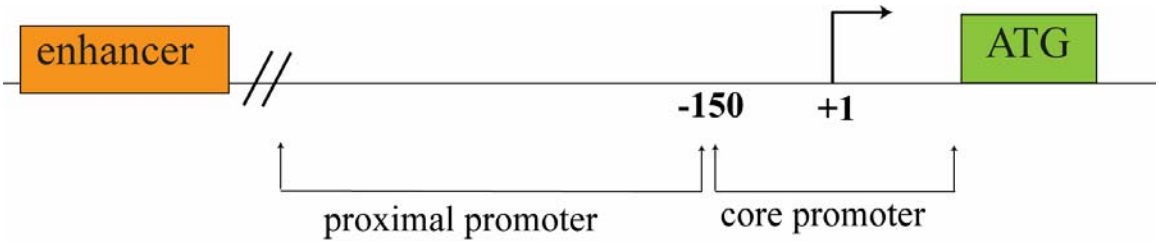

Figure I-4. The transcription of each gene is regulated by regulatory DNA sequences, the promoter and the enhancer. Shown is a schematic of a typical gene promoter. The transcription initiation site is indicated by the arrow and is denoted +1. The core promoter flanks the transcription initiation site and can extend up to 100 to 200 base pairs upstream of the transcription initiation site. Further upstream and directly adjacent to the core promoter is the proximal promoter. Finally, enhancers can exist at great distances and may not be continuous with the proximal promoter itself.

GTFs function at the core promoter. There are six GTFs (TFIIA, TFIIB, TFIID, TFIIE, TFIIF, and TFIIH). The GTFs, along with RNA Pol II and the DNA at the transcription initiation site, form the preinitiation complex, or PIC. The process of PIC formation begins with the binding of TFIID to specific sequences in the core promoter. TFIIA contributes to the stabilization of the binding of TFIID to the core promoter. TFIIB is recruited next into the complex, followed by TFIIF and RNA Pol II, and finally, by TFIIE and TFIIH. TFIIH then phosphorylates the largest subunit of RNA Pol II; upon phosphorylation, RNA Pol II dissociates from the rest of the PIC. Adenosine triphosphate hydrolysis facilitates the opening of the DNA helix and RNA Pol II, along with TFIIE and TFIIH, proceeds to move along the gene and catalyze transcription (Figure I-5) (1).

Overview of transcription activation

Accurate initiation of transcription is crucial to ensure that mRNAs of the correct sequence and size are produced. Accurately transcribed mRNAs will be translated into proteins that can carry out the myriad of functions that are crucial to cellular structure and function.

However, it is not enough that correctly functioning proteins are produced. For a cell to function smoothly, it must be able to produce each protein at the optimal concentration needed for efficient function. The optimal concentration of a given protein is determined by environmental factors, which fluctuate constantly. Cells have evolved mechanisms to sense these environmental factors, and to respond to changes in these factors by upregulating or downregulating the concentrations of certain proteins.

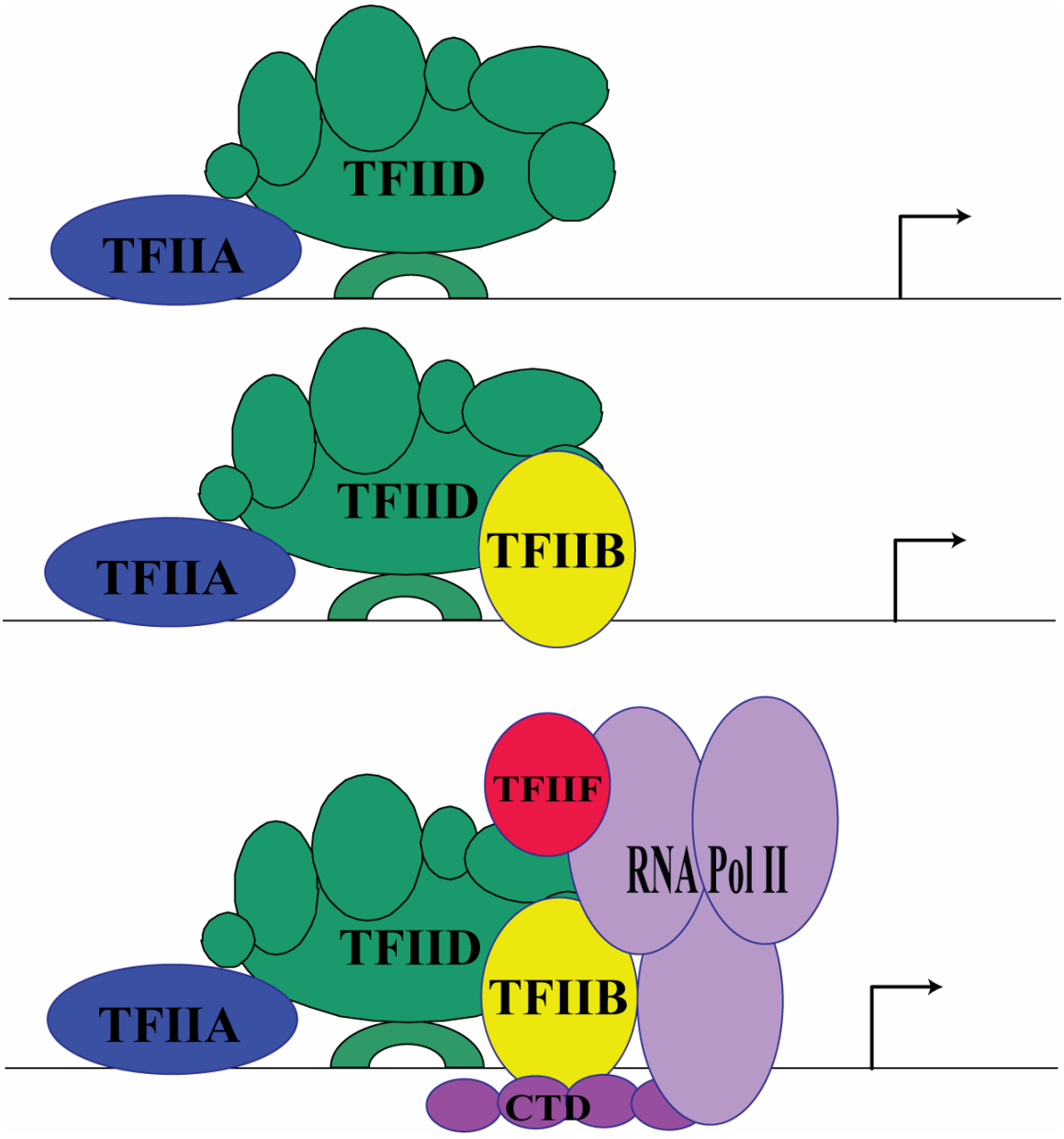
TFIID
TFIIA
TFIID
TFIIB
TFIIA
TFIIF
RNA Pol II
TFIID
TFIIB
TFIIA
CTD

Figure I-5.

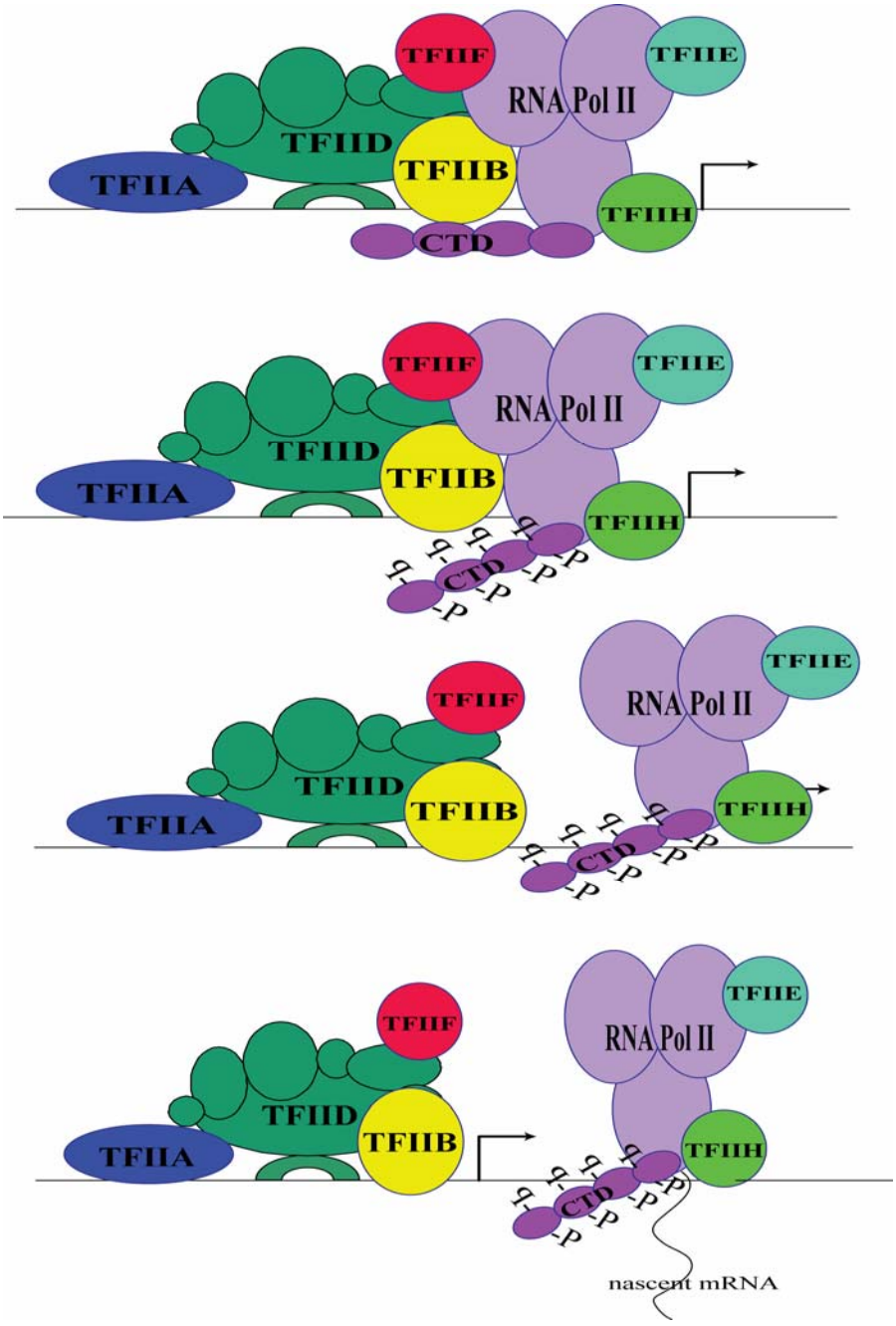

Figure I-5. (*continued*)

Figure I-5. Formation of the preinitiation complex, or PIC, is a complex process. . Preinitiation complex (PIC) formation begins with TFIID binding to the core promoter. TFIIA contributes to the stabilization of the binding of TFIID to the core promoter. Next, TFIIB is recruited to the core promoter, followed by RNA Pol II and TFIIF. Finally, TFIIE and TFIIH are recruited into the complex. TFIIH catalyzes the phosphorylation of the C terminal domain (CTD) of the largest subunit of RNA Pol II. Upon phosphorylation, RNA Pol II, TFIIE and TFIIH dissociate from the rest of the PIC. RNA Pol II, along with TFIIE and TFIIH, catalyzes RNA transcription in response to the template base sequence as it travels along the gene. In each panel, the arrow denotes the transcription initiation site.

Improper adjustment of concentrations of proteins can have deleterious consequences. For example, many cancers may arise due to the inappropriate overexpression of oncogenes; elevated expression of these oncogenes results in unrestrained cellular proliferation, thus leading to tumorigenesis.

The concentration of a specific protein can be regulated at several points in the protein production pipeline. Protein levels can be adjusted by regulating protein stability, translation rate, mRNA stability, and mRNA transcription. In this thesis, I will focus on the regulation of protein concentration at the level of mRNA transcription.

As discussed in the preceding section (**Overview of transcription initiation**), GTFs recruit RNA pol II to the correct transcription initiation site of a gene, thus ensuring that accurately initiated mRNA transcripts are produced. In addition to, and concomitant with, their function in accurately initiating transcription, GTFs also function to regulate the mRNA levels of a gene. GTFs do this through interaction with another class of proteins, transcription factors. Transcription factors are proteins that recognize and bind to specific DNA sequences in the proximal promoter and in enhancers. Transcription factors stimulate gene transcription by interacting with and recruiting components of the PIC and/or chromatin remodeling complexes.

Interaction between transcription factors and PIC components result in several consequences, including: increased recruitment of PIC components to the core promoter; stabilization of GTF binding to the core promoter; and conformational changes in GTFs that stimulate their function. The net result is an increase in the levels of transcript produced. Transcription factors themselves are regulated, either directly or indirectly, by changes in the cellular environment. Depending on the environmental context, the

binding of a transcription factor at the proximal promoter or enhancer can increase or decrease, resulting in increases or decreases in transcript levels, respectively (Figure I-6).

The transcription level of each gene is regulated in a unique way. This arises from the properties of the gene promoter and of the transcription factors themselves. First, a given transcription factor can recognize and bind efficiently to DNA elements of a specific sequence (some degeneracy or limited variation may be allowed). The proximal promoter of a given gene contains only a subset of transcription factor recognition sites, thus rendering each gene responsive to only a subset of transcription factors. Second, each given transcription factor responds to only a subset of environmental signals and, among transcription factors that respond to the same environmental signal, the manner in which a given transcription factor responds (either positively or negatively) and to what extent, differs. As a result, each gene is responsive only to certain environmental cues, and responds to different environmental cues by either increasing or decreasing levels of transcription to different extents in a way that is dependent on the details of the promoter's DNA sequence.

The role of TFIID in the regulation of transcription initiation

TFIID is a large protein complex composed of the TATA-box binding protein (TBP) and fourteen tightly bound TBP-associated factors (Taf_{II}s). The structure and function of TFIID has been highly conserved throughout eukaryotic evolution. Homologs of TBP and all but one of the TAF_{II}s exist in a spectrum of eukaryotic species, from the

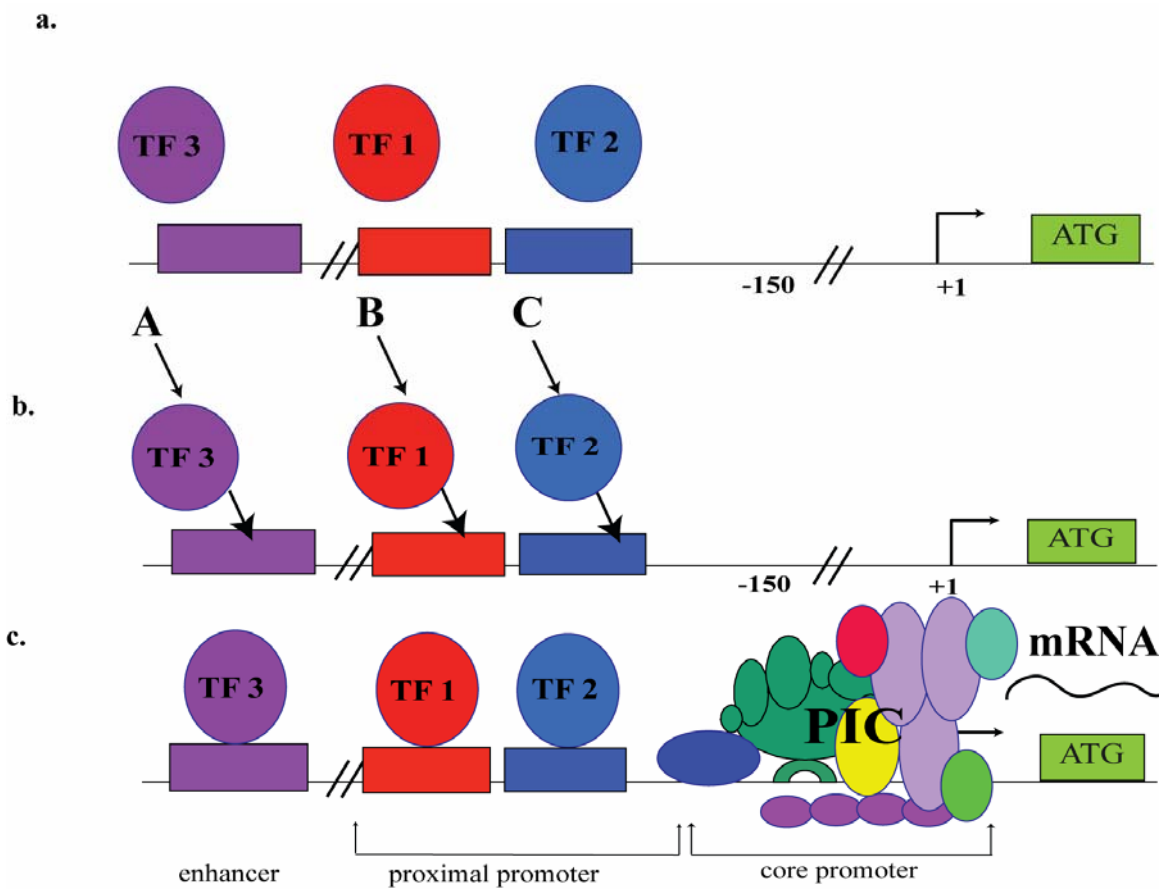

Figure I-6. Transcriptional output is increased in response to binding of transcription factors to the proximal promoter and enhancers. Shown is a schematic depicting the simple scenario in which transcription of a gene is upregulated in response to binding of transcription factors in the proximal promoter and enhancer.
a. In the absence of environmental cues, no transcription factors are bound to the proximal promoter and enhancer, and there is no transcriptional output.
b. In response to a subset of environmental cues (designated A, B, and C), transcription factors bind to their cognate binding sites in the proximal promoter and the enhancer.
c. Transcription factors bound to the proximal promoter and the enhancer increase the formation and/or stabilization of the PIC, thus resulting in an increase in transcriptional output. In each panel, the arrow denotes the transcription initiation site.
TF = transcription factor; PIC = preinitiation complex.

budding yeast, *Saccharomyces cerevisae*, to *Drosophila melanogaster* to *Homo sapiens* (2,3). Furthermore, the trilobed, three-dimensional structure of *S. cerevisiae* TFIID is nearly superimposable on the three-dimensional structure of *H. sapiens* TFIID (4). Lastly, TFIID functions to regulate gene transcription by similar mechanisms in *S. cerevisiae*, *D. melanogaster*, and *H. sapiens* (1, 5, 6, 7, 8, 9, 10, 11).

As discussed in **Overview of transcription initiation**, the process of PIC formation begins with the binding of TFIID to specific sequences in the core promoter. The binding of TFIID to the core promoter is thought to be the rate-limiting step in PIC formation, and this step can stimulated by certain transcription factors. In this way, TFIID plays a central role in regulating both the accurate initiation of gene transcription and the level of transcriptional output. Below, the mechanisms by which TFIID is thought to regulate both these aspects of transcription will be discussed separately.

Role of TFIID in core promoter selectivity

Initial studies of TFIID function indicated that TFIID recognized and bound to a consensus DNA sequence, known as the TATA box, in the core promoter (1). Recognition of the TATA box is mediated by TBP, a subunit of TFIID, which binds the TATA box with high affinity. The TATA box is typically found within 25 base pairs upstream of the transcription initiation site in metazoans but, in yeast, can even be as far as 100 base pairs away. However, TFIID can also bind to core promoters that do not contain a consensus TATA box. In addition, some Taf_{II}s can contact DNA directly, usually immediately downstream of the transcription initiation site, but the sequence specificity of such interactions is not well understood. These Taf_{II}-DNA contacts are

thought to increase the affinity of TBP to core promoters that do not contain a consensus TATA box. Furthermore, TFIID does not bind to all core promoters that have a consensus TATA box. Lastly, another GTF, TFIIA, is thought to contribute to stabilizing TFIID binding to the core promoter. Once bound to the core promoter, TFIID recruits, either directly or indirectly, the remainder of the components of the PIC.

However, TFIID is not required in regulating transcription of all genes inside the cell. For example, in a series of promoter-manipulation studies performed by Shen et al. (9), it was shown that while transcription from the *ADH1* core promoter was not regulated by TFIID, transcription from the core promoters of *RPS5*, *RPS30*, and *CLN2* was regulated by TFIID. The differences could not be explained simply by the presence or absence of a consensus TATA box, as the *ADH1* core promoter contains a consensus TATA box, whereas the *RPS5* core promoter does not contain a consensus TATA box. The mechanisms by which PIC formation occurs on TFIID-independent promoters are not well understood.

Role of TFIID as coactivator

Initial *in vitro* studies of TFIID function indicated that TBP alone could support PIC formation and accurate initiation of transcription. However, the Taf_{II}s were necessary for the stimulation of gene transcription mediated by transcription factors (1). The concept and definition of coactivator was developed from these *in vitro* studies on activated gene transcription. A coactivator possesses the following characteristics: first, the coactivator and transcription factor must directly interact with each other; second, interaction between the coactivator and transcription factor is necessary to recruit the

coactivator to the core promoter; and third, interaction between the coactivator and transcription factor is necessary to drive stimulation of gene transcription mediated by the transcription factor (Figure I-7).

The ability to assemble Taf_{II}-TBP complexes *in vitro*, using purified recombinant proteins, allowed detailed biochemical dissection of the role of individual Taf_{II}s in response to transcription factors (1, 5, 7). Two key points came out of this work. First, an intact TFIID complex was not necessary to mediate responses to transcription factors. Instead, only a subset of Taf_{II}s was required to mediate transcription in response to transcription factors. Second, different transcription factors required different subsets of Taf_{II}s to stimulate transcription.

There are several caveats, however, to these *in vitro* studies. First, the promoters that were used to drive transcription were oversimplified, artificial constructs consisting of a core promoter and a proximal promoter containing multiple binding sites, in tandem, of only one transcription factor. Regulation of transcription of naturally occurring genes, however, is much more complicated. Transcription from naturally occurring genes is often stimulated by a combination of different transcription factors. The proximal promoters of these genes, therefore, contain binding sites for several different transcription factors. Furthermore, multiple copies of a binding site for a given transcription factor may exist in the promoter but they may not be in tandem with each other, and may even be separated by a distance of 100 base pairs or more. Second, these *in vitro* studies largely ignored the contributions from distal enhancers.

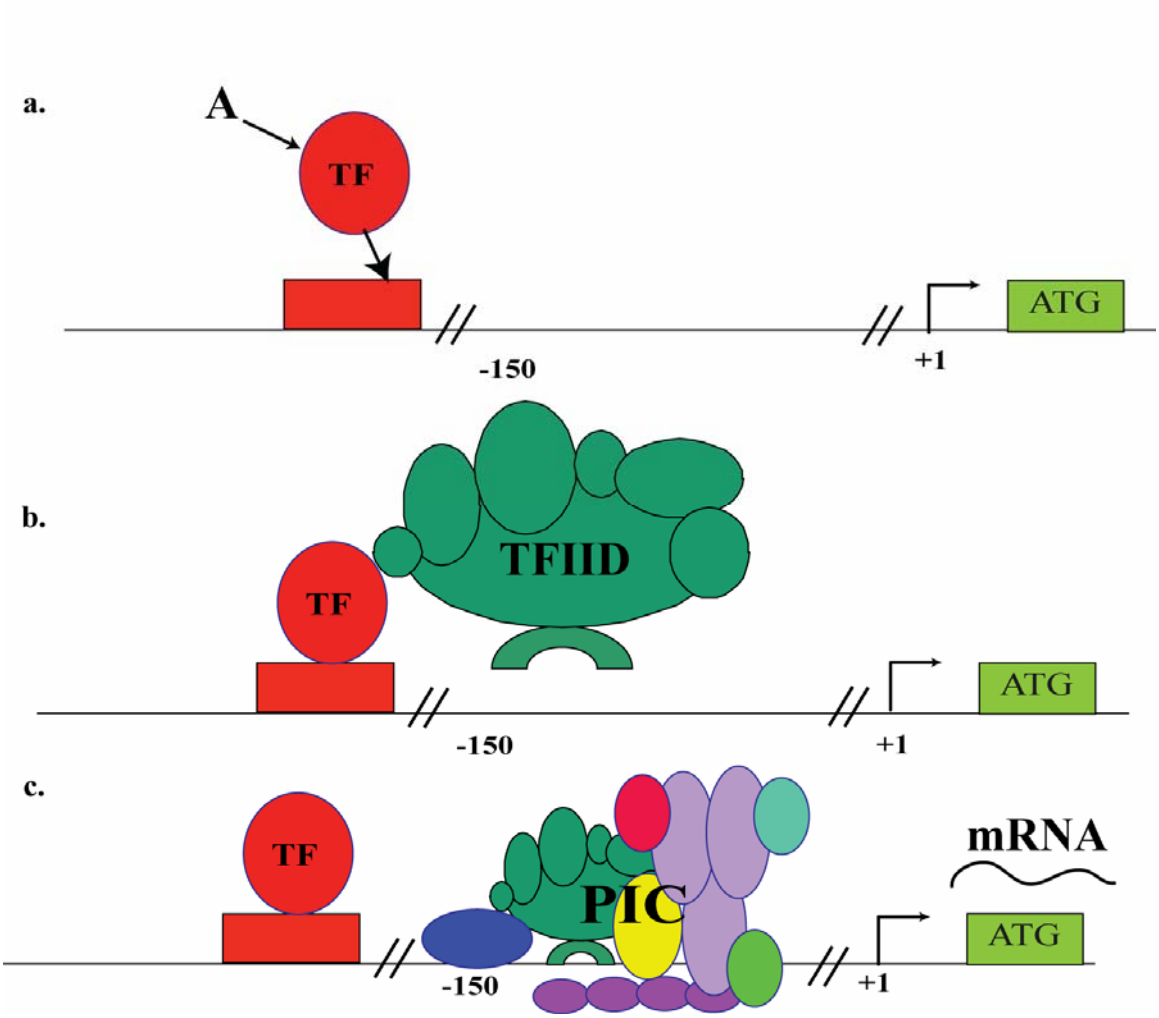

Figure I-7. TFIID functions as a coactivator for transcription factors. Shown is a simple schematic depicting the coactivator model of TFIID.
a. A transcription factor binds to its cognate binding site in the proximal promoter in response to an environmental cue.
b. The transcription factor recruits TFIID to the core promoter through direct interactions with a subset of TFIID subunits.
c. TFIID nucleates the formation of the PIC, thus resulting in an increase in transcriptional output. In each panel, the transcription initiation site is denoted by an arrow and +1.
TF = transcription factor; PIC = preinitiation complex.

The third caveat is that these simplified *in vitro* systems were used to study only one set of interactions, between that of a single transcription factor and a single Taf_{II}-TBP complex. The ability of mutated transcription factors to bind a particular subset of Taf_{II}s was correlated with the ability of these mutant transcription factors to stimulate transcription via that subset of Taf_{II}s. For example, the transcription factor, p53, can interact with Taf6p *in vitro* via its transcriptional activation domain. Mutations in the activation domain of p53 disrupt interaction with Taf6p (7). Not surprisingly, p53 requires a minimal Taf_{II}-TBP complex that must containTaf6p to stimulate transcription *in vitro*, and again as predicted, the mutant p53 that was defective in interacting with Taf6p could not stimulate transcription via this minimal Taf_{II}-TBP complex containing Taf6p. Therefore, the conclusion was drawn that p53 requires interaction with Taf6p to stimulate transcription. Of course, the situation is more complex *in vivo*, as different transcription factors work together to stimulate gene transcription. Because distinct subsets of Taf_{II}s mediate interaction with different transcription factors, altering one set of interactions by mutating a single transcription factor may provoke a change in other sets of interactions mediated by other transcription factors that could lead to changes in gene expression *in vivo* that could not be predicted from studying one set of interactions *in vitro*.

Therefore, an important question is: how exactly does TFIID stimulate transcription *in vivo*? One hypothesis is that TFIID stimulates transcription *in vivo* as it does *in vitro*, that is, via mutationally sensitive, direct interactions between a given transcription factor and a subset of Taf_{II}s.

Evidence that TFIID may serve as a coactiavtor for Swi6p

As discussed in the preceding section (**The role of TFIID in the regulation of transcription initiation: Role of TFIID as coactivator**), a pressing question in the field of gene transcription is how exactly TFIID stimulates transcription *in vivo*. To be able to answer this question, it is first important to identify transcription factors that likely interact with TFIID *in vivo*.

In our laboratory, mass spectrometric analyses of proteins associated with TFIID that had been immunopurified from yeast identified several transcription factors. One of these transcription factors was Swi6p (12). Swi6p was first identified in a screen of mutants defective for transcription of the cell-cycle regulated gene, *HO* (13). Many studies since then have illuminated the mode of action of Swi6p, and several aspects of Swi6p structure and function are worth mentioning. First, Swi6p is thought to function in conjunction with one of two other transcription factors, Swi4p and Mbp1p, forming the complexes known as SBF and MBF, respectively. SBF and MBF regulate the expression of a group of genes that are expressed at the G_1/S phase boundary of the yeast cell cycle. SBF and MBF recognize and bind to specific DNA binding sites found in the promoters of many of its target genes, CACGAAA and ACGCGTNA, respectively. Swi4p and Mbp1p provide the DNA binding specificity, whereas Swi6p does not (14, 15, 16, 17 , 18). As predicted, Swi6p does not contain any recognizable DNA binding domain. However, in reporter gene studies using a series of deletion mutants of Swi6p, an activation domain was identified both in the N-terminal and the C-terminal halves of the protein (19). These two activation domains are separated by a putative leucine zipper and four to five ankyrin repeats; both of these domains are known to function as protein-

protein interaction domains in other proteins (19, 20). Finally, Swi6p has been shown to interact with Swi4p and Mbp1p via its C-terminus (21) (Figure I-8).

The role of Swi6p in regulating gene transcription, however, is still not well understood. Studies in *swi6Δ* mutant yeast show that the expression of many SBF and MBF target genes, other than *HO*, is not significantly impaired, if at all, in asynchronous cultures of yeast (13, 17, 22, 23, 24). However, in synchronized cultures of *swi6Δ* yeast, the characteristic peak of expression of these target genes at the G_1/S phase boundary was abolished, resulting in a near steady state level of gene expression throughout the yeast cell cycle (23). In conclusion, Swi6p appears to function in activating gene transcription in a specific cellular context, the G_1/S phase transition of the yeast cell cycle. Consistent with this view is the fact that the intracellular location of Swi6p is regulated as a function of the cell cycle: during G_2 and mitosis, Swi6p is predominantly cytoplasmic but becomes nuclear in G_1 (25).

At present, however, the molecular mechanisms by which Swi6p activates gene transcription are not understood. Does Swi6p regulate transcription by relieving the repressive effects of chromatin or by upregulating levels of transcription initiation or both? Therefore, does Swi6p regulate transcription by recruiting chromatin remodeling complexes or GTFs or both?

TFIID and cell-cycle regulation

Previous work has strongly suggested that TFIID plays a role in regulating the expression of genes at the G_1/S phase transition. Studies using a temperature sensitive (ts) allele of one of the yeast Taf_{II}s, *TAF1*, demonstrated that *TAF1* regulates the G_1/S phase

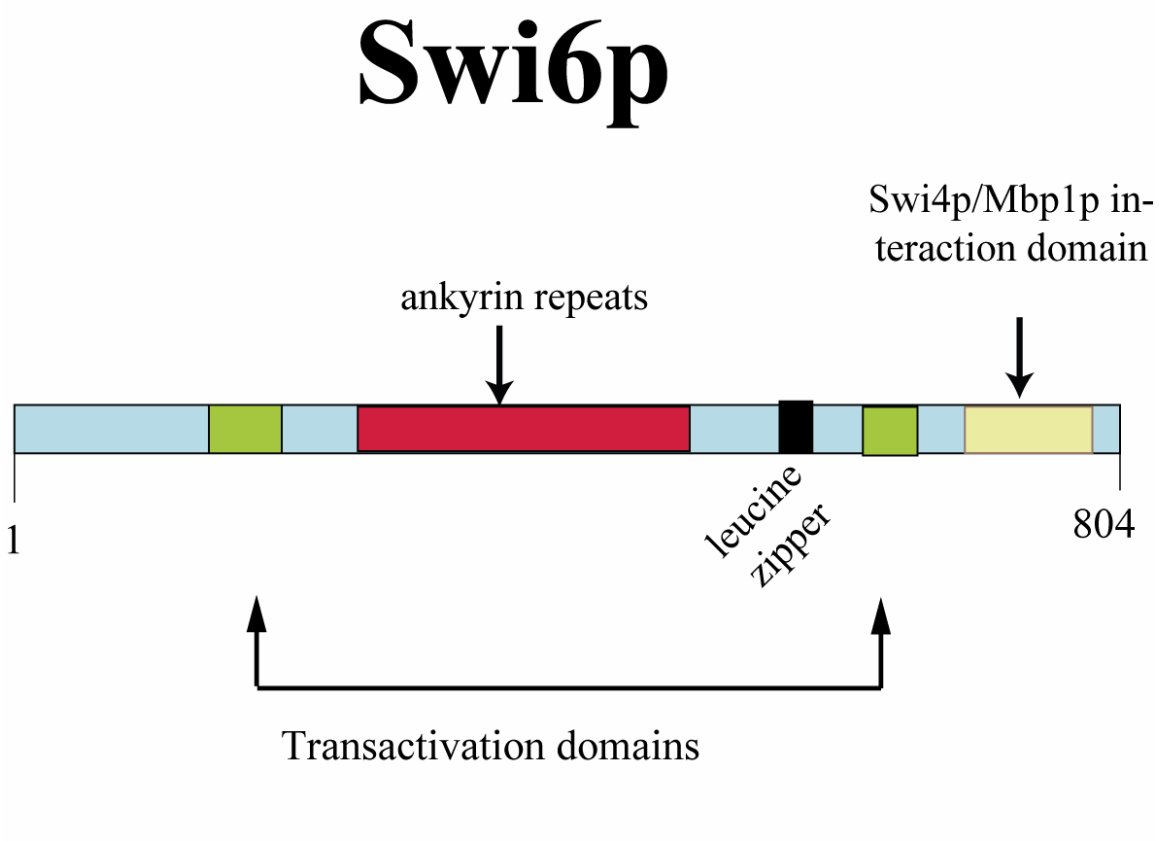

Figure I-8. Domain map of Swi6p. Shown is a diagram depicting the functional and structural domains contained within Swi6p.

transition of the yeast cell cycle, since *taf1* ts mutant yeast incubated at the restrictive temperature showed a uniform cell cycle arrest in G_1 (26). This observation was correlated with the fact that the expression levels of several SBF and MBF target genes were severely impaired in mutant yeast at the restrictive temperature (10). In addition, the stimulation of expression of these genes at the G_1/S phase transition was all but abolished in synchronized mutant yeast at the restrictive temperature (10).

Second, analogous studies in mammalian cells pointed to a conserved role of TFIID in the regulation of expression of cell cycle genes in metazoans. Hamster cells harboring a ts allele of human *TAF1* also arrested in G_1 at the restrictive temperature (27). Furthermore, the expression of several cell cycle regulated genes was impaired at the restrictive temperature in this mutant. This defect was shown to be at the transcriptional level, as indicated by the results of nuclear run-on assays (28).

A specific role for Taf9p as coactivator for Swi6p

As discussed above, there is compelling data that shows that TFIID has a role in the expression of a group of genes at the G_1/S phase transition of the cell cycle. In addition, studies using a ts allele of a yeast Taf_{II}, yeast Taf9p, demonstrated a synthetic growth defect at the permissive temperature between *TAF9* and *SWI6* (18). This mutation in *TAF9* is a single point mutation that converts a tryptophan codon to a premature stop codon that would result in the translation of a truncated protein missing 25 amino acids from the C terminus (henceforth, this mutation will be referred to as the *taf9W133stop* mutation) (Figure I-9). Furthermore, the peak in expression of two cell-cycle regulated genes, *PCL2* and *CLB5*, was reduced in G_1 at the permissive temperature in synchronized

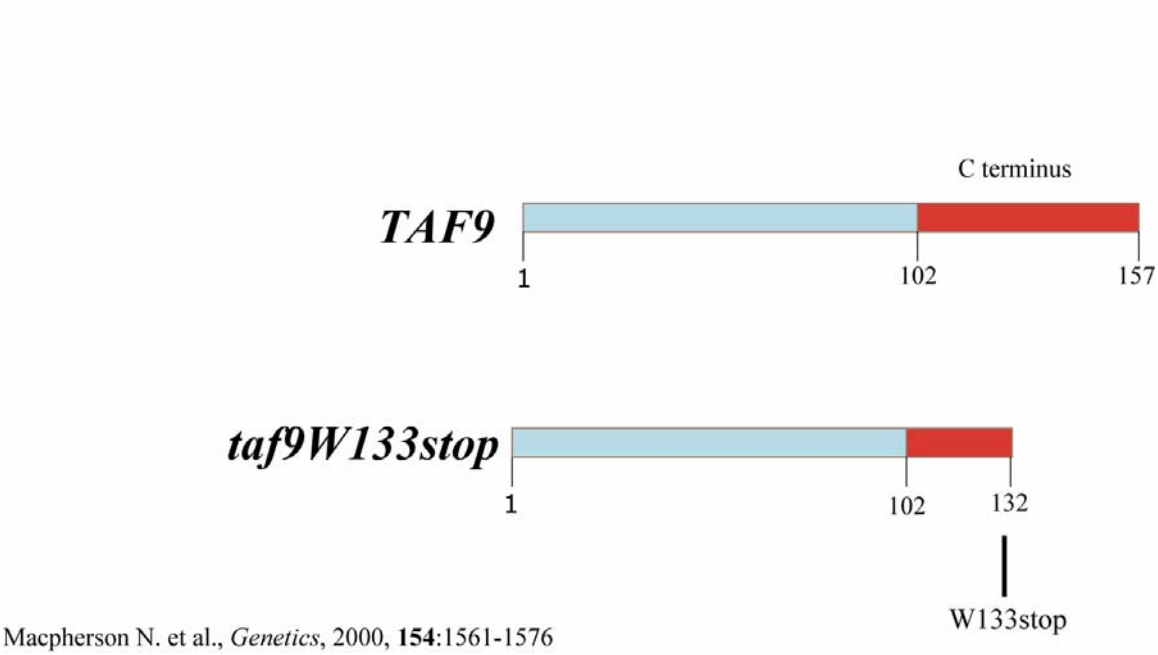

Figure I-9. Diagram of the protein predicted to be encoded by *the taf9W133stop* mutation.
(Top) Shown is a diagram of wild-type yeast Taf9p, and
(bottom) mutant Taf9p that may be expressed in yeast harboring the *taf9W133stop* mutation. In the mutant yeast, a single point mutation converts a tryptophan codon into a premature stop codon; this mutation is expected to encode a protein that is missing the 25 amino acids from the C terminus of the wild-type protein.

taf9W133stop yeast. Interestingly, the C terminus of yeast Taf9p has been conserved in metazoans (Figure I-10).

In addition, in our laboratory, it was found that Swi6p could interact with a subset of Taf_{II}s (Taf8p, Taf12p, and Taf7p) in wild-type yeast whole cell extracts, and that this interaction was disrupted in yeast harboring the *taf9W133stop* mutation (12) (Figure I-11).

Taken together, the observations discussed in the preceding two sections support a model in which TFIID stimulates transcription of a group of genes at the G_1/S phase transition by serving as a coactivator for Swi6p via direct, mutationally sensitive interactions between Swi6p and Taf9p.

Hypothesis and specific aims

I hypothesize that TFIID serves as a coactivator for Swi6p at the promoters of Swi6p-regulated genes. Because of the genetic and biochemical data that suggests an interaction between Swi6p and Taf9p, I also hypothesize that Taf9p plays an important role in mediating the coactivator function of TFIID for Swi6p.

My original specific aims had centered on the role of Taf9p. My original aims were as follows:

1) characterize the mode of interaction of Taf9p with SBF and MBF;
2) (investigate the) role of Taf9p in regulating *PCL2* transcription at Start; and
3) characterize interaction of SBF and MBF with Taf9p at endogenous *PCL2* and *CLB5* promoters.

During the course of this research, attention shifted away from Taf9p as a result of the variability observed in the *taf9W133stop* mutant and from the lack of evidence supporting a direct interaction between Taf9p and SBF (discussed in **Chapter III** and **Chapter II**, respectively).

Therefore, I modified my original specific aims to the following:

1) characterize the interaction of Swi6p/SBF with TFIID, and

2) characterize the interaction of Swi6p/SBF with TFIID at promoters of co-regulated genes *in vivo*.

For the first specific aim, I characterized further the interaction between Swi6p and the TFIID complex through co-immunoprecipitation analyses of Swi6p with various Taf_{II}s in wild-type yeast and yeast harboring the *taf9W133stop* mutation. These experiments are discussed in **Chapter III**. I also identified the subunit(s) of TFIID that mediate interaction with Swi6p through Far Western analyses of interaction between TFIID subunits and SBF. The Far Western analyses are discussed in **Chapter II**.

For the second specific aim, I performed Northern blot analyses of gene expression in *taf12* temperature sensitive mutant yeast and in *swi6Δ* yeast. These experiments are discussed in **Chapter II**.

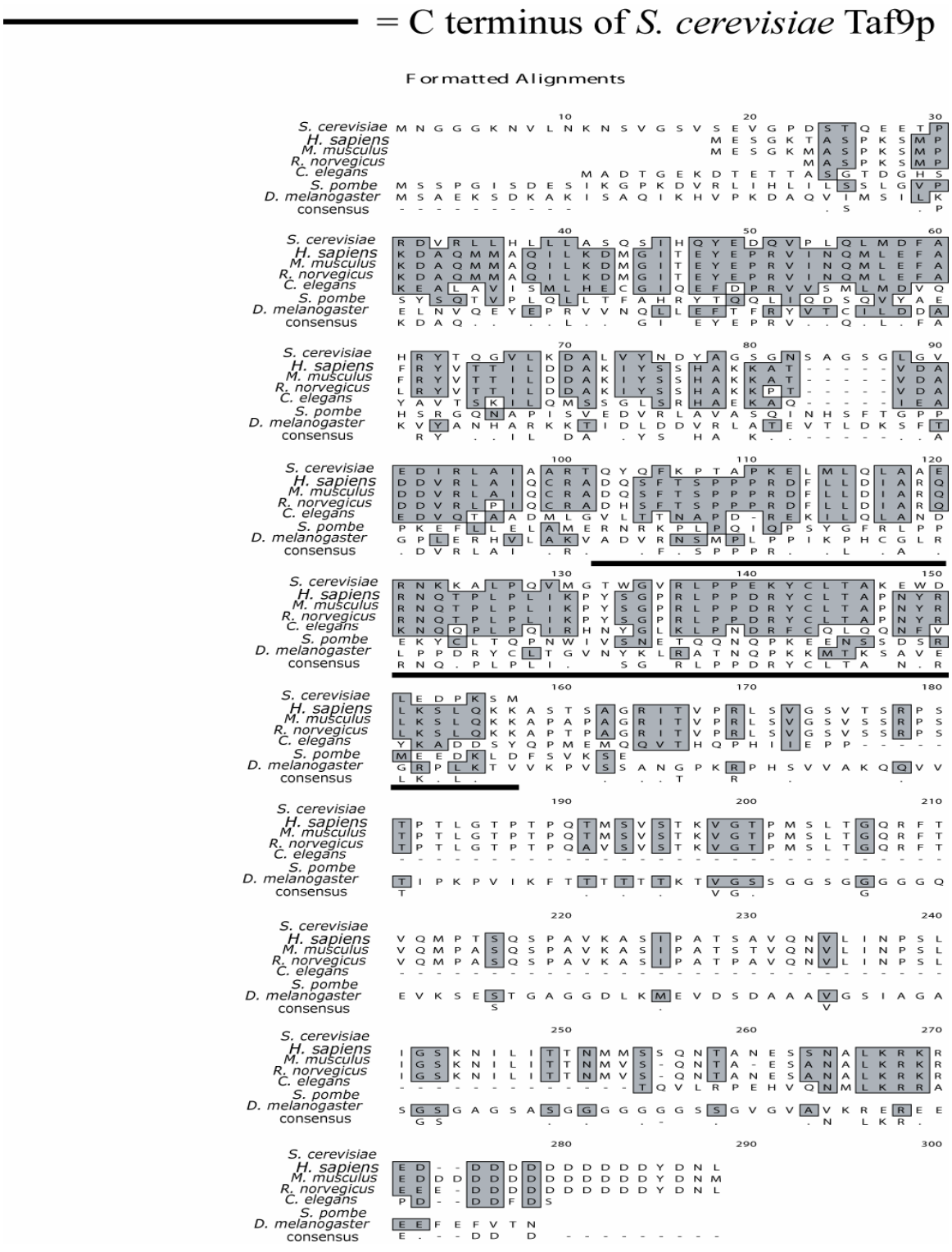
= C terminus of S. cerevisiae Taf9p
Formatted Alignments
S. cerevisiae
H. sapiens
M. musculus
R. norvegicus
C. elegans
S. pombe
D. melanogaster
consensus

Figure I-10.

Figure I-10. The C terminus of *Saccharomyces cerevisiae* Taf9p is conserved across several metazoan species. Shown are the amino acid alignments of Taf9p from two species of yeast and several metazoan species. The sequences were aligned in MacVector. The sequences are numbered according to the Taf9p sequence from *S. cerevisiae*. Beneath the sequences is a suggested consensus sequence.
S. cerevisiae = *Saccharomyces cerevisiae*; *H. sapiens* = *Homo sapiens*; *M. musculus* = *Mus musculus*; *R. norvegicus* = *Rattus norvegicus*; *C. elegans* = *Caenorhabditis elegans*; *S. pombe* = *Schizosacchromyces pombe*; *D. melanogaster* = *Drosophila melanogaster*.

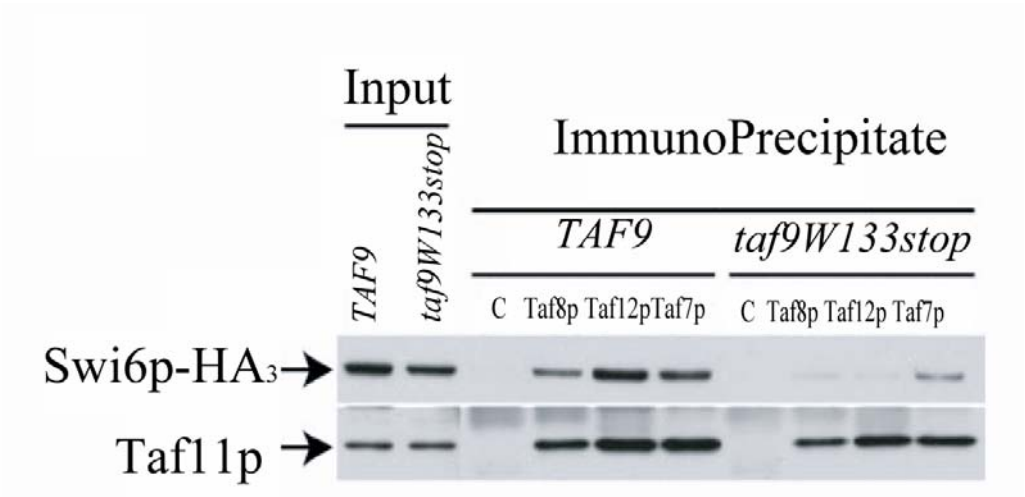

Sanders SL., et al. *Mol. Cell. Biol.*, 2002, **22**:4723-4738

Figure I-11. In *taf9W133stop* yeast, the co-immunoprecipitation of Swi6p with three Taf_{II}s was impaired. Portions of whole cell extract (WCE) were immunoprecipitated with polyclonal antibodies against Taf8p, Taf12p, or Taf7p. The proteins detected in the immunoprecipitate by immunoblot are indicated at the left. Swi6p co-immuonprecipitated with Taf8p, Taf12p and Taf7p in wild-type yeast but this interaction was impaired in *taf9W133stop* yeast. "*TAF9*" and "*tafW133stop*" refer to yeast strains that are wild-type and mutant, respectively.
C = control immunoprecipitation.

CHAPTER II

IDENTIFYING TFIID SUBUNITS AS CANDIDATES FOR PROVIDING COACTIVATOR FUNCTION FOR SWI6P

The first, and most critical, criterion for demonstrating that TFIID is a coactivator for Swi6p is that TFIID must interact directly with Swi6p. Since Swi6p functions *in vivo* as part of the SBF and MBF complexes, I decided to examine interaction between TFIID and Swi6p in the context of these complexes. For sake of simplicity and availability of reagents, I decided to focus on one of these complexes, SBF. Initial studies of TFIID coactivator function *in vitro* had shown that transcription factors activated transcription through direct interaction with only a subset of Taf_{II}s (1, 5, 7). Furthermore, mutations in transcription factors that impaired interaction with these Taf_{II}s also impaired transcriptional activation *in vitro*. Therefore, I hypothesized that SBF may also activate transcription through only a subset of Taf_{II}s. I performed Far Western analyses to answer two questions simultaneously: does SBF interact with TFIID *in vitro*, and if so, does SBF interact with only a subset of Taf_{II}s?

I found that SBF did interact *in vitro* selectively with a subset of Taf_{II}s (Taf12p, Taf4p, and Taf5p). With this information, I performed Northern blot analyses in asynchronous cultures of *swi6Δ* and a temperature sensitive (ts) mutant of *TAF12* to identify a gene(s) that is (are) co-regulated by Swi6p and TFIID. I found that several cell-cycle regulated genes are regulated by *TAF12* in asynchronous yeast, but none of these genes were regulated by *SWI6* in asynchronous yeast.

Materials and Methods

In vitro studies of protein-protein interaction

Production of anti-Swi6p antibodies. I cloned DNA encoding the C terminal half of Swi6p into a pET19b expression vector. The DNA had been generated by PCR of genomic yeast DNA (Invitrogen) using primers specific for the coding region of that portion of *SWI6*. See Table II-1 for the sequences of the primers used in the PCR. The cloned vectors were transformed into a DH5α *E. coli* strain. The plasmids were purified and the inserts were sequenced. The plasmids were then transformed into BL21 pLysS and BL21 Codon plus *E. coli* strains.

The pET19b expression vector adds an N terminal His_{10} tag to the insert. Therefore, the C terminal Swi6p fragment was purified by a one-time pass of bacterial lysate on a Ni^{2+}NTA column under denaturing conditions, and the bound protein was eluted with increasing concentrations of imidazole (Figure II-1). Upon renaturation by dialysis, about 50% of the protein precipitated. The soluble protein was sent to Bethyl Laboratories, where it was used to immunize rabbits. The remaining insoluble protein was re-solubilized with a non-detergent sulfobetaine (NDSB 201). The re-solubilized protein was covalently cross-linked to cyanogen bromide (CNBr)-activated sepharose. Ten mL of serum from immunized rabbits were filtered through a 0.8μM membrane. Antibodies were purified from the filtered serum as follows: the serum was incubated with the antigen cross-linked to CNBr-activated sepharose, unbound antibody was washed from the resin with an increasing NaCl concentration gradient, and the Swi6p-antibodies bound to the resin were eluted with 0.1M Na citrate, pH 2.8. The eluates were

Table II-1. Details on cloning the C terminal half of Swi6p.
(Top) Sequences of primers used in PCR of an insert encoding the C terminal fragment of Swi6p. The locus ID for *SWI6* was obtained from the online Saccharomyces Genome Database.
(Bottom) The sequence of the multiple cloning site in the pET19b vector (Novagen).

Gene	Locus ID	Sequence of forward primer	Sequence of reverse primer	Size of His-tagged fusion peptide (no. of amino acids)
		NdeI site	BamHI site stop codon	
SWI6	*YLR182W*	GCGGAGAGCATATGCACCATATCATTA TTACG	GGCCTATCGGATCCCTCATGAAGCATG CTTTTTT	435

pET19b cloning and expression region

His_{10}-tag	Enterokinase site	NdeI site	XhoI site	BamHI site	
CATCATCATCATCATCATCATCATCAC	AGCAGCGGCCATATCGACGACGACGACAAG	CATATG	CTCGAG	GATCCGGCTGCTAACAAA	·····

T7 terminator

····· **TAGCATAACCCCTTGGGGCCTCTAAACGGGTCTTGAGGGGTTTTTTG**

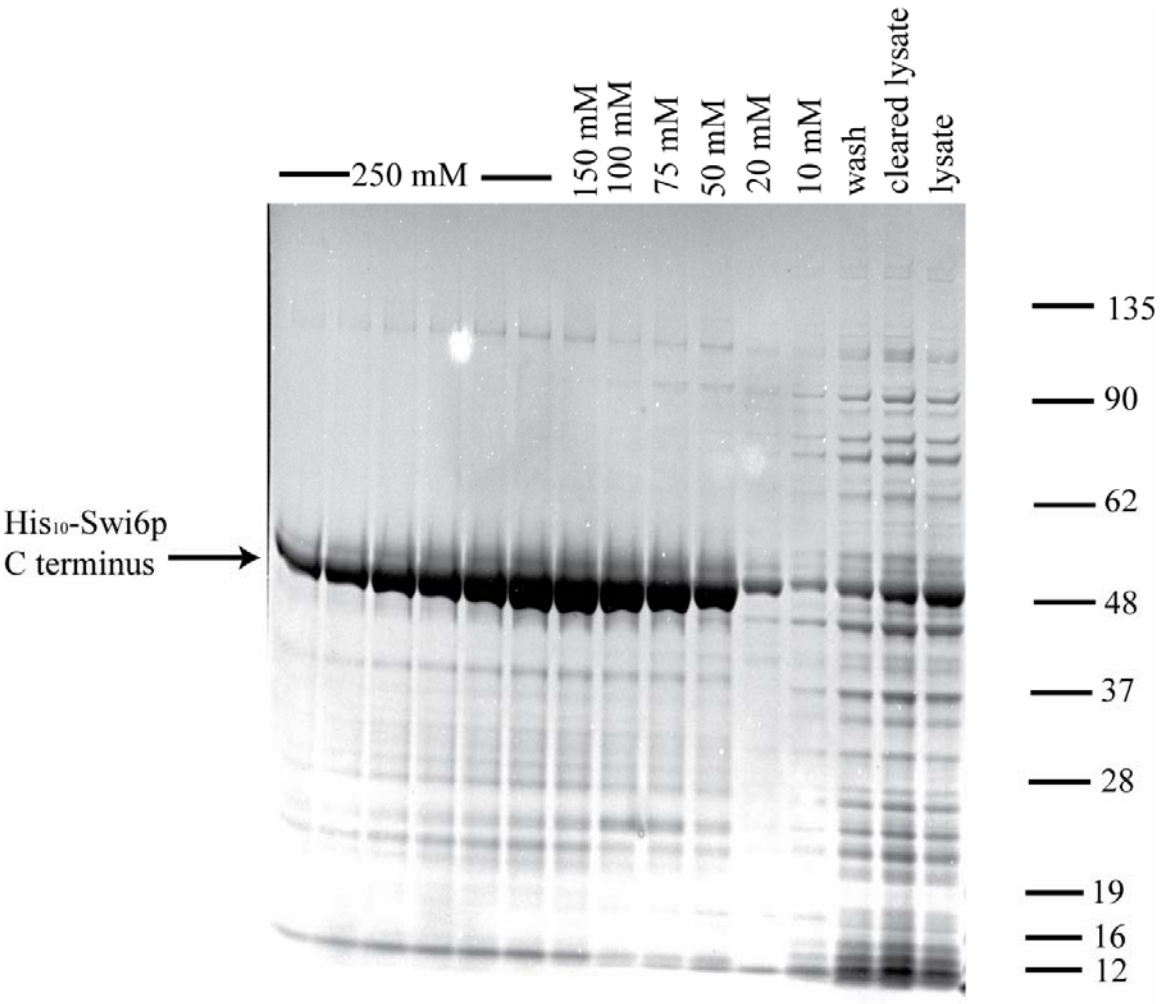

Figure II-1. The C terminal half of Swi6p was successfully expressed in *E. coli*. A Coomassie stain of the purification of a His_{10}-tagged, C terminal fragment of Swi6p. Lanes designated as "XmM" refer to imidazole concentrations. The numbers to the right of the gel are the MWs, in kDa.

collected in 600 μL fractions in chilled 1.5mL-eppendorf tubes containing 60 μL of 1M Tris acetate pH 9.0; the pH of the eluates was verified to be a pH of 7 with pH paper.

The optimal dilution of anti-Swi6p for detection purposes was determined by probing increasing amounts of the recombinant, His_{10}-tagged C terminal fragment of Swi6p immobilized on a 0.45 μM PVDF membrane with different dilutions of anti-Swi6p. The specificity of anti-Swi6p was determined by probing yeast WCEs from the strains indicated in Table II-2 (Figure II-2).

Far Western assay. 20X Transfer buffer consisted of the following per liter of buffer: 81.6 g bicine; 104.8 g bis-Tris; 6.0 g EDTA; and 0.2g chlorobutanol. Binding buffer consisted of the following: 20mM HEPES-KOH pH 7.6; 75mM KCl; 2.5mM $MgCl_2$; 0.1mM EDTA; and 0.05% (v/v) NP-40. TBS-T consists of the following: 25mM Tris-HCl pH 7.6; 150mM NaCl; and 0.05% Tween-20 (v/v).

See Figure II-3 for a basic schematic of a Far Western assay. A purified yeast TFIID preparation that contained a TAP-tagged Taf1p was loaded in two lanes on a 4-12% bis-Tris gel separated by a lane containing prestained Benchmark MW markers (Invitrogen). TFIID subunits were separated by SDS-PAGE. The proteins were electroblotted onto a 0.45 μM PVDF membrane for two hours in 1x transfer buffer/10% methanol (v/v). One lane of TFIID was stained with 0.05% (w/v) Coomassie R-250, whereas the adjacent lane of TFIID was further subjected to Far Western analyses. In some experiments, recombinant His_6-tagged Taf_{II}s were

Table II-2. Yeast strains used to test polyclonal anti-Swi6p.

Strain	Genotype	Source
YSLS163	*Matα ura3-52 lys2-801 ades-107 TRP1 his3Δ200 leu2Δ1 SWI6::HA $_3$-KAN^r*	Tony Weil lab
YSLS164	*Matα slm7-1(taf17W133^{amber}) SWI6::HA $_3$-KAN^r TRP1 ura3 leu2 lys2 ade2*	Tony Weil lab
BY4741	*MATa leu2Δ0 ura3Δ0 his3Δ1 LYS2 met15Δ0*	Research Genetics
swi6Δ	*MATa leu2Δ0 ura3Δ0 his3Δ1 LYS2 met15Δ0 swi6::KAN^r*	Andrew Link lab
W303 haploid ⧾	*Mat⧾ ura3-1 his3-11, 15 ade2-1 leu2-3, 112 trp1-1 can1-100*	Jeff Flick lab
Z1373	*YLR182W SWI6-MYC18 in W303 haploid* ⧾	Richard Young lab

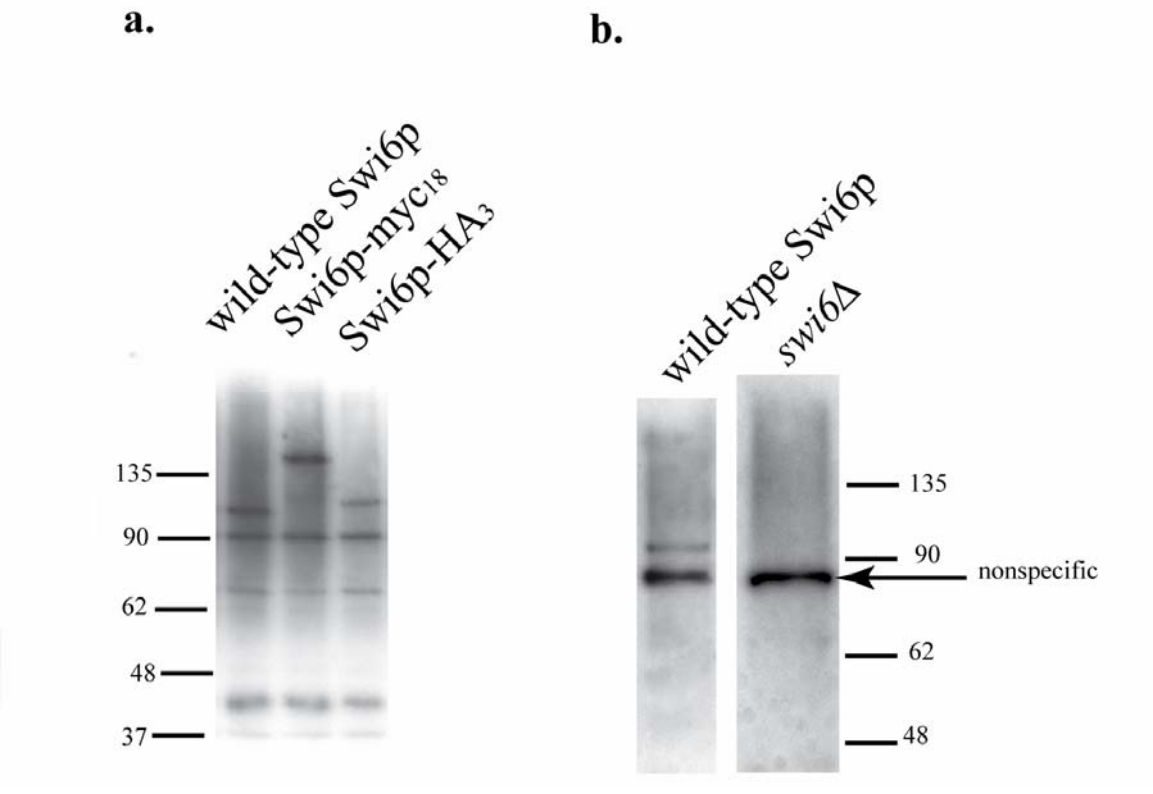

Figure II-2. The polyclonal antibodies raised against the C terminal half of recombinant Swi6p specifically detect yeast Swi6p.

a. Shown are the results of an immunoblot in which WCEs prepared from wild-type yeast and yeast that express HA_3 or myc_{18}-tagged Swi6p were probed with polyclonal anti-Swi6p.

b. Shown are the results of a separate immunoblot in which WCEs prepared from wild-type yeast and *swi6Δ* yeast were probed with polyclonal anti-Swi6p.

In **a.** and **b**., the top most band seen in the figure is Swi6p (either untagged or tagged with HA_3 or myc_{18} epitopes). The numbers to the left of the immunoblot in **a.** and the numbers to the right of the immunoblot in **b.** are the MWs, in kDa.

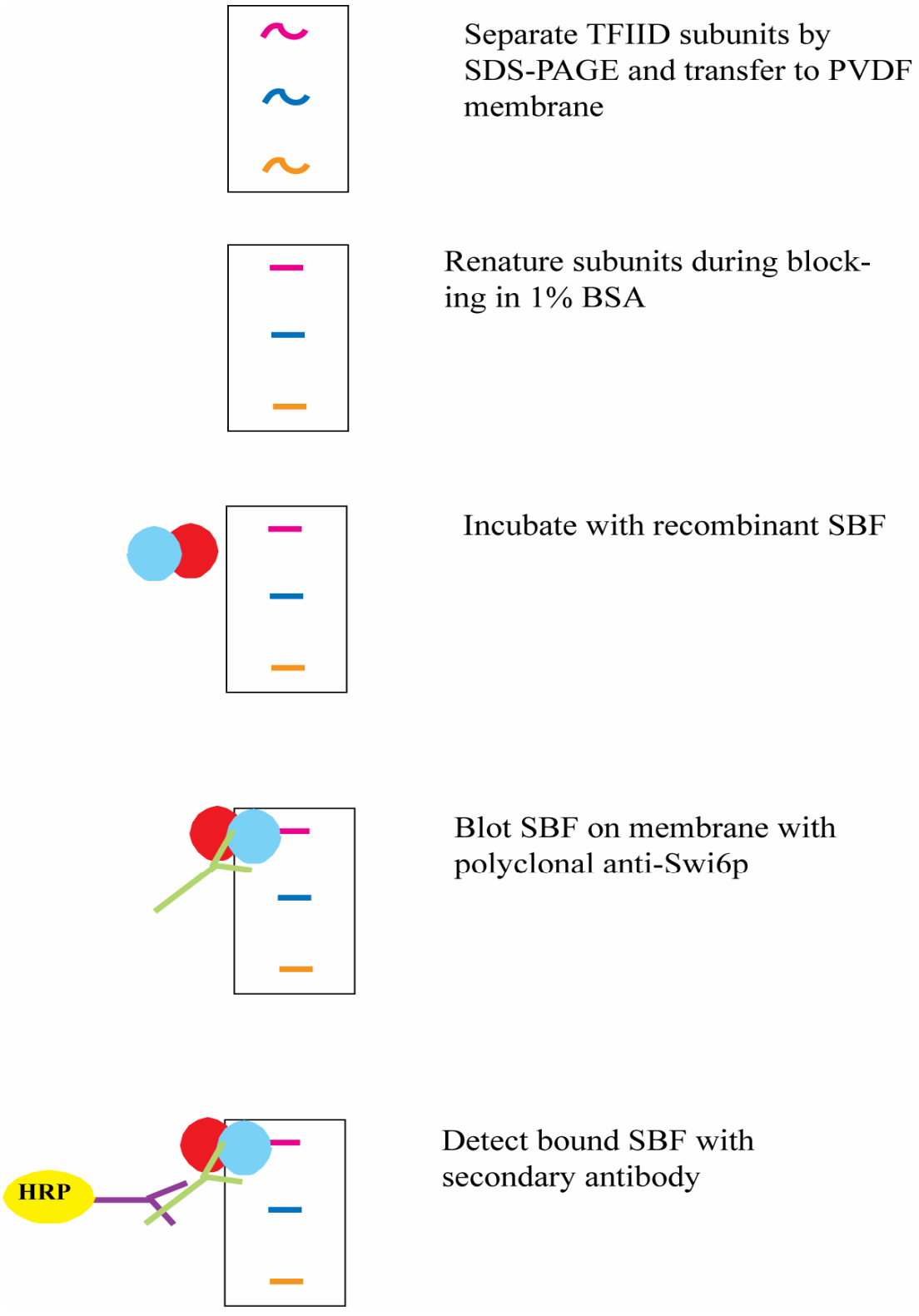
Separate TFIID subunits by SDS-PAGE and transfer to PVDF membrane
Renature subunits during block-ing in 1% BSA
Incubate with recombinant SBF
Blot SBF on membrane with polyclonal anti-Swi6p
HRP
Detect bound SBF with secondary antibody

Figure II-3.

Figure II-3. Schematic of a Far Western assay. First, yeast TFIID was subjected to SDS-PAGE. Proteins were then electroblotted onto a PVDF membrane, and renatured during blocking in 1%BSA/binding buffer/1mM DTT. The membrane was then incubated with soluble, recombinant SBF. Unbound SBF was washed away, and bound SBF was detected with polyclonal anti-Swi6p antibodies in a standard immunoblot. HRP = horseradish peroxidase.

electrophoresed on the same gel as yeast TFIID. The amount of recombinant Taf_{II} loaded was equal to the amount of the corresponding Taf_{II} in the portion of yeast TFIID that was loaded on the gel and subjected to Far Western analysis. The membrane was blocked for one to two hours in binding buffer with 1% BSA/binding buffer/1mM DTT at either room temperature or in the cold room, and then probed with SBF, which had been purified from baculovirus-infected insect cells, for 14-21 hours. The membrane was rinsed once with 1%BSA/binding buffer/1mMDTT, and then rinsed three times with binding buffer/1mM DTT only. The membrane was then subjected to Western blot as follows: the membrane was incubated with purified anti-Swi6p, diluted 1:5000 in 1% nonfat milk/TBS-T, either overnight in the cold room or for several hours at room temperature. The membrane was then rinsed once with 1% nonfat milk/TBS-T followed by three rinses with TBS-T only. The membrane was incubated with goat anti-rabbit Fc cross-linked to HRP for 30 minutes, and the membrane was then washed as described above. Bound SBF was visualized on the membrane by enhanced chemiluminescence (Roche). The images were detected by exposure to Kodak BioMax film. TFIID subunits that bound SBF were identified by aligning the Coomassie-stained strip of TFIID with the bands seen on the film. The positions of the prestained MW markers were used as reference points for the alignment.

The recombinant SBF used in this analysis was purified as untagged proteins by a member of our laboratory, Krassimira A. Garbett. The components of SBF, Swi4p and Swi6p, were expressed simultaneously by separate baculovirus vectors in insect S2 cells. The baculovirus vectors had been obtained from the lab of Brenda Andrews. I probed purified SBF with my polyclonal anti-Swi6p, and showed that the antibodies detected

Swi6p and not Swi4p (Figure II-4). The TAP-TFIID used in these studies was purified by another member of our laboratory, Manish K. Tripathi. Nearly all the recombinant His_6-Taf_{II}s used in this study had been purified by Steven Sanders, except for His_6-Taf4p, which had been purified by Belgin Cenkci. Each recombinant His_6-Taf_{II} had been separately expressed as a His_6-tagged protein in *E. coli* or in baculovirus-infected insect cells (Figure II-5).

Far Western competition assay*.** This assay was performed as described above (see ***Far Western assay) except that a 2.5 to 10 fold molar excess of recombinant His_6-Taf12p or His_6-Taf6p was incubated simultaneously with SBF (Figure II-6). In one set of competition experiments, His_6-Taf12p or His_6-Taf6p was tested for their ability to compete with yeast TFIID immobilized on the membrane for binding to SBF. In another set of experiments, His_6-Taf12p or His_6-Taf6p was tested for their ability to compete with recombinant His_6-Taf12p immobilized on the membrane for binding to SBF. "Molar excess" refers to multiples of the pmol of Taf12p or of Taf6p that are in 1.62 μg of yeast TFIID, which was the amount of TFIID loaded on the gel and subjected to Far Western analysis.

In vivo studies of Taf_{II} regulation of cell-cycle regulated genes

See table II-3 for yeast strains used in this analysis.

***Temperature shift assay*.** A *taf12* temperature sensitive (ts) strain and its cognate wild-type (strains YSB547 and YSB452, respectively) were subjected to a temperature shift experiment. For each strain, the following was performed: yeast were streaked onto the appropriate

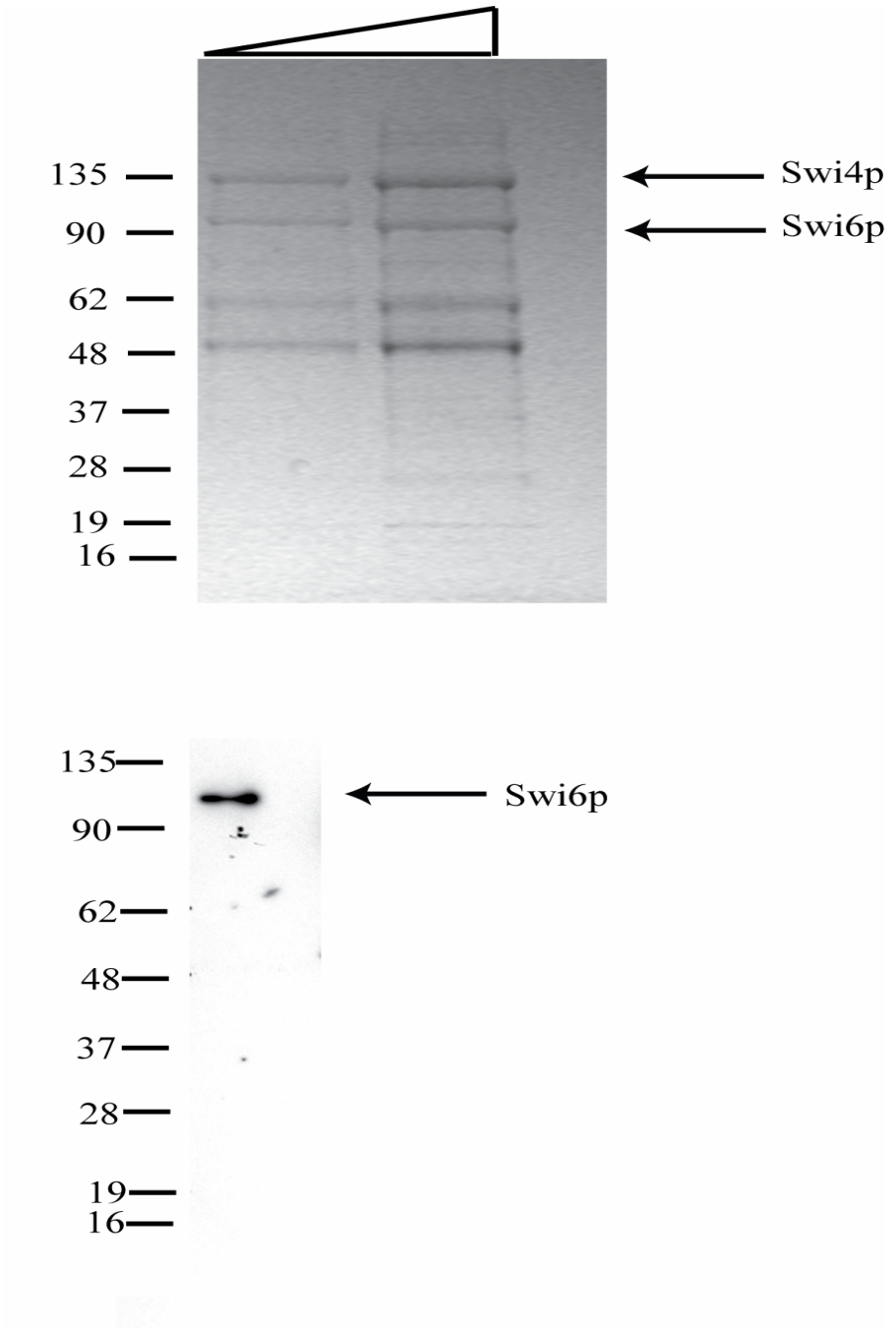

Figure II-4. Polyclonal anti-Swi6p detects Swi6p, not Swi4p, in purified, recombinant SBF that had been expressed in baculovirus-infected insect cells.
(Top) Coomassie-stained gel of recombinant SBF. From left to right, SBF was loaded in increasing amounts across two lanes.
(Bottom) Anti-Swi6p immunoblot of the same batch of SBF that is shown in the Coomassie-stained gel.
In both top and bottom panels, the numbers to the left of the gel or immunoblot are the MWs, in kDa.

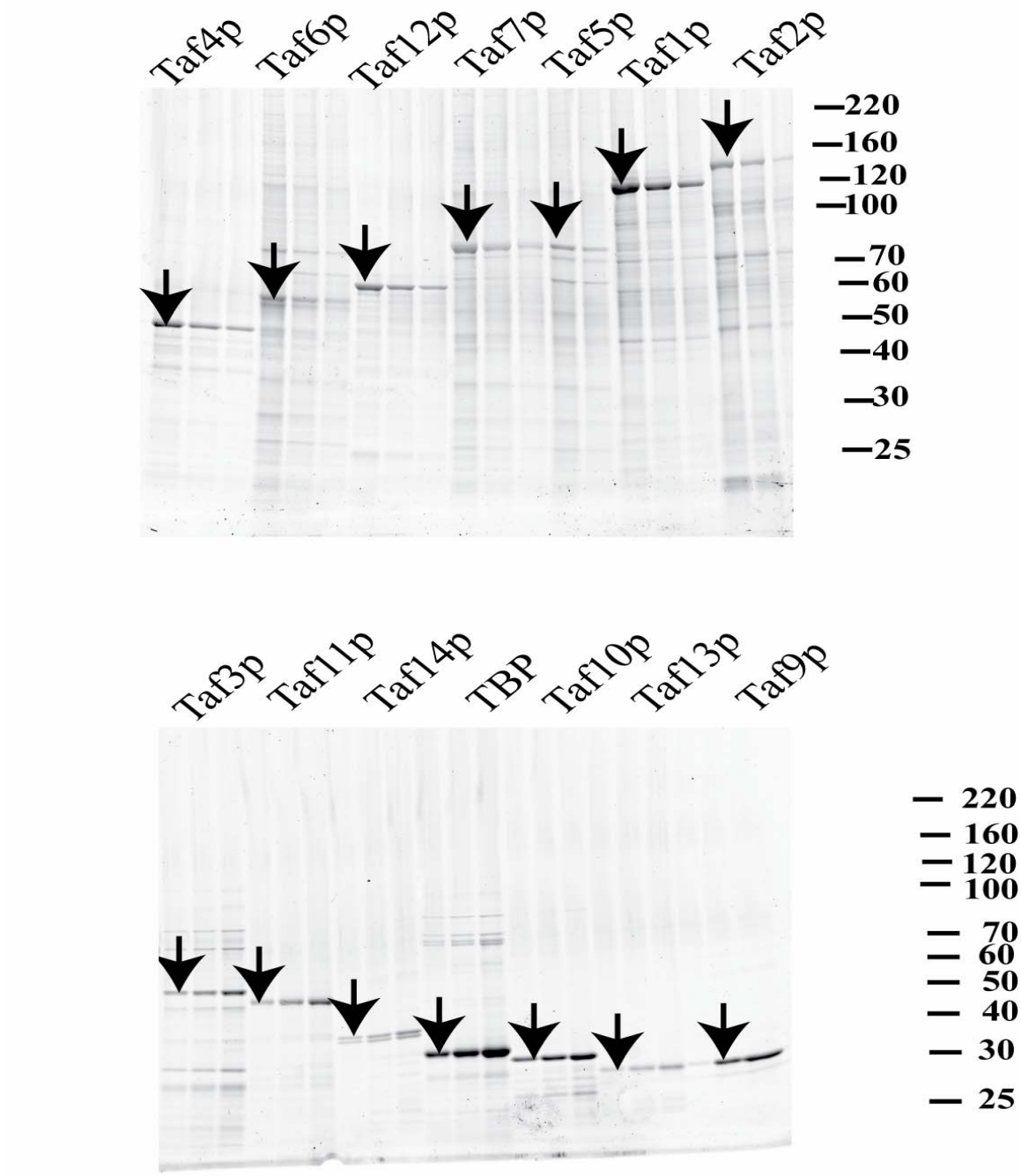

Figure II-5. Sypro Ruby-stained gels of each recombinant His_6-TFIID subunit, except Taf8p. The numbers to the right of each gel are the MWs, in kDa. In the top gel, each recombinant TFIID subunit was loaded onto the gel in decreasing amounts (left to right) over two or three lanes. In the bottom gel, each recombinant TFIID subunit was loaded onto the gel in increasing amounts (left to right) over three lanes. The arrows indicate the position of each full-length recombinant TFIID subunit.

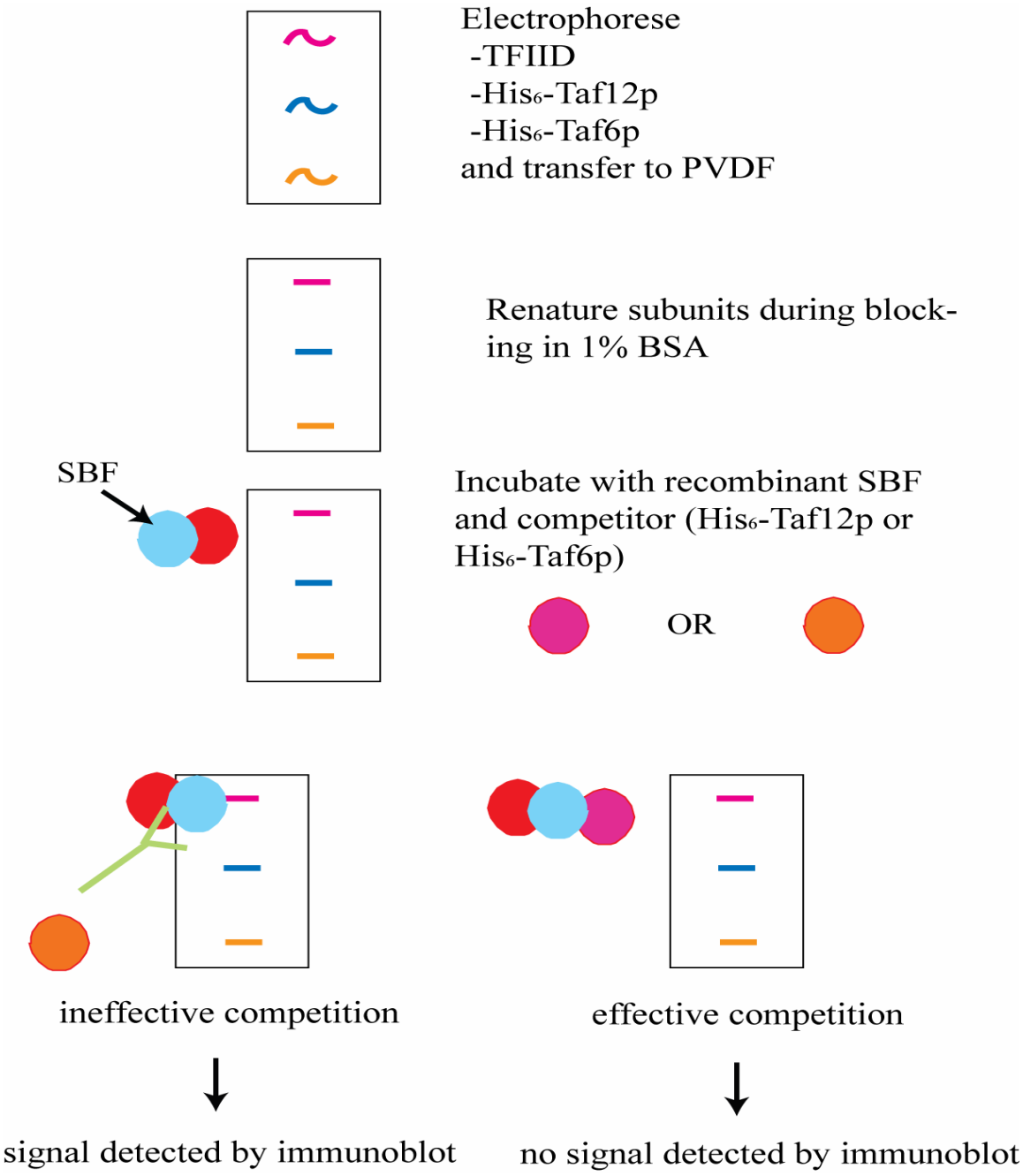

Figure II-6. Schematic of a Far Western competition assay. The experiment is as described in Figure II-3, except that either His_6-Taf12p or His_6-Taf6p was incubated simultaneously with SBF.

drop-out synthetic media plate from frozen lab glycerol stocks and incubated at 30°C for two days. A 50 mL starter culture was prepared in YPAD and inoculated with a single colony from the plate culture. Starter cultures were incubated, with shaking in an open-air incubator, at room temperature until the starter cultures were saturated. Six hundred ml of YPAD was inoculated with a volume of starter culture so that the starting OD_{600}/mL was 0.125. The culture was incubated with shaking in an air incubator at 30°C. The growth of the culture was monitored by OD_{600} and by cell counting in a hemocytometer. When the culture reached an average cell density of two to four million cells per ml, two 50mL aliquots were harvested as follows: cells from each aliquot were collected by vacuum filtration onto a 5.0μm polycarbonate membrane (Millipore), washed once with 25 mL of cold sterile water, and flash frozen on dry ice in pre-chilled 15mL-conical tubes. The frozen cells were then stored at -80°C. In addition, one ml was taken from each culture to perform a temperature shift plate assay (see below). The remaining culture was harvested by vacuum filtration on a 1.0 μm mixed cellulose ester membrane and washed once with 50 mL of cold sterile water. The cells were eluted from the membrane by shaking in a 50ml aliquot of pre-warmed YPAD in a 37°C air incubator for five minutes. The membrane was discarded and the 50 mL of suspended cells were added to a pre-warmed aliquot of 500 mL of YPAD, thus bringing the total volume of the culture to 550 mL.

The culture was then incubated, with shaking, in the 37°C air incubator; the culture was removed from the air incubator to room temperature briefly at 30 minutes and 60 minutes incubation to collect two 50mL aliquots of culture in 50mL-conical tubes

(Falcon). These aliquots were harvested and stored at -80°C, as described in the preceding paragraph.

Plate assay for temperature sensitivity. Fifty μL of the one mL aliquot harvested previously (see ***Temperature shift assay***), was plated onto each of two YPAD plates. One plate was incubated at 30°C whereas the other was incubated at 37°C. Plates were examined one day later (Figure II-7).

Growing and harvesting swi6Δ yeast. Cultures of a *swi6Δ* strain and its cognate wild-type strain (BY4741) were grown and harvested at the permissive temperature only. For each strain, the following was performed: yeast were streaked onto YPAD plates from frozen lab glycerol stocks and incubated at 30°C for two days. A 7.5mL starter culture was prepared in YPAD and inoculated with a single colony from the plate culture. Starter cultures were incubated, with shaking in a 30°C incubator, until the starter cultures were saturated. Two hundred and fifty ml of YPAD was inoculated with a volume of starter culture so that the starting OD_{600}/mL was 0.125. The culture was incubated with shaking at 30°C. The growth of the culture was monitored by OD_{600} and by cell counting in a hemocytometer. When the culture reached an average cell density of two to four million cells per ml, two 50mL aliquots were harvested as follows: cells from each aliquot were collected by vacuum filtration onto a 5.0μm polycarbonate membrane (Millipore), washed once with 25 mL of cold sterile water, and flash frozen on dry ice in pre-chilled 15mL-conical tubes.

Table II-3. Yeast strains used in Northern blotting studies.

Strain	Genotype	Source
YSB452	*Mata ura3-52 leu2::PET56 trp1Δ1 his3Δ200 ade2 taf12Δ259::LEU2[pJA73 (CEN URA3 KAN^r TAF12)]*	Stephen Buratowski lab
YSB547	*Mata ura3-52 leu2::PET56 trp1Δ1 his3Δ200 ade2 taf12Δ259::LEU2[pRS313 (CEN HIS3 taf12-23 ts)]*	Stephen Buratowski lab
BY4741	*MATa leu2Δ0 ura3Δ0 his3Δ1 LYS2 met15Δ0*	Research Genetics
swi6Δ	*MATa leu2Δ0 ura3Δ0 his3Δ1 LYS2 met15Δ0 swi6::KAN^r*	Andrew Link lab

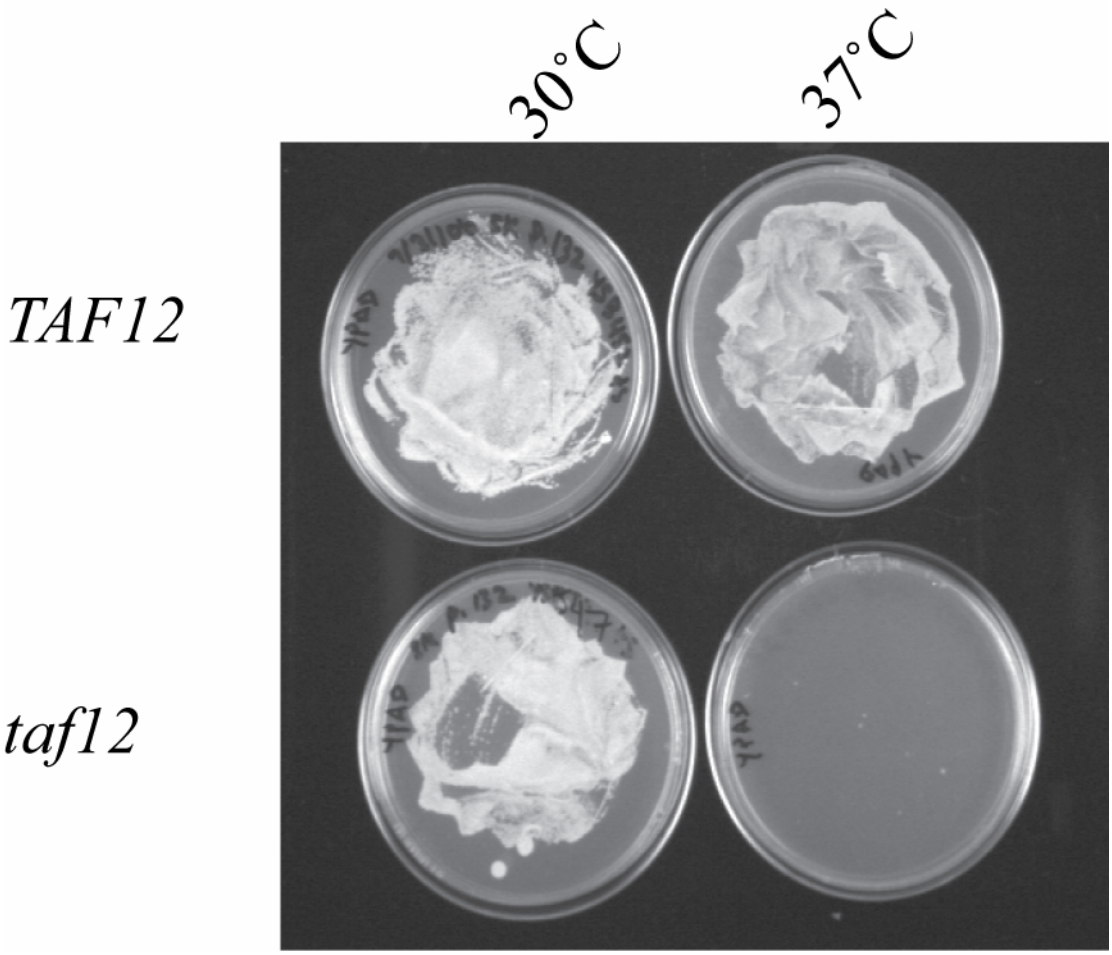

Figure II-7. Plate assay confirming the temperature sensitivity of the *taf12* temperature sensitive yeast strain. Shown is the result of the plate assay of the *taf12* ts strain (YSB547, *taf12* in figure) and its cognate wild-type (YSB452, *TAF12* in figure). Across the top are the temperatures at which the plates had been incubated.

RNA isolation. TE consisted of 10mM Tris-HCl pH 8.0 and 1mM EDTA pH 8.0, whereas T0.1E consisted of 10mM Tris-HCl pH 8.0 and 0.1mM EDTA pH 8.0

RNA was isolated from each 50mL aliquot harvested previously (see ***Temperature shift assay*** and ***Growing and harvesting swi6Δ yeast***) as follows: 1.5mL of acid saturated phenol:chloroform (125:5:1 phenol:$CHCl_3$:isoamyl alcohol, equilibrated to pH 4.7, Sigma) was added directly to each membrane in the 15mL collection tube. Most of the cells were eluted from the membrane with vigorous vortexing. Then, 1.5mL of TE+0.5%SDS (w/v) was added to the membrane, and the remainder of the cells was eluted with vigorous vortexing. The aqueous phase was separated with centrifugation in a Beckman Coulter centrifuge for five minutes at 4°C. About one mL of aqueous phase was recovered, which was divided between two 1.5mL-eppendorf tubes. Five hundred μL of acid saturated phenol was added to each aqueous phase. RNA was isolated by hot phenol extraction as follows: the aqueous phase was vortexed for ten seconds, incubated in a 65°C water bath for ten minutes, and spun in a microfuge at room temperature for three minutes at 14krpm. The cycle of vortexing, incubation, and spinning was repeated for a total of six times.

The aqueous phase was transferred to a new 1.5mL-eppendorf tube after the last cycle, and then extracted once with acid saturated phenol and twice with choloroform. RNA was precipitated overnight from the aqueous phase at -80°C in one-eighth the volume of Na acetate pH 5.2 and twice the volume of cold 100% ethanol (these volumes are relative to the volume of the final aqueous phase obtained after extraction, which was typically 400 μL). The RNA pellet was recovered by spinning for 25 minutes in a

microfuge at top speed in the cold room. The pellet was then washed once with cold 80% ethanol, and air-dried for one hour. The pellet was then dissolved in fifty μL of T0.1E+0.1%SDS (w/v) for 30 to 40 minutes in a 65°C water bath.

Radioactively labeling probes for Northern blot. The probe for each gene examined was generated by PCR of yeast genomic DNA (Invitrogen) using a pair of gene-specific primers. See table II-4 for the sequences of the primers that were used to amplify each gene. Each reaction consisted of the following components: 1X PCR buffer II (Applied Biosystems); 1.5mM $MgCl_2$; 0.25μM forward primer; 0.25μM reverse primer; 0.2mM dNTPs; 8pg/μL yeast genomic DNA (Invitrogen); and Taq polymerase (made in our laboratory). The reaction conditions were the following: initial denaturation step for three minutes at 95ºC; 30 cycles of denaturation, annealing, and product extension; and a terminal extension step for five minutes at 72°C. Each cycle consisted of the following: denaturation for 30 seconds at 95ºC, annealing for one minute, and product extension for two minutes at 72°C. The annealing temperature varied for each primer pair; optimal annealing temperatures had been determined empirically for each primer pair. PCR was carried out using the BioRad iCycler. Each probe was purified by gel elution and phenol:$CHCl_3$ extraction from 16 PCR reactions, and quantitated by EthBr (1 μg/mL) staining of PCR product electrophoresed on a 1.2% agarose gel.

Table II-4. Sequences of primers used to amplify mRNAs of genes analyzed by Northern blot. The locus ID for each gene was obtained from the online Saccharomyces Genome Database. bp = base pairs.

Gene name	Locus ID	size of yeast mRNA (bp)	Sequence of forward primer	Sequence of reverse primer	size of probe (bp)
CLN2	YPL256C	1639	AAACGGTCAATGGTGTTCTACCC	CTATTTATGGTCCCAGTTGGCG	550
TOS4	YLR183C	1471	TCAGCACCATTACTGTAGGGCG	GTCTCAGGGTTTGTTCCTCGTG	657
GIC1	YHR061C	946	AGGAAAGAGGCTGCAACAGATG	CGCACTCAACTCTCTTGGCTTG	802
HCM1	YCR065W	1696	GGTAAGGGTCATTTCTGGGAGGTC	GGGGTTTTCTCTAAGCCATCGG	797
SWE1	YJL187C	2461	CGTCGCTAAACCTAACCAATCAGC	CTATGTGTTTGAGATGTTGCCCC	681
YHP1	YDR451C	1063	GACAATGCTCGGTTAGCTCGTC	TGAAAGAATTGAGATCGACCTCCC	553
SCR1	SCR1	522	AACAAATCCTTCCTCGCGGCTAGA	GAACGGCCACAATGTGCGAGTAAA	434

The PCR-generated probes were labeled with α^{32}P-dCTP by the Klenow fragment of DNA polymerase I. Each reaction consisted of the following components: 25ng of probe; 1x labeling buffer (10x labeling buffer from New England Biolabs); 20 μM each of dGTP, dCTP and dTTP (100 mM stocks from New England Biolabs); 2.5 μL of α^{32}P-dCTP (6000 Ci/mMol); one μL of Klenow fragment of DNA polymerase I (New England Biolabs); and nuclease-free water (Promega) to bring the final volume of the reaction to 50μL. The reactions were incubated at room temperature from five to seven hours. The reaction was terminated with addition of five μL of 0.5M EDTA pH8.0. Each reaction was purified by passing the reaction over a Sepahdex G-50 column. Each labeled probe was eluted with 300 μL of TE pH 8.0. Three hundred and fifty μL of each eluate was recovered and stored in the refrigerator overnight before use.

Northern blots. Denaturation mix consisted of the following: 66% (v/v) deionized formamide; 1.3x MOPS running buffer; and 8% formaldehyde**.** A formaldehyde-agarose gel consisted of the following: 0.6M formaldehyde; 1.5% agarose; and 1X MOPS running buffer. 10X MOPS running buffer consisted of the following: 0.2M MOPS; 50mM Na acetate; and 10mM Na_2EDTA. The pH of the buffer was adjusted to a pH of 7.0. 20X SSPE consisted of the following: 3.6M NaCl; 0.2M NaH_2PO_4; and 20mM NaEDTA. The pH of the buffer was adjusted to a pH of 7.2-7.4. Therefore, 5X SSPE was a 1:4 dilution of 20X SSPE in sterile water.

Hybridization solution consisted of the following: 5X SSPE; 5X Denhardt's solution; 0.1% (w/v) SDS; 50% (v/v) deionized formamide; and 30 μg/mL sonicated salmon sperm DNA. (5X Denhardt's solution was made according to the composition described in Molecular Cloning: A Laboratory Manual by Maniatis et al). Right before

adding the salmon sperm DNA, the DNA was heated in boiling H_2O for 7.5 minutes, chilled on ice for five to 7.5 minutes, and spun brielfy at 12krpm in the cold room to recover the condensate.

Concentrations of isolated RNA were determined by measuring A_{260} of duplicate samples. A sample for measurement consisted of either 2.5 µL or 1.3 µL of RNA diluted in 500 µL of nuclease-free water. A_{260} measurements of all samples were either 0.6 or less. Two hundred and twenty µg of RNA was then dissolved in denaturation mix to a final volume of 275 µL, heated in a 65°C water bath for 10 minutes, chilled on ice for 10 minutes, and spun briefly in the cold room to recover condensate. Twenty µg of each RNA was loaded onto a formaldehyde-agarose gel and electrophoresed for two to 2.5 hours at 120V in 1X MOPS running buffer. The gel was then rinsed in sterile water three times, 20 minutes per rinse. The gel, Hybond-N membrane (Amersham Biosciences), and filter papers were then incubated in 20X SSPE for 30 minutes. RNA was blotted onto the membrane in 20X SSPE for 12-14 hours by upward capillary transfer. Following transfer, the membrane was rinsed in 5X SSPE for 30 minutes and air-dried. The RNA was crosslinked to the membrane by UV (Auto function, UV Stratalinker 2400, 1200J). The membrane was then stained with 0.02%methylene blue/0.3M Na acetate pH 5.2, and scanned with a regular light scanner.

In parallel with the gel used in membrane transfer, another formaldehyde-agarose gel was loaded with RNA and electrophoresed as described above. Instead of undergoing membrane transfer, however, this gel was rinsed overnight with sterile water, stained with EthBr (1 µg/mL) for 30 minutes, rinsed with sterile water, and photographed under UV (Figure II-8).

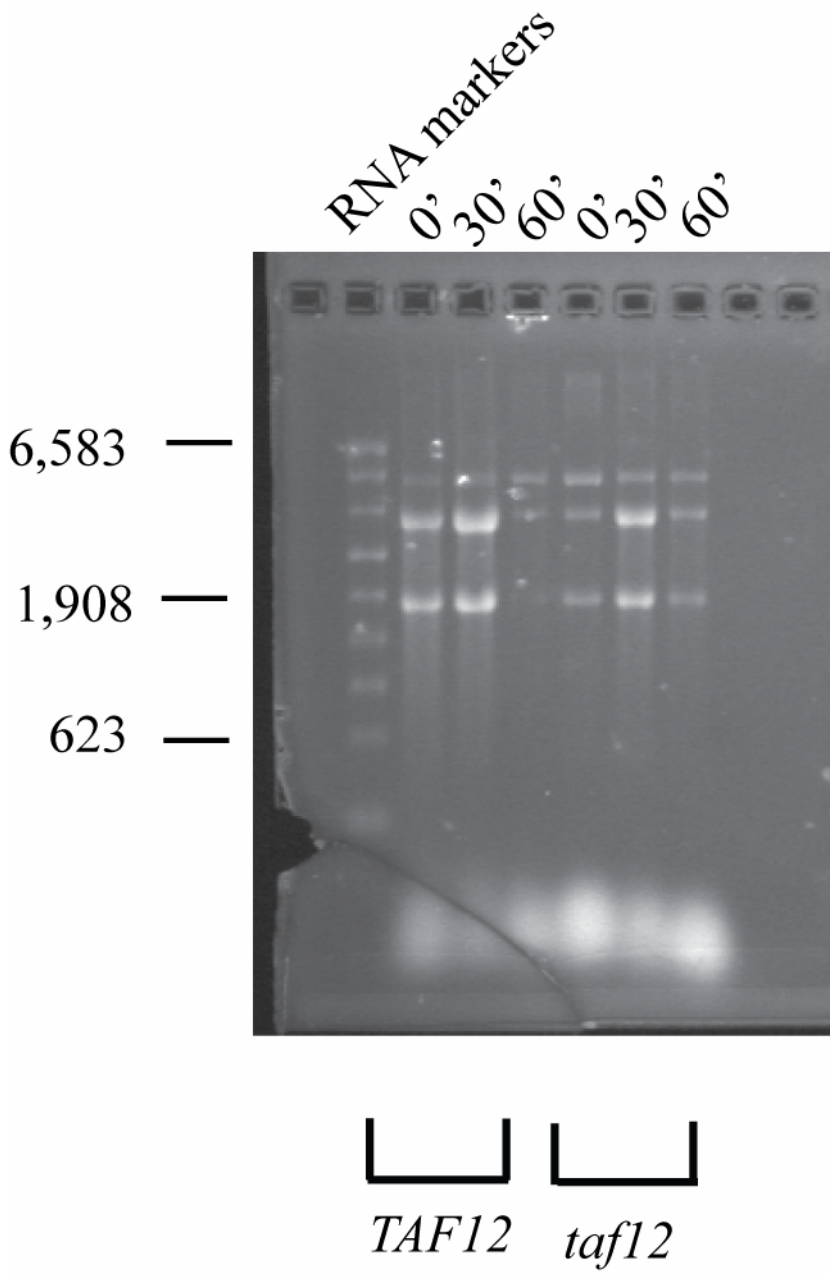

Figure II-8. The integrity of isolated RNA was determined by EthBr staining. RNA was isolated from different strains incubated at the permissive temperature (0') and at various times at the restrictive temperature (30', 60'). The (') symbol indicates minutes. *TAF12* = cognate strain of *taf12* ts strain; *taf12* = *taf12* ts strain. The numbers to the left are the sizes of the RNA markers, in base pairs.

Each membrane was incubated in 10 mL of hybridization solution for two and a half hours at 42°C. Right before adding to the hybridization solution, the radioactively labeled probe was heated in boiling H_2O for five minutes, chilled on ice for five minutes, and spun for 30 seconds at 12krpm in a microfuge in the cold room. Three hundred and fifty μL of radioactively labeled probe was added to the hybridization solution, and the membrane was incubated with probe for 21 hours in a 42°C hybridization oven. The temperature control was then turned off. When the oven temperature reached about 30°C, the membrane was washed twice with 2X SSPE/0.5%SDS (w/v) and then twice with 0.2X SSPE/0.5%SDS (w/v). The membrane incubated in the last wash solution as the oven temperature was brought back up to 42°C, and then the membrane was washed again twice with 0.2X SSPE/0.5%SDS. Temperature control was turned off, and the membrane was rinsed finally with 2X SSPE. In each wash, the membrane had been washed with 25 mL of wash buffer for 15 minutes, except for the last rinse, which had been for five minutes. The membrane was air-dried, enclosed in Saran Wrap plastic film, and exposed to a phosphorimaging K screen. The signals from the K screen were detected with an FX imager, and analyzed using Quantity One software.

Results

In vitro studies of protein-protein interaction

Far Western analyses of binding between yeast TFIID and SBF showed that SBF does indeed interact directly with a subset of $Taf_{II}s$ *in vitro* (Figure II-9a). SBF interacted most strongly with Taf12p/Taf8p, with weaker binding to Taf5p/Taf7p, Taf1p, and to

Taf4p. Unexpectedly, interaction with Taf9p was not detected. Due to gel resolution, Taf5p and Taf7p co-migrated as did Taf12p and Taf8p, so it was not clear from these results alone which Taf_{II} out of each pair was interacting directly with SBF.

As negative controls, experiments were performed in which either SBF or anti-Swi6p was omitted during the procedure (Figure II-9b). These controls verify that the interaction between SBF and the subset of yeast Taf_{II}s is real, rather than an artifact of interaction between TFIID and either the primary or secondary antibody.

Far Western analysis of SBF binding to all recombinant Taf_{II}s revealed results similar to those for TFIID purified from yeast (Figure II-10). SBF interacted with His_6-Taf12p, and also with His_6-Taf5p and His_6-Taf4p. However, no interaction between SBF and His_6-Taf1p and His_6-Taf7p was observed. Furthermore, the recombinant forms of those yeast TFIID subunits that did **not** interact with SBF (which includes Taf9p) also did **not** interact with SBF.

SBF probably does not interact with yeast Taf7p since SBF did not interact with His_6-Taf7p. Because recombinant Taf8p was unavailable and difficult to purify in sufficient quantities, I could not assay for direct interaction between SBF and recombinant Taf8p. However, SBF probably does not directly interact with yeast Taf8p since the specific activity of SBF binding to yeast Taf12p/Taf8p was equivalent to SBF binding to an amount of His_6-Taf12p that was equivalent to the amount of yeast Taf12p in the Far Western assay. If SBF also interacted directly with Taf8p, then one would expect that the specific activity of binding between SBF and His_6-Taf12p would be less than binding between SBF and yeast Taf12p/Taf8p. Finally, differences in post-translational modifications in yeast Taf1p and in His_6-Taf1p may explain why SBF was

a.

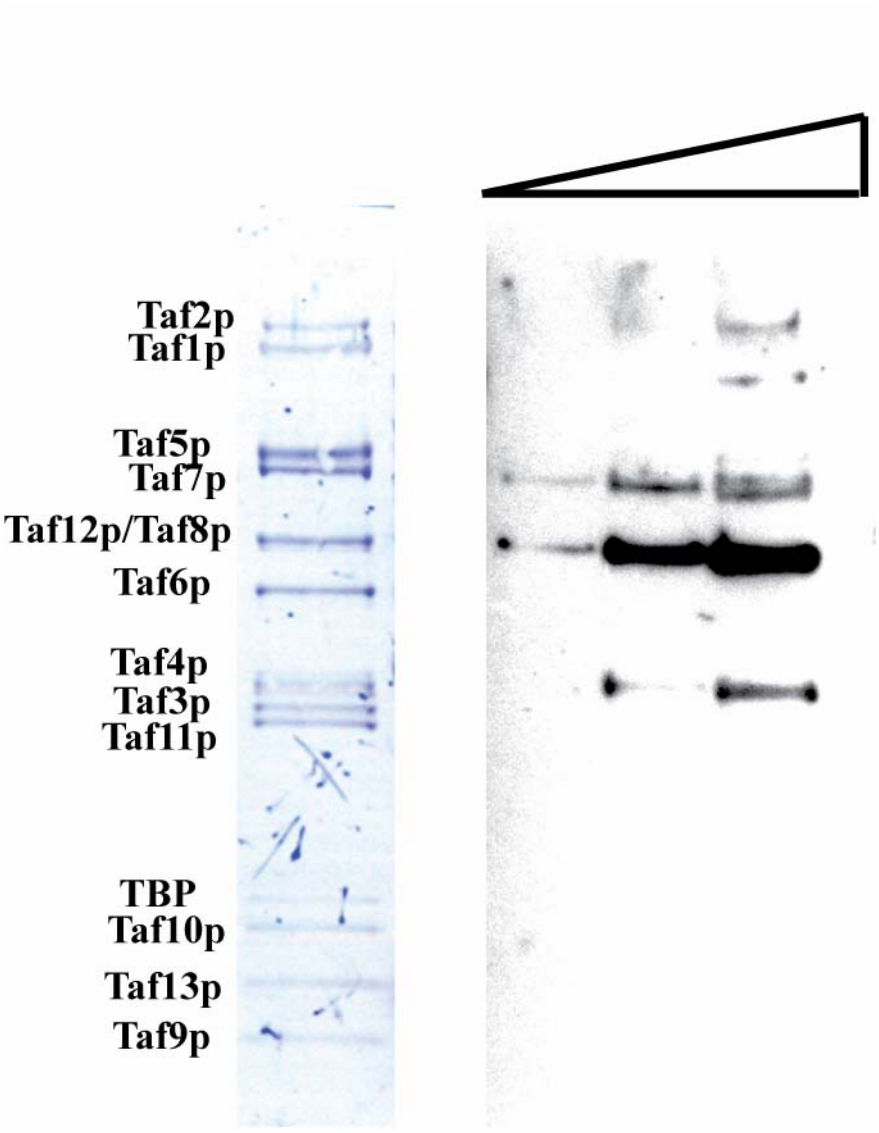
Taf2p
Taf1p
Taf5p
Taf7p
Taf12p/Taf8p
Taf6p
Taf4p
Taf3p
Taf11p
TBP
Taf10p
Taf13p
Taf9p

Figure II-9.

b.

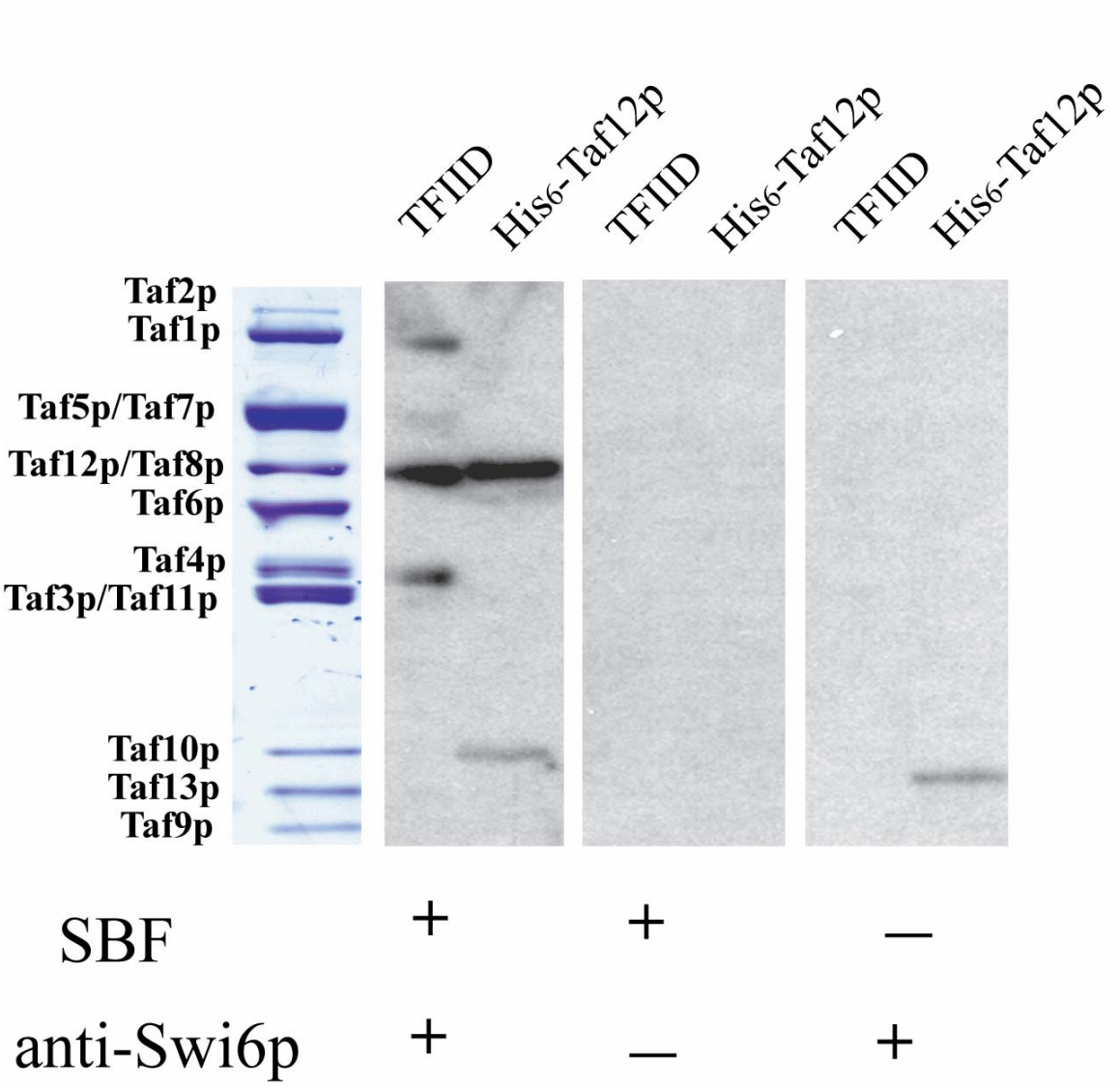

Figure II-9. SBF interacts *in vitro* with a subset of Taf_{II}s in yeast TFIID.
a. Shown is the result of a Far Western assay in which interaction was detected between SBF and yeast TFIID. From left to right, increasing amounts of TFIID were probed (0.8 µg, 1.6 µg, and 3.3 µg). Bound SBF was detected by polyclonal antibodies against Swi6p. To the far left is a Coomassie-stained strip of 2.3 µg of yeast TFIID.
b. (Far left) Coomassie stain of 2.4 µg of yeast TFIID separated by SDS-PAGE and immobilized on PVDF. (Second panel from the left) Interaction was detected between SBF and 1.6 µg of yeast TFIID. (Third and fourth panels from the left) results of the Far Western assay with either anti-Swi6p or SBF omitted during the procedure. The second through fourth panels also show the results of SBF interaction with recombinant His_6-Taf12p loaded in the lane adjacent to yeast TFIID.

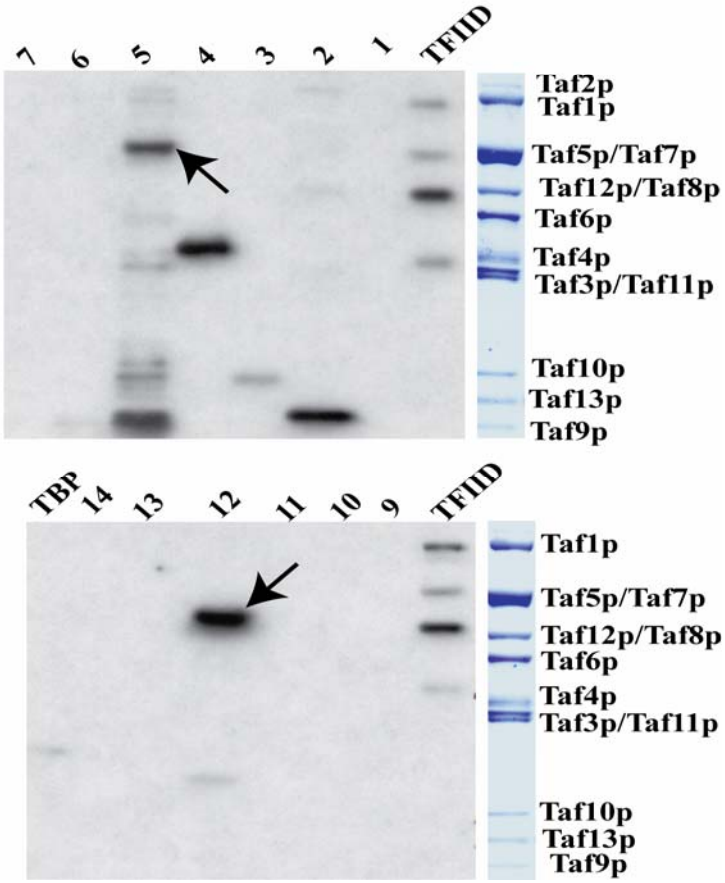

Figure II-10. SBF interacts with recombinant counterparts of most of the Taf_{II}s that it interacted with in the context of yeast TFIID. (Far right) Coomassie stain of yeast TFIID separated by SDS-PAGE and transferred to PVDF. (All other lanes) Far Western analysis of yeast TFIID and of the recombinant counterparts of all the TFIID subunits except Taf8p. The arrows indicate the full-length proteins in lanes in which more than one band is evident. The numbers across the top of each lane correspond to the various Taf_{II}s (1 = Taf1p; 2 = Taf2p, etc.)

able to interact with yeast Taf1p but not with the recombinant Taf1p, although the amount of His_6- Taf1p in these assays was equivalent to the amount of Taf1p in yeast TFIID. The observation that SBF bound to both the yeast and recombinant versions of a subset of Taf_{II}s suggests that the interaction between SBF and these Taf_{II}s is mediated by the primary amino acid sequence of these Taf_{II}s independent of any post-translational modifications.

The specificity of the interaction between SBF and the Taf_{II}s was determined through a series of competition assays. First, I demonstrated that a ten molar excess of recombinant His_6-Taf12p in solution could block interaction between SBF and the subset of interacting yeast Taf_{II}s (Taf12p, Taf4p, Taf1p, and Taf5p) identified previously (compare Figure II-9 and Figure II-10 with Figure II-11a). His_6-Taf12p could also block interaction between SBF and recombinant His_6-Taf12p that was immobilized on the membrane.

As a negative control, competition experiments were also performed with His_6-Taf6p; Taf6p had been shown not to interact with SBF in previous experiments (Figure II-9 and Figure II-10). A ten fold molar excess of His_6-Taf6p did not significantly impair interaction between SBF and His_6-Taf12p immobilized on the membrane (Figure II-11a). Also, binding between SBF and yeast Taf4p or yeast Taf1p was not significantly affected. However, there was some decrease in binding observed between SBF and yeast Taf12p immobilized on the membrane. Interestingly, this was accompanied by an increase in binding between SBF and yeast Taf5p. Nonetheless, it was obvious that, as a competitor, His_6-Taf12p was much more effective than His_6-Taf6p.

In another set of experiments, recombinant His_6-Taf12p in solution blocked SBF interaction with recombinant His_6-Taf12p bound to the membrane in a linear fashion, whereas recombinant His_6-Taf6p could not effectively compete with His_6-Taf12p bound to the membrane for binding to SBF (Figure II-11b).

Together, both sets of competition experiments indicate that the interaction between SBF and the Taf_{II}s is specific.

In vivo studies of Taf_{II} regulation of cell-cycle regulated genes

The expression of six cell-cycle regulated genes (*CLN2*, *TOS4*, *GIC1*, *HCM1*, *SWE1*, and *YHP1*) was examined by Northern blot in *swi6*Δ yeast at the permissive temperature, and in yeast harboring a ts allele of *TAF12* at both the permissive and restrictive temperatures (see Table II-5 for more details on these genes).

I focused further on Taf12p because Taf12p has been implicated as a coactivator for the mammalian transcription factor, ATF (29). Furthermore, Taf12p may mediate interaction between a yeast transcription factor, Gcn4p, and another coactivator complex, SAGA (30). Therefore, Taf12p may play an important role in mediating interaction between transcription factors and coactivators in general.

Expression of all genes was lower or even absent in *taf12* ts yeast relative to wild-type at the permissive temperature (Figure II-12). However, the effects of heat shock may not have been well controlled for in this experiment as there were changes in gene expression in *TAF12* wild-type yeast at the restrictive temperature (data not shown). Therefore, no definitive conclusions can be drawn. In future iterations of this experiment, controlling the temperature of the yeast cultures with a water bath may be better than

incubation in an air incubator for controlling effects of heat shock. Also, the time course of incubation at the restrictive temperature should be extended up to two hours, as it takes about this long for yeast to recover completely from heat shock.

Nonetheless, the observation that expression of all genes in the *taf12* yeast was significantly lower than in *TAF12* yeast at the permissive temperature suggests that expression of these genes is impaired in *taf12* yeast. Therefore, I conclude that all the genes that I tested are likely to be regulated by Taf12p. Interestingly, one of the genes identified was *CLN2*, which had already been shown to be dependent on another TFIID subunit, Taf1p (10). Furthermore, it has been recently shown by ChIP assay that Swi6p associates with the *CLN2* gene promoter in a cell cycle-dependent fashion (31).

I also compared expression of these genes in *swi6Δ* yeast and its cognate wild-type at the permissive temperature. I did not detect reduction in expression of any of the genes in *swi6Δ* yeast relative to wild-type (Figure II-13); some genes were even expressed at a higher level in *swi6Δ* relative to wild-type. In studying the literature, these results are not surprising. Other than the *HO* gene, the expression of several putative SBF-target genes showed only modest reduction, if at all, in asynchronous *swi6Δ* cultures (17, 22, 23, 24).

One possible mechanism for this modest effect is that Swi6p may play a limited role in gene expression in that it simply modulates the periodicity of gene expression but is not absolutely required for gene expression. Indeed, studies have shown that, in synchronized cultures of *swi6Δ* yeast, either the periodicity of expression of some genes is abolished or only the peak level of expression of some genes is dampened without any

a.

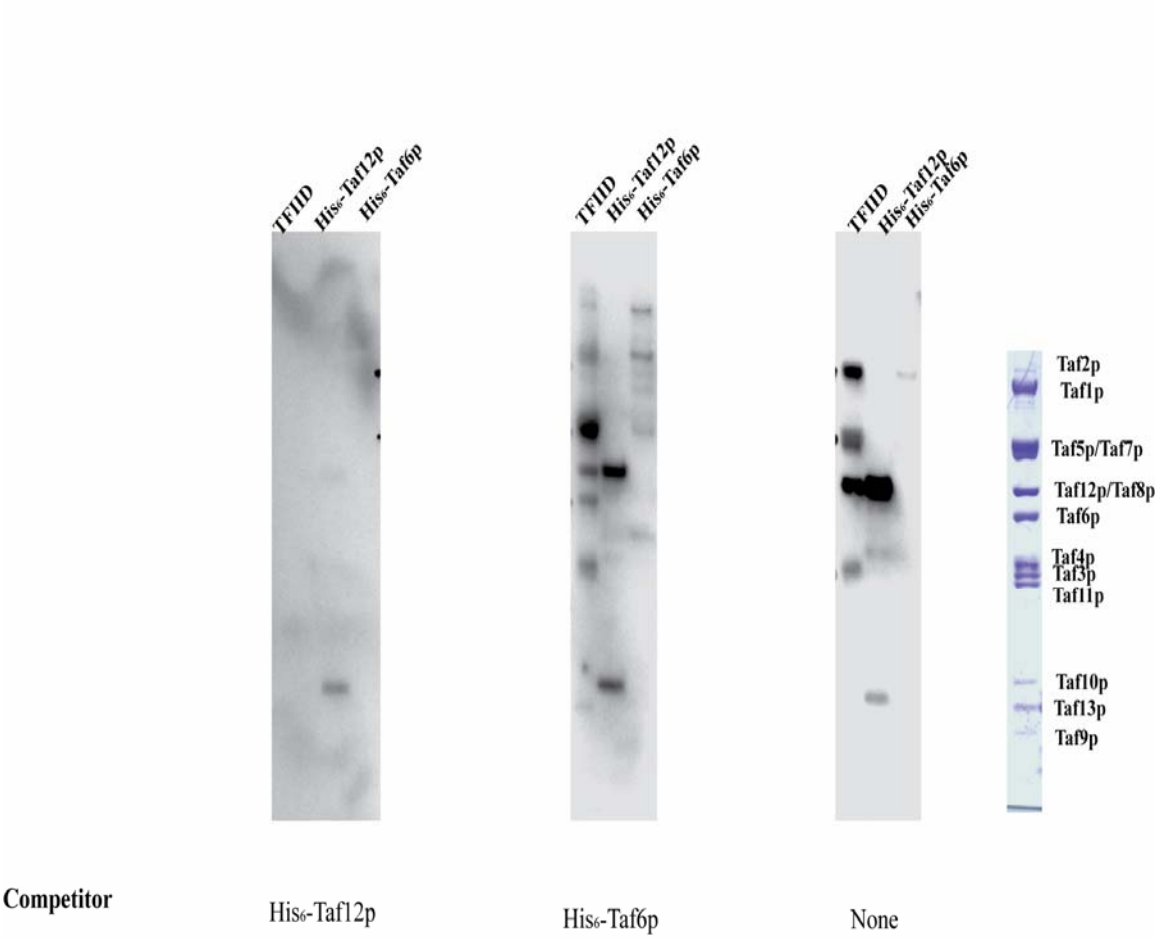

Figure II-11.

b.

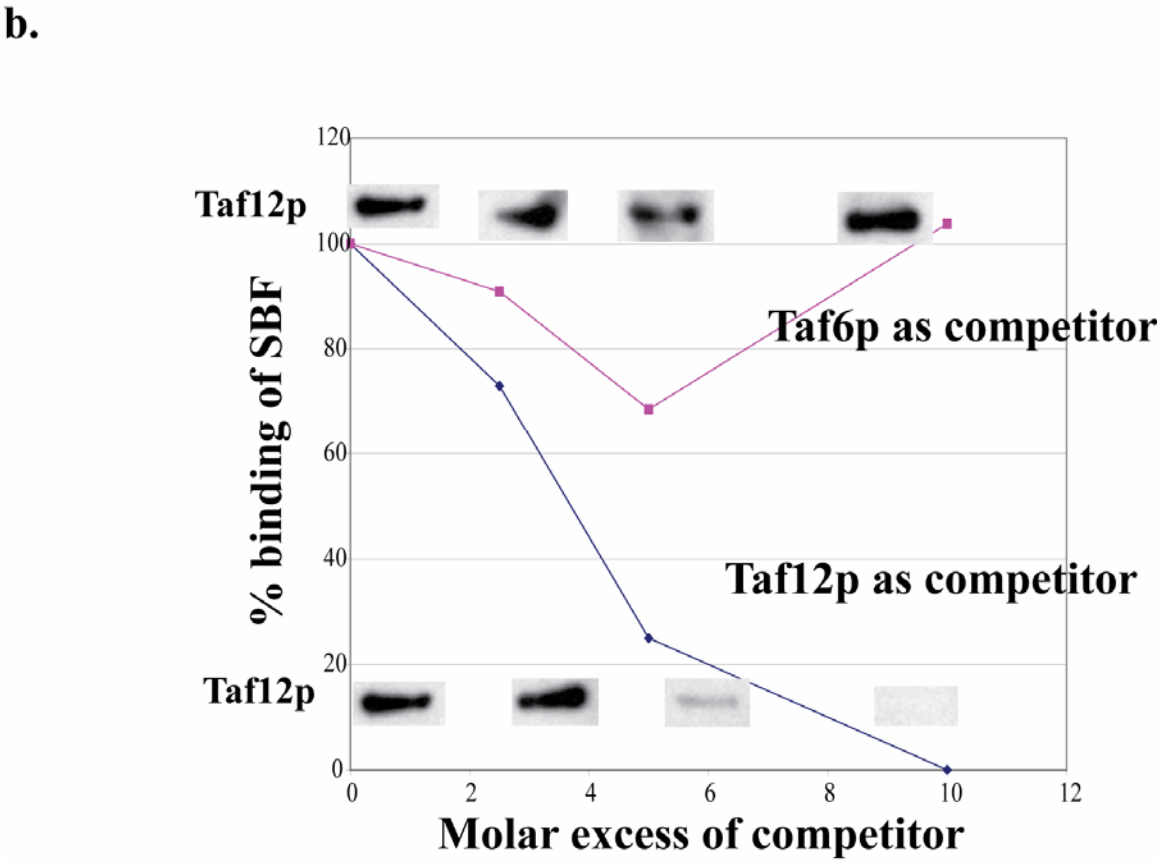

Figure II-11. Interaction between SBF and Taf_{II}s is specific.
a. His_6-Taf12p competes with yeast TFIID immobilized on PVDF for binding to SBF, whereas His_6-Taf6p could not compete effectively with immobilized yeast TFIID for binding to SBF. On the far right is a Coomassie-stained strip of yeast TFIID.
b. His_6-Taf12p competes with His_6-Taf12p immobilized on PVDF for binding to SBF, whereas His_6-Taf6p could not compete with immobilized His_6-Taf12p for binding to SBF.

Table II-5. Information on the cell cycle regulated genes that were assayed by Northern blot.

Gene	[1] Change in expression in *taf12* ts				[4]No. of mRNA copies in yeast cell	
cell cycle control	Fold change	[2]Presence of TATA box?	No. of SCBs and/or MCBs?	[3]Change in expression (log_{10}ratio) in *swi6* Δ	data from the lab of Patrick Brown	data from the lab of Richard Young
SWE1	-1.8	no	4	-0.026	1.2	0.4
CLN2	-1.1	yes	5	0.097	1.5	1.2
transcription factors						
HCM1	-2	no	15	-0.014	0.8	0.7
TOS4	-1.3	no	6	-0.078	1.6	0.6
YHP1	-1.2	yes	1	-0.375	1	0.6
cell wall						
GIC1	-4.1	no	2	-0.022	0.8	0.3

1. Online data for Lee et al. *Nature* , 2000, **405**: 701-704
2. Supplementary data from Basehoar et al. *Cell* , 2004, **116**: 699-709
3. Supplementary data from Hughes et al. *Cell* , 2000, **102**: 109-126
4. Online data: http://www-genome.stanford.edu/turnover/tresults.shtml

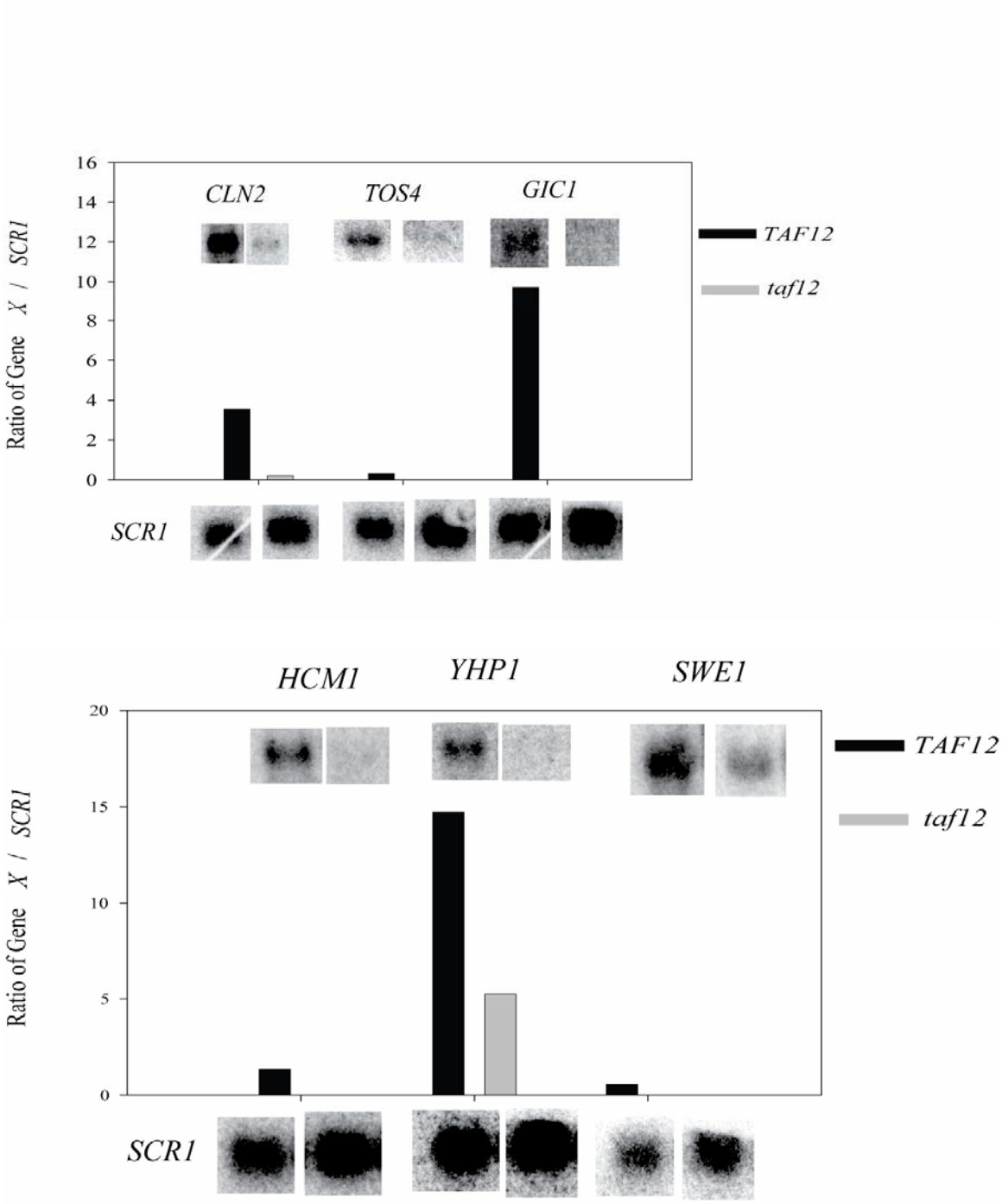

Figure II-12. Gene expression in a *taf12* ts mutant. mRNA levels of selected genes were analyzed by Northern blotting, and as shown here, normalized to levels of *SCR1*. Bars have been omitted for those data points for which RNA was not detectable (assume a value of zero for those data points).

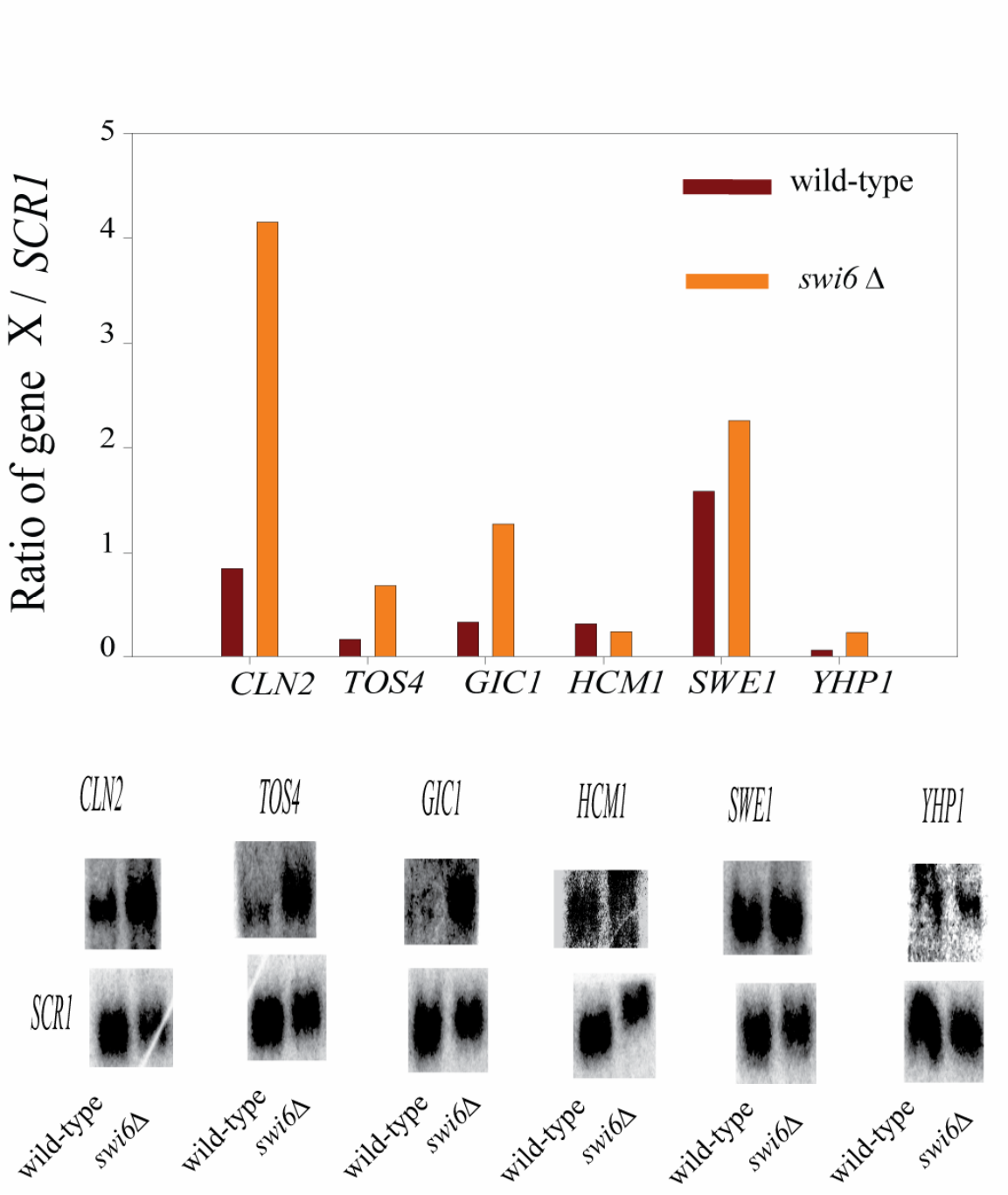

Figure II-13. Gene expression was not downregulated in a *swi6Δ* mutant relative to wild-type. mRNA levels of selected genes were analyzed by Northern blotting, and as shown here, normalized to levels of *SCR1*.

significant effect on expression itself (23). The net result would be a modest to no reduction in expression of otherwise Swi6p-regulated genes in asynchronous *swi6Δ* cultures.

Therefore, analysis of gene expression in synchronized cultures of *swi6Δ* yeast may be necessary to uncover a dependence on Swi6p.

Discussion

As discussed in the **Introduction** (**Chapter I**), one of the pressing questions in the field of TFIID biology is how exactly TFIID stimulates gene transcription *in vivo*. Based on experiments performed *in vitro*, the following model has been proposed: through direct, mutationally sensitive interactions with a subset of TFIID subunits, transcription factors recruit and/or stabilize TFIID occupancy of the gene promoter. Once localized to the promoter, TFIID, through the formation of the PIC, recruits RNA Pol II to the gene promoter, resulting in an increase in transcriptional output.

Through Far Western experiments, I have generated evidence of direct interaction between Swi6p and TFIID, specifically between SBF and a specific subset of Taf_{II}s (Taf12p, Taf4p, and Taf5p). In addition, through Northern blotting studies, I have generated evidence that one of these interacting Taf_{II}s, Taf12p, regulates expression of some putative Swi6p-target genes.

At this point, the data I have generated are consistent with a model in which Swi6p stimulates gene transcription by recruiting TFIID to the gene promoter through direct interactions between SBF and a subset of Taf_{II}s (Figure II-14).

One caveat of the Far Western assays is that it is not known which component of SBF, Swi6p or Swi4p, mediates direct interaction between the Taf_{II}s and SBF. Three scenarios can be envisioned: first, Swi6p mediates direct interaction between SBF and the Taf_{II}s; second, Swi4p mediates direct interaction between SBF and the Taf_{II}s; or, third, both Swi6p and Swi4p mediate direct interaction between SBF and the Taf_{II}s (Figure II-15a). However, it is also possible that, during the course of the experiment, SBF dissociates into its constituent subunits, Swi6p and Swi4p. Swi6p and Swi4p then each interact separately with either a redundant or separate subset of TFIID subunits (Figure II-15b).

Several questions regarding interaction between SBF and TFIID need to be answered. What is the form of Swi6p that is mediating interaction with Taf12p, Taf4p, and Taf5p? In other words, is it the intact SBF complex or Swi6p alone that is mediating interaction with these Taf_{II}s? Does Swi4p make any contacts on its own with other Taf_{II}s that were not detected in the Far Western assays (for example, Taf9p)? Do SBF and/or Swi6p interact with the intact TFIID complex? Preliminary results from a cryo electron microscopy (EM) analysis of interaction between SBF and TFIID indicate that interaction occurs between intact SBF and TFIID complexes (unpublished communications with collaborator, Patrick Schultz). However, it was not determined which subunit (Swi6p or Swi4p) mediated direct interaction with TFIID. Intriguingly, SBF contacted a subdomain of TFIID which contains Taf12p, Taf4p, Taf5p, and Taf9p.

The next step is to study TFIID occupancy *in vivo* on the promoters of Swi6p-regulated genes in wild-type yeast, and then ultimately, test how promoter occupancy of TFIID on these gene promoters is affected in yeast that express mutants of Swi6p that

could not interact with TFIID *in vitro*. Occupancy of promoters *in vivo* can be determined by chromatin immunoprecipitation (ChIP) analysis. However, one caveat of these studies is that any defect in TFIID occupancy may not be attributable, either entirely or in part, to defects in interaction with Swi6p alone as other transcription factors also regulate transcription of cell-cycle regulated genes. To circumvent this problem, it is suggested that TFIID occupancy be measured in synchronized yeast. Since transcription of cell-cycle regulated genes at the G_1/S phase transition is controlled by Swi6p (discussed in **Results**), one can predict that TFIID occupancy of cell-cycle regulated gene promoters in G_1/S phase will also be regulated by Swi6p. Therefore, one can predict that TFIID occupancy of these gene promoters will increase in the G_1/S phase transition in parallel with an increase in Swi6p occupancy. Finally, the increase in TFIID occupancy at the G_1/S phase transition would be diminished or abolished in yeast that express mutants of Swi6p that could not interact with Taf12p, Taf4p, and Taf5p *in vitro*.

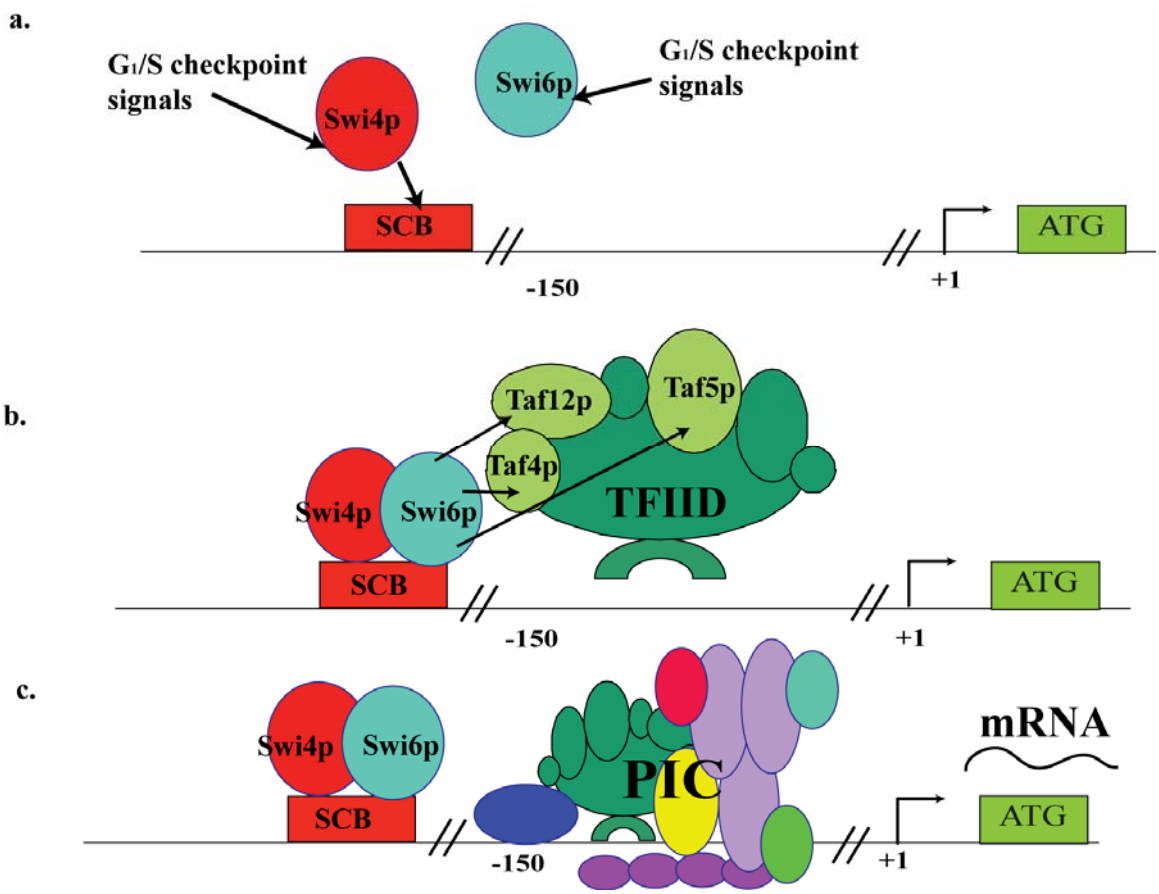

Figure II-14. Model of the mechanism by which TFIID may regulate the expression of cell-cycle regulated genes.
a. SBF (Swi6p and Swi4p heterodimer) binds to the promoters of its target genes in G_1 in response to G_1/S checkpoint signals.
b.Through direct interactions with a subset of Taf_{II}s, SBF recruits TFIID to the gene promoter.
c. Once at the promoter, TFIID nucleates the formation of the PIC, resulting in an increase in transcriptional output.

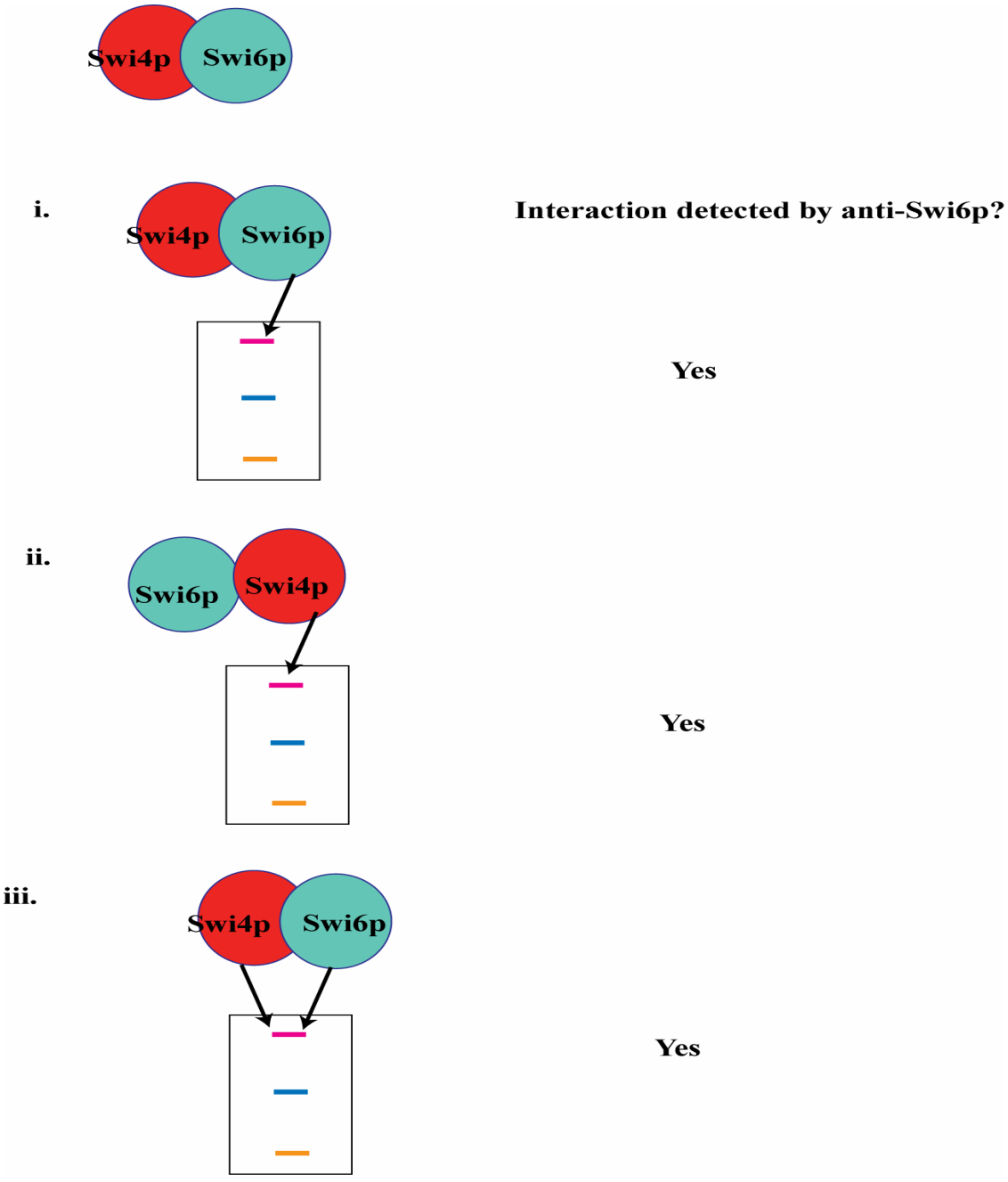

Figure II-15. Possible modes of interaction between SBF and Taf_{II}s.
a. Interaction occurs between SBF and Taf_{II}s.
i. Swi6p mediates interaction between SBF and Taf_{II}s.
ii. Swi4p mediates interaction between SBF and Taf_{II}s.
iii. Both Swi6p and Swi4p mediate interaction between SBF and Taf_{II}s.

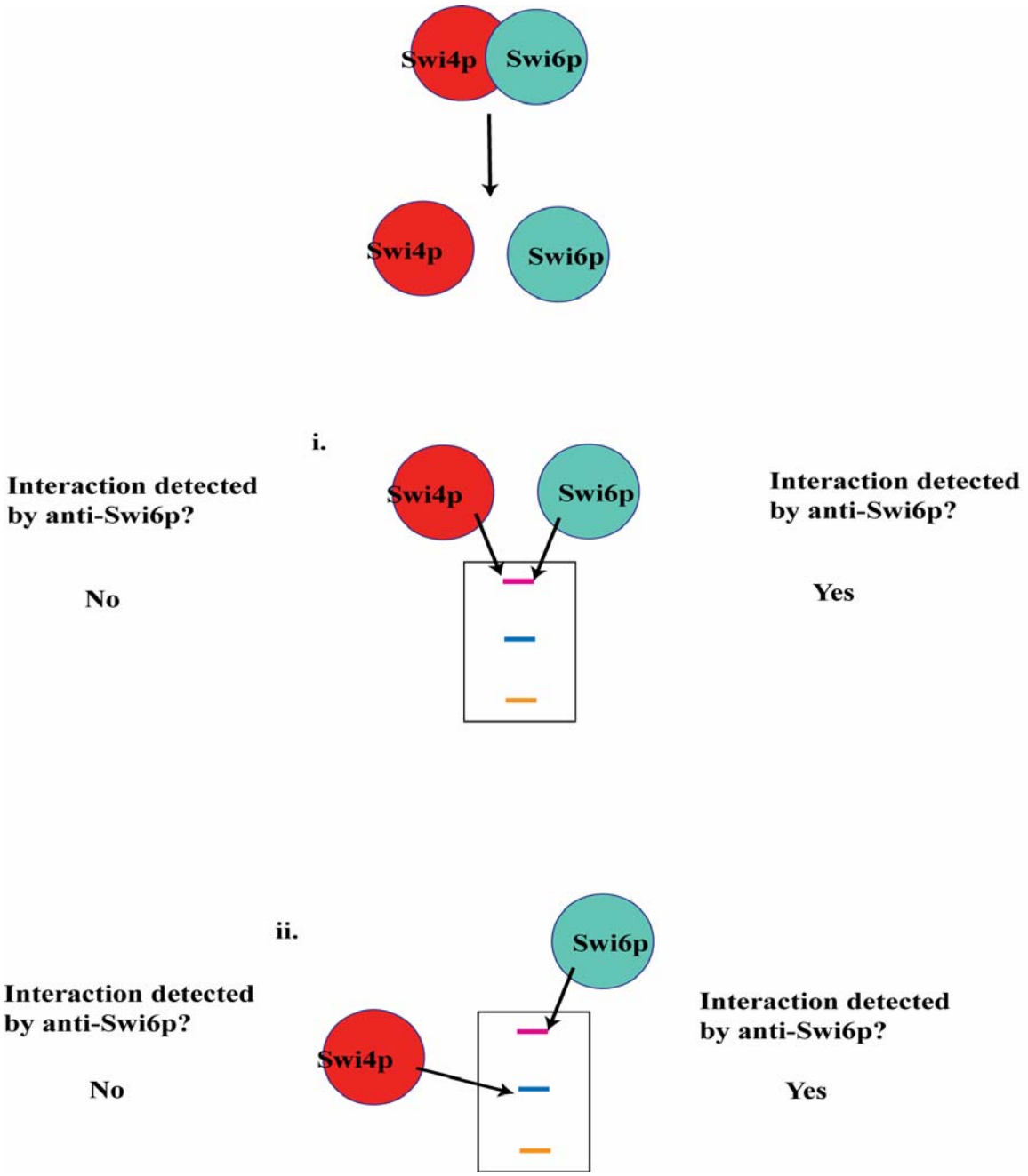

Figure II-15. Possible modes of interaction between SBF and Taf_{II}s.
b. During the course of the experiment, SBF dissociates into its constituent subunits, Swi6p and Swi4p. Swi6p and Swi4p then each interact with

i. a redundant subset of TFIID subunits, or

ii. a separate subset of TFIID subunits.

CHAPTER III

INVESTIGATING TAF9P AS A CANDIDATE FOR PROVIDING COACTIVATOR FUNCTION FOR SWI6P

As discussed in the **Introduction**, studies of yeast harboring the *taf9W133stop* mutation yielded two observations that supported a role for Taf9p as coactivator for Swi6p. First, the *taf9W133stop* mutation displayed a synthetic growth defect in combination with a *swi6Δ* mutation (18). Second, the association of Swi6p with a subset of Taf_{II}s (Taf12p, Taf8p, and Taf7p) in yeast WCE was disrupted in the *taf9W133stop* mutant (12). The simplest interpretation of these observations is that Taf9p mediates direct interaction between Swi6p and TFIID. If this were the case, then Taf9p would fulfill the first and essential criterion of a coactivator, which is that the coactivator and transcription factor must directly interact with each other.

To test for a direct interaction between Taf_{II}s and Swi6p, I studied interaction *in vitro* between all the TFIID subunits and Swi6p; these experiments are described in detail in **Chapter II**. I also tested for an interaction between Taf_{II}s and Swi6p *in vivo* through co-immunoprecipitation experiments; these experiments are discussed within this chapter.

The initial Swi6p-TFIID co-immunoprecipitation experiments were performed by Steven Sanders in our laboratory. Through these experiments, he found that Swi6p co-immunoprecipitated with some Taf_{II}s (Taf8p, Taf12p, and Taf7p) and that this association was disrupted in *taf9W133stop* yeast (12). These experiments, however, only indirectly assay possible interactions between Taf9p and Swi6p *in vivo*. Therefore, to

directly study interaction between Taf9p and Swi6p *in vivo*, I carried out co-immunoprecipitation experiments in which I immunoprecipitated Taf9p directly and probed for Swi6p in the immunoprecipitate. To obtain additional background information, I also repeated the initial experiments carried out by Steven Sanders.

Materials and Methods

Strains used in these studies

The *taf9W133stop* yeast and its cognate wild-type were obtained from the laboratory of Brenda Andrews. A member of our laboratory, Steven Sanders, tagged the *SWI6* allele in each yeast strain with a triple HA epitope at the C terminus. The 21R wild-type and 21R Taf9p-HA_3 strains were obtained from the laboratory of Karsten Melcher. Specific details are shown in Table III-1.

Co-immunoprecipitation analysis in wild-type and *taf9W133stop* yeast

Lysis buffer consisted of the following: 20mM HEPES pH 7.9; 10% glycerol (v/v); 150mM NaCl; 5mM DTT; 0.1% NP-40; one complete mini-protease inhibitor tablets (Roche) in ten mL of buffer; 2mM EGTA; 2mM EDTA; 5mM benzamidine; 2 μg/mL pepstatin; 5 μg/mL leupeptin; 5 μg/mL aprotinin; 12 μg/mL TPCK; 12 μg/mL TLCK; and 0.2 mM PMSF**.** Tris buffered saline with Tween-20 (TBS-T) consisted of the following: 25mM Tris-HCl pH 7.6; 150mM NaCl; and 0.05% Tween-20 (v/v). 20X Transfer buffer consisted of the following per liter of buffer: 81.6 g bicine; 104.8 g bis-Tris; 6.0 g EDTA; and 0.2g chlorobutanol

Table III-1. Yeast strains used in immunoprecipitation studies. Shown is strain information for the yeast strains that harbor the *taf9W133stop* or *swi6Δ* mutation or that express Taf9p-HA_3.

Strain	Genotype	Source
YSLS163	*Matα ura3-52 lys2-801 ades-107 TRP1 his3Δ200 leu2Δ1 SWI6::HA $_3$-KAN^r*	Tony Weil lab
YSLS164	*Matα slm7-1(taf17W133^{amber}) SWI6::HA $_3$-KAN^r TRP1 ura3 leu2 lys2 ade2*	Tony Weil lab
21R Melcher WT	*MATa ura3-52 leu2-3, 221 ade1 MEL1*	Karsten Melcher lab
21R-TAF17HA $_3$	*MATa ura3-52 leu2-3, 221 ade1 MEL1 TAF9-HA $_3$*	Karsten Melcher lab
swi6Δ	*MATa leu2Δ0 ura3Δ0 his3Δ1 LYS2 met15Δ0 swi6::KAN^r*	Andrew Link lab

Stripping solution consisted of the following: 2% SDS (w/v), 30mM Tris acetate pH 6.7, and 100mM β-mercaptoethanol.

Each strain was grown as follows: yeast were streaked from frozen glycerol stocks onto a YPAD plate containing G418 and incubated at 30ºC for two to four days. A single colony from the plate culture was inoculated into a starter culture of 7mL YPAD/G418 and incubated, with shaking at 250rpm, at 30ºC until the culture became saturated. A starter culture was inoculated into 200 mL of YPAD so that the starting OD_{600}/mL was about 0.125 OD_{600}/mL. The 200mL culture was incubated at 30ºC, with shaking at 250rpm, until the culture reached an OD_{600}/mL of about 1.3-2.4 OD_{600}/mL. Four 50mL-aliquots were collected in 50mL-conical tubes (Falcon) and harvested by centrifugation in a Beckman centrifuge for 10 minutes at 4°C. Each pellet was washed once with 25 mL of cold sterile water. Each pellet was suspended in one mL of PBS (made according to composition in Molecular Cloning: A Laboratory Manual by Maniatis et al), transferred to 1.5mL-screw top tubes (Sarstedt) and pelleted by spinning for three minutes at 6500 rpm in a microfuge. The supernatant was discarded, the pellet was frozen on dry ice, and stored at -70 to -80°C.

Each yeast cell pellet was thawed in the cold room. Each pellet was beat with a mini-bead beater in 600 μL of lysis buffer and 500 μL of glass beads in the cold room. The cells were beat for a total of seven cycles, with each cycle consisting of beating for 1.5 minutes followed by a two-minute incubation on ice. Five μL of each lysate were examined under an Olympus microscope, and the lysis efficiency, as determined by visual inspection, was over 95%. Four hundred μL of WCE were obtained from each lysate by spinning the lysates for ten minutes at 14krpm in the cold room. Each WCE was

pre-cleared with 175 μL of a 1:1 slurry of Protein A sepharose in lysis buffer for five minutes on a tiltboard in the cold room. Four hundred and eighty μL of each pre-cleared WCE were obtained by spinning for two minutes at 6krpm in the cold room. The protein concentration of pre-cleared WCEs was determined by Bradford assay, using BSA (1.8-25 μg/mL) as a standard.

Anti-Taf12p immunoprecipitations. Each immunoprecipitation consists of the following: 550 μg of pre-cleared WCE, 0.025 μg/ μL EthBr, antibody, and lysis buffer to bring the final volume of the reaction to 200 μL. The antibodies consisted of one of the following: ten μg of 12CA5 cross-linked to Protein A sepharose beads, 10.5 μg of nonspecific rabbit IgG cross-linked to Protein A sepharose beads, and ten μg of free polyclonal anti-Taf12p. In those immunoprecipitations containing free antibody, five μL of Protein A sepharose were added. Immunoprecipitations were generally incubated on a tiltboard in the cold room for 14 hours (overnight), except for one set of experiments in which the immunoprecipitations were incubated for seven hours. The shorter duration of the reaction did not affect the co-immunoprecipitation of Swi6p with Taf12p. Immunoprecipitates were harvested by a one minute spin at 12krpm in the cold room. Each immunoprecipitate was washed three times with lysis buffer, 500 μL of lysis buffer per wash.

Anti-Taf4p immunoprecipitations. Swi6p was not detected in the anti-Taf4p immunoprecipitate when the experiment was performed as described above for anti-Taf12p immunoprecipitations, so the reaction was scaled up and the experiment was performed as described in this section. Each immunoprecipitation consisted of 950 μg of pre-cleared WCE, 0.025 μg/ μL EthBr, antibody, and lysis buffer to bring the final

volume of the reaction to 400 µL. Each reaction contained 20 µg of either polyclonal anti-Ta4p or nonspecific rabbit IgG (both were cross-linked to CNBr-activated sepharose beads). Immunoprecipitations were incubated for 16 hours (overnight) in the cold room on a tiltboard. Immunoprecipitates were harvested with a one minute spin in the cold room at 12krpm, and each immunoprecipitate was washed twice with lysis buffer, 700 µL of buffer each wash.

SDS-PAGE analysis and immunoblot of immunoprecipitations. The immunoprecipitate was solubilized in LDS PAGE sample buffer for ten minutes in a boiling water bath or in a 100°C heating block, cooled at room temperature for ten minutes, and spun briefly at 12krpm to recover condensate. Inputs and portions of the immunoprecipitates were subjected to SDS-PAGE analysis. Samples were loaded on a 4-12% gradient bis-Tris gel, and run in 1xMOPS-SDS running buffer for 50 minutes to one hour at 200V. Proteins were electroblotted onto PVDF (0.45 µM) for two hours at 12V in 1x transfer buffer/10% methanol (v/v). Membranes were blocked in 10% milk/TBS-T for one to two hours at room temperature, and incubated in primary antibody overnight on a tiltboard in the cold room. Antibodies used in detection were: polyclonal anti-Taf11p (1:5000 or 1:3300); anti-HA cross-linked to HRP (1:2000); polyclonal anti-Taf12p (1:10,000); polyclonal anti-Taf4p (1:2500); and polyclonal anti-Swi6p (1:5000). All blots, except those probed with anti-HA HRP, were rinsed once in 1% milk/TBS-T, washed three times in TBS-T, and incubated with goat anti-rabbit Fab cross-linked to HRP, 1:20,000 in 1% milk/TBS-T, for 30 minutes at room temperature. Then, all blots, including those probed with anti-HA HRP, were rinsed and washed as described above. Protein was visualized with enhanced chemiluminescence, and signals were either

detected directly with a ChemiDoc XRS scanner or by exposure to Kodak BioMax Light film.

Some blots probed with anti-Swi6p and anti-HA HRP were stripped and re-probed with either polyclonal anti-Swi6p at a higher concentration (1:3300) or with a fresh lot of anti-HA cross-linked to HRP at 1:2000. The blots were stripped in stripping solution for 30 minutes in a 65°C water bath and washed four times with TBS-T. The stripped blots were then probed with primary antibody and processed as described above.

Films of immunoblots were scanned with a regular light scanner. Scanned films or blots detected directly with a ChemiDoc XRS scanner were analyzed in Quantity One software (Biorad) with the volume rectangle tool. Immunoprecipitation efficiency was calculated for a given protein as follows: immunoprecipitation efficiency of protein X = {100/% of immunoprecipitate subjected to immunoblot * [(adjusted volume of protein X in immunoprecipitate /adjusted volume of protein X in input)* %input]}. If, for a given protein, there was any background signal detected in the negative control (the rabbit IgG immunoprecipitations), then the adjusted volume of this background signal was first subtracted from the adjusted volume of the signal detected in the anti-Taf_{II} immunoprecipitations; this corrected value was then used instead in the formula described above.

SDS-PAGE analysis of total protein in WCE. Pre-cleared portions of yeast WCE were subjected to SDS-PAGE analysis as described above, and the resulting gel was either stained with Coomassie or with Sypro Ruby.

Coomassie staining was performed as follows: the gel was stained with microwave-heated Coomassie stain (0.05% w/v Coomassie Blue R-250 in 10% v/v acetic acid and 25% v/v isopropanol) for 40 minutes, and destained twice (40 minutes per incubation) with 40%v/v methanol and 10%v/v acetic acid. The gel was scanned with a regular light scanner, lane analysis was performed with Quantity One software, and lane intensities were plotted with Microsoft Excel.

Sypro Ruby staining was performed as follows: the gel was fixed twice in 50% methanol(v/v)/7% acetic acid (v/v) (15 minute each incubation), stained with Sypro Ruby protein gel stain (Molecular Probes, Invitrogen) overnight for 22 hours, and destained with 10% methanol (v/v)/7% acetic acid (v/v) for 30 minutes. The gel was then scanned with a Molecular Imager FX scanner. The gel was analyzed further in Quantity One with a volume rectangle tool. The entirety of each lane had been enclosed in volume boxes of equivalent length and width.

Growth curve analysis of wild-type and *taf9W133stop* yeast

Yeast cells were streaked and incubated on YPAD plates containing G418 at 30°C for three days. Cells from the following glycerol stocks were streaked on separate plates: the lab cognate wild-type stock, my own cognate wild-type stock derived from the lab wild-type stock, the lab *taf9W133stop* stock, and my own *taf9W133stop* stock derived from the lab *taf9W133stop* stock. Single colonies from each plate were inoculated in

separate, 5mL-YPAD starter cultures containing G418. Four wild-type colonies were inoculated in separate liquid cultures (two colonies per glycerol stock), whereas 20 *taf9W133stop* clones were inoculated in separate liquid cultures (10 colonies per glycerol stock). These cultures were grown to saturation. For each clone, two OD of the starter culture was inoculated into 15 mL of fresh liquid YPAD media. Immediately after inoculation, the initial OD_{600} of each 15mL-culture was measured with duplicate samples. The 15mL-cultures were then grown at 30°C, with shaking at 200rpm. The growth of the culture was monitored by OD_{600}. At each time point, measurements of duplicate samples of each culture were taken. Initially, measurements were taken of samples of culture without dilution, but when readings of the culture surpassed a value of 1, measurements were taken of a sample of the culture that had been diluted 1:10 in YPD.

Co-immunoprecipitation analysis in 21R wild-type and 21R Taf9p-HA_3 yeast strains

Lysis buffer consisted of the following: 20mM HEPES pH 7.9; 10% glycerol (v/v); 300mM or 150mM NaCl; 1mM DTT; 0.1% NP-40; and one complete mini-protease inhibitor tablet (Roche) per ten mL of buffer. Stripping solution consisted of the following: 2% SDS (w/v), 30mM Tris acetate pH 6.7, and 100mM β-mercaptoethanol. Tris-buffered saline with Tween-20 (TBS-T) consisted of the following: 25mM Tris-HCl pH 7.6; 150mM NaCl; and 0.05% Tween-20 (v/v). 20X Transfer buffer consisted of the following per liter of buffer: 81.6 g bicine; 104.8 g bis-Tris; 6.0 g EDTA; and 0.2g chlorobutanol

Each strain was grown as follows: yeast were streaked from frozen glycerol stocks onto YPAD plates containing G418 (21R Taf9p-HA_3) or YPAD alone (21R wild-

type) and incubated at 30ºC for about a day and a half. A single colony from the plate culture was inoculated into a starter culture of 5mL YPAD and incubated, with shaking at 250rpm, at 30ºC until the culture became saturated. A starter culture was inoculated into 100 mL of YPAD so that the starting OD_{600}/mL was about 0.125 OD_{600}/mL. The 100mL culture was incubated at 30ºC, with shaking at 250rpm, until the culture reached an OD_{600}/mL of about 1.3-1.5 OD_{600}/mL. Two 50mL-aliquots were collected in 50mL-conical tubes (Falcon) and harvested by centrifugation in a Beckman centrifuge for 10 minutes at 4°C. The pellets were washed once with 25 mL of cold phosphate buffered saline (PBS). Each pellet was suspended in one mL of PBS, transferred to 1.5mL-screw top tubes (Sarstedt) and pelleted by spinning for three minutes at 6500 rpm in a microfuge. The supernatant was discarded, the pellet was frozen on dry ice, and stored at -70°C.

WCE was obtained from each cell pellet as follows: the cell pellet was thawed on ice from -70°C, and then beat with a mini-bead beater with 500 µL of glass beads and 600 µL of lysis buffer (containing 300mM NaCl) in the cold room. The cells were beat for a total of four cycles, with each cycle consisting of beating for 30 seconds, followed by incubation on ice for two minutes. The pellets were then agitated for 30 minutes in an IKA-Vibrax-VKR vibrator in the cold room at a setting of 2200. The pellets were beat again with a bead beater as described above for two additional cycles. Finally, the pellets were agitated in the vibrator as described above for an additional 15 minutes. Five µL of each lysate were examined with an Olympus light microscope, and the lysis efficiency was determined by visual inspection to be over 90-95%. Four hundred µL of WCE was obtained by spinning the lysate for 10 minutes at 14krpm in the cold room in a

microfuge. The WCE was then pre-cleared with 175 μL of a 1:1 slurry of Protein A Sepharose in lysis buffer for five minutes on a tiltboard in the cold room. Four hundred and eighty μL of pre-cleared WCE was obtained by spinning for two minutes at 6krpm in the cold room. The protein concentration of the pre-cleared extract was measured by Bradford assay. BSA, over a concentration range of 2μg/mL-20 μg/mL, was used as a standard in the Bradford assay.

Each immunoprecipitation consisted of the following: 540 μg of pre-cleared WCE, antibody, 0.025 μg/ μL EthBr, and lysis buffer to bring the final volume of the reaction to 200 μL. The antibody used was 12 μg of 12CA5 antibody cross-linked to agarose. As a negative control, some immunoprecipitations were performed without antibody; in these reactions, five μL of Protein A-sepharose were added instead. In addition, the lysis buffer added to raise the volume of each reaction had a NaCl concentration of either 300mM or 150mM.

In general, the immunoprecipitations were incubated for 14-20 hours (overnight) in the cold room on a tiltboard. The pellets were harvested by a rapid one minute spin in the microfuge. The pellets were then washed three times with lysis buffer, 500 μL each wash. The pellet was then suspended in LDS PAGE sample buffer, and heated in a 75°C heating block for five minutes. The samples were cooled for five minutes at room temperature, and spun briefly in a microfuge at room temperature to bring down condensate. A portion of the immunoprecipitates was then analyzed by SDS-PAGE followed by immunoblot.

SDS-PAGE analysis and immunoblot of immunoprecipitations. Portions of pre-cleared WCE (inputs) and of the LDS-solubilized immunoprecipitates were analyzed further by SDS-PAGE and immunoblot. Each input consisted of an amount that was equal to 1% of the total protein that was subjected to immunoprecipitation. Inputs and immunoprecipitates were electrophoresed on a 4-12% gradient bis-Tris gel for one hour at 200V. Protein was electroblotted onto a 0.45μM PVDF membrane in 1x transfer buffer/10% methanol (v/v) for over two hours at 12V. The membrane was blocked for two hours in 10% nonfat milk/TBS-T and incubated with polyclonal anti-Swi6p (see **Chapter II**) at 1:5000 in 1% milk/TBS-T overnight in the cold room. The blots were then rinsed three times with TBS-T, incubated with goat anti-rabbit Fc cross-linked to horseradish peroxidase (HRP) for 45 minutes, and rinsed again with TBS-T three times. The protein was visualized with enhanced chemiluminescence and the images were detected by exposure of the membrane to Kodak BioMax Light film.

Blots probed with anti-Swi6p were stripped and re-probed with either polyclonal anti-Taf8p at 1:10,000 or anti-HA cross-linked to HRP at 1:2000. The blots were stripped in stripping solution for 40 minutes in a 65°C water bath and washed four times with TBS-T. The stripped blots were then probed with primary antibody and processed as described above, except that the blots were incubated with primary antibody at room temperature for four to seven hours, and the anti-HA blots were not incubated with secondary antibody.

Films of immunoblots were scanned with ChemiDoc XRS and analyzed in Quantity One software (Biorad) with the volume rectangle tool. Immunoprecipitation

efficiency was calculated for a given protein as follows: immunoprecipitation efficiency of protein X = {100/% of immunoprecipitate subjected to immunoblot * [(adjusted volume of protein X in immunoprecipitate/adjusted volume of protein X in input) * %input]}

Results

Swi6p interaction with Taf_{II}s in *taf9W133stop* yeast

The initial Swi6p-TFIID co-immunoprecipitation experiments were performed by Steven Sanders in our laboratory. Through these experiments, he found that Swi6p co-immunoprecipitated with some Taf_{II}s (Taf8p, Taf12p, and Taf7p) and that this association was disrupted in *taf9W133stop* yeast (12).

I successfully repeated the experiment with polyclonal anti-Taf12p antibodies. In addition, I modified the experimental procedure, using a much lower concentration of salt (150mM NaCl) than had been used by Sanders (300mM potassium acetate). Under these mild salt conditions, I found that polyclonal antibodies raised against Taf12p were able to specifically immunoprecipitate Swi6p as well as another TFIID subunit, Taf11p, from yeast WCEs. Furthermore, interaction between Swi6p and Taf12p was disrupted in *taf9W133stop* yeast. However, the interaction between Taf12p and Taf11p was not disrupted in this mutant (Figure III-1). These results are in agreement with what has been previously published (12). My co-immunoprecipitation results also suggest that the association between Taf12p and Swi6p is sub-stoichiometric since the efficiency by which anti-Taf12p antibodies can co-immunoprecipitate Swi6p is 3.5-5% in the wild-type

strain. The immunoprecipitation efficiency, with respect to Taf12p, was 38%, so that the low levels of Swi6p detected in the immunoprecipitate may not likely be attributed to insufficient capture of antigen. Furthermore, the immunoprecipitation efficiency, with respect to Taf12p, was similar in the *taf9W133stop* WCEs, at 34%. Lastly, as indicated by the inputs, the expression levels of the Swi6p and of Taf12p were similar between wild-type and mutant WCEs.

The results of these experiments are consistent with the interpretation that the *taf9W133stop* mutation decreases the affinity of TFIID for interaction with Swi6p. However, I made some other observations that led me to revise this interpretation.

First, I soon discovered that the observation that the Swi6p-Taf_{II} interaction was disrupted in *taf9W133stop* yeast was not reproducible. In further repeats of the anti-Taf12p immunoprecipitation, I observed that interaction between Swi6p and Taf12p in *taf9W133stop* yeast WCEs was similar to wild-type (Figure III-2). Anti-Taf12p was able to co-immunoprecipitate Swi6p with an efficiency of 6% in the wild-type and 4.5% in the mutant. Again, as indicated by the inputs, the expression level of Swi6p-HA_3 in wild-type and mutant input WCEs was the same.

Second, I isolated a *taf9W133stop* mutant clone that expressed lower levels of Taf_{II}s and Swi6p relative to wild-type. In another repeat of this experiment, I had successfully co-immunoprecipitated Swi6p with polyclonal anti-Taf4p antibodies in wild-type yeast (Figure III-3). I found that, in one mutant clone (mutant B), the co-immunoprecipitation of Swi6 was unaffected, whereas, in a second mutant clone (mutant A), the co-immunoprecipitation of Swi6p was reduced. But, most importantly, the expression levels of Taf4p and of Swi6p were also reduced in the inputs in mutant A

relative to wild-type. The level of Swi6p in mutant A was 26% of wild-type, and Taf4p was not even detected in the input in mutant A. I observed that the level of another Taf_{II}, Taf12p, was reduced as well, with a mutant level that was 21% of wild-type (Figure III-3a, b). In contrast, the expression of Swi6p and Taf_{II}s in mutant B was similar to wild-type.

Also, analysis of the growth curves revealed that, at the permissive temperature, mutant A grew slower wild-type and mutant B (Figure III-3c). This was the first time I had isolated a mutant clone that grew slower than wild-type; previously, I had noted that the *taf9W133stop* yeast always grew at a rate similar to wild-type. However, the original description of *taf9W133stop* yeast by the Andrews lab had also noted that the mutant grows slower than wild-type at permissive temperature (18).

To summarize, I have observed three phenotypes of the *taf9W133stop* mutant. In one phenotype (type A), interaction between Swi6p and the Taf_{II}s are reduced, the expression levels of Swi6p and some of the Taf_{II}s are reduced, and the growth rate is slower than wild-type. In the second phenotype (type B), interaction between Swi6p and Taf_{II}s is intact, and the expression levels of Swi6p and some of the Taf_{II}s and the growth rate is similar to wild-type. In the third phenotype (type C), interaction between Swi6p and Taf_{II}s is reduced, but the expression levels of Swi6p and some of the Taf_{II}s and the growth rate is similar to wild-type. See Table III-2 for a summary of the various phenotypes of the *taf9W133stop* mutant.

I hypothesized that the most severe phenotype of mutant A was the result of the *taf9W133stop* mutation alone, whereas phenotypes of mutant B and C were the result of the *taf9W133stop* mutation and mutations that were acquired during logarithmic growth. I

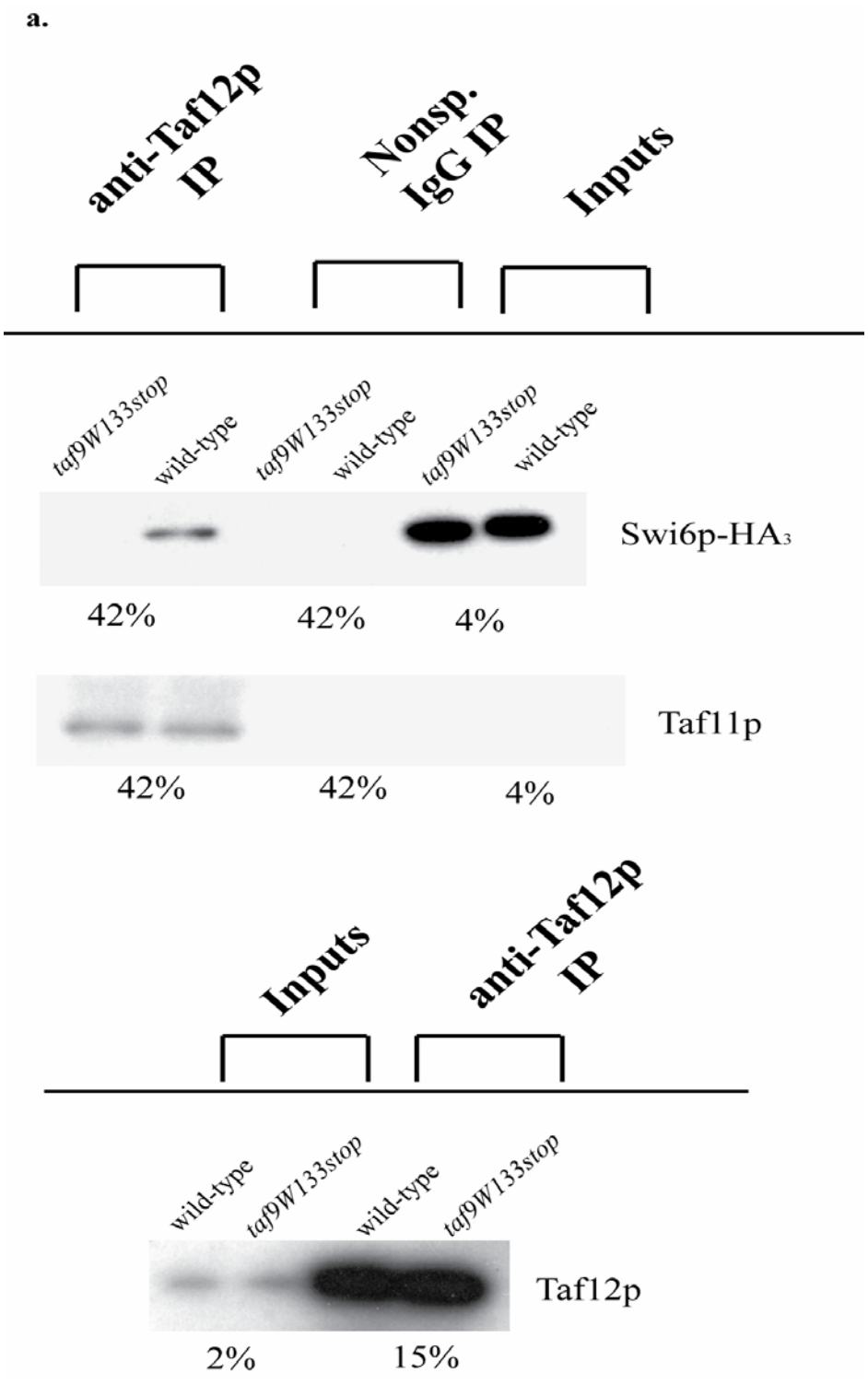
a.
anti-Taf12p IP
Nonsp. IgG IP
Inputs
taf9W133stop
wild-type
taf9W133stop
wild-type
taf9W133stop
wild-type
Swi6p-HA3
42%
42%
4%
Taf11p
42%
42%
4%
Inputs
anti-Taf12p IP
wild-type
taf9W133stop
wild-type
taf9W133stop
Taf12p
2%
15%

Figure III-1.

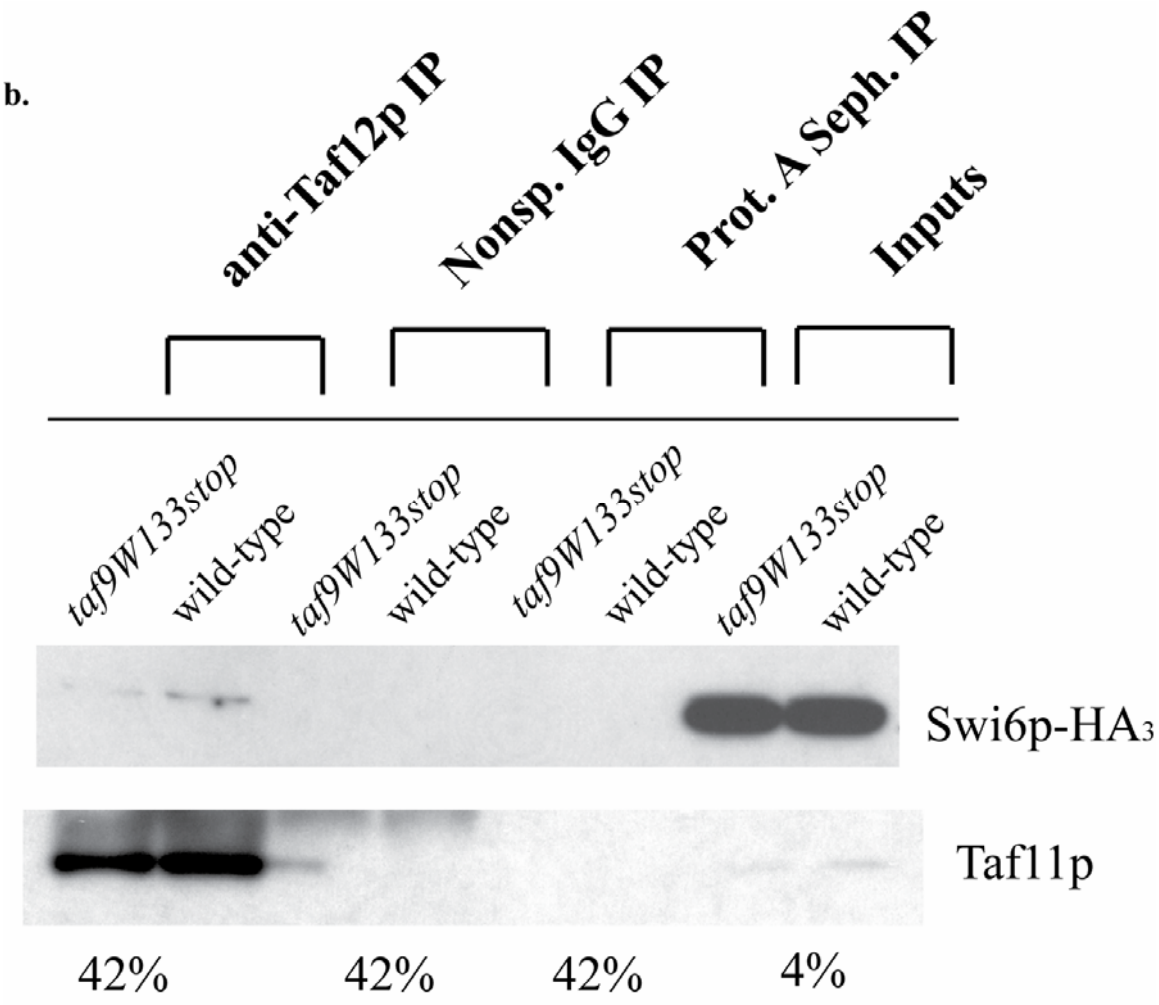

Figure III-1. The interaction of Swi6p-HA$_3$ withTaf12p is disrupted in yeast bearing the *taf9W133stop* mutation. a, b. Yeast WCE was immunoprecipitated with polyclonal anti-Taf12p antibodies for 14 hours, and the immunoprecipitate was analyzed by SDS-PAGE and immunoblot. Shown in panels **a.** and **b.** are the results of two separate immunoprecipitation experiments. The proteins that were probed in the immunoprecipitate are indicated on the right. The number beneath inputs indicates the percentage of total protein subjected to immunoprecipitation, whereas the numbers beneath the immunoprecipitates indicates the percentage of the volume of LDS-solubilized immunoprecipitate that was subjected to immunoblot analysis. The protein signals in the inputs and immunoprecipitates had been detected by exposure to Kodak Biomax Light film. The labels directly above each lane denote the yeast strain.
IP=immunoprecipitate, Nonsp. IgG = nonspecific rabbit IgG,
Prot. A Seph. = protein A sepharose.

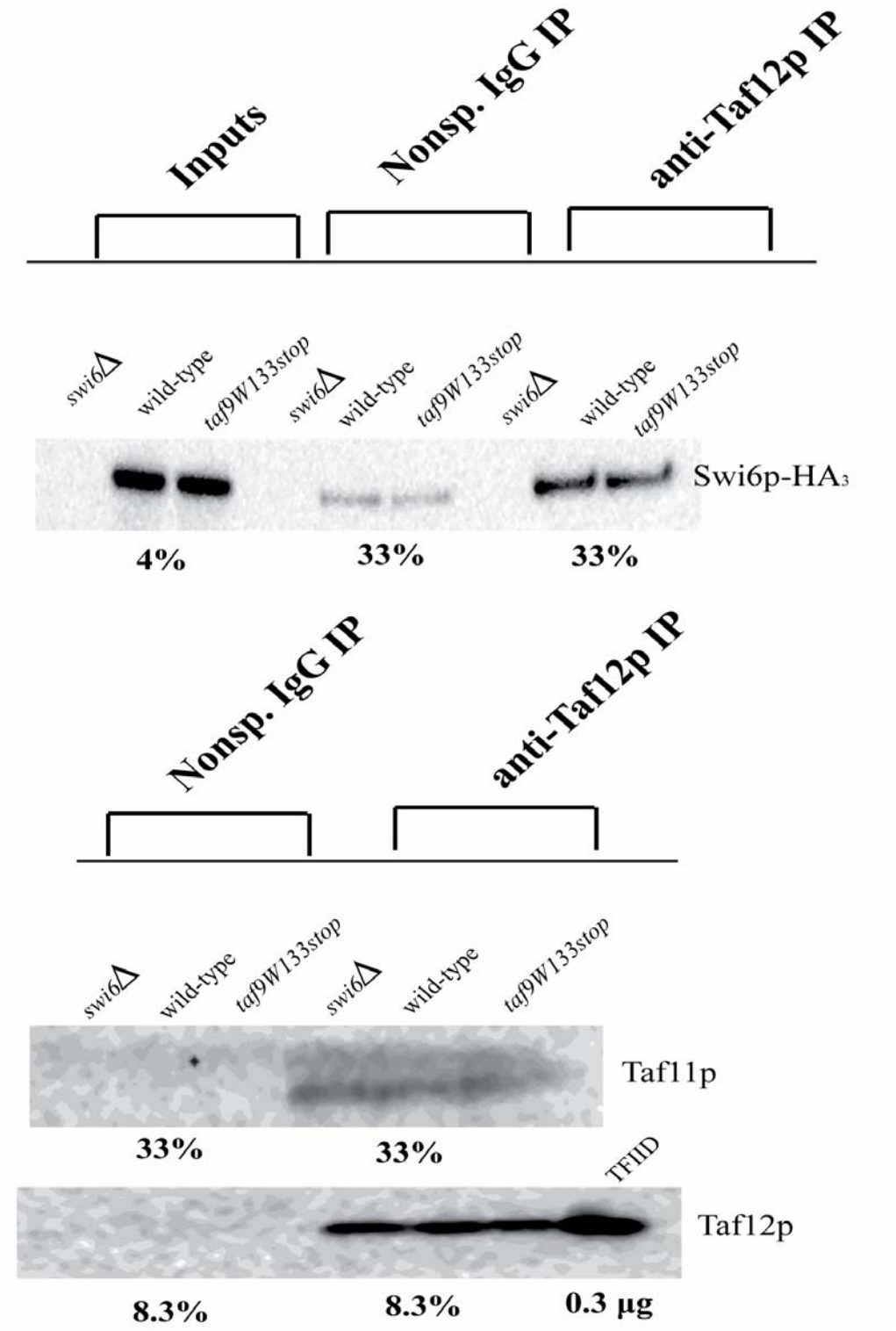
Inputs
Nonsp. IgG IP
anti-Taf12p IP
swi6Δ
wild-type
taf9W133stop
swi6Δ
wild-type
taf9W133stop
swi6Δ
wild-type
taf9W133stop
Swi6p-HA3
4%
33%
33%
Nonsp. IgG IP
anti-Taf12p IP
swi6Δ
wild-type
taf9W133stop
swi6Δ
wild-type
taf9W133stop
Taf11p
33%
33%
TFIID
Taf12p
8.3%
8.3%
0.3 µg

Figure III-2.

Figure III-2. The interaction between Swi6p-HA_3 and Taf12p was not always impaired in *taf9W133stop* yeast. Yeast WCE was immunoprecipitated with polyclonal anti-Taf12p for seven hours, and the immunoprecipitate was analyzed by SDS-PAGE and immunoblot. The proteins that were probed in the immunoprecipitate are indicated on the right. 0.3 μg of purified yeast TAP-tagged TFIID had also been analyzed by SDS-PAGE and immunoblot in an adjacent lane. The number beneath inputs indicates the percentage of total protein that had been subjected to immunoprecipitation. Note that the number beneath each immunoprecipitate refers to the percentage of the combined volume of two LDS-solubilized immunoprecipitates that had been harvested from two identical immunoprecipitations performed in parallel. Two immunoprecipitates had been combined in order to increase the otherwise faint signal of Swi6p-HA_3 in the immunoprecipitate. The protein signals in the inputs and immunoprecipitates had been detected directly with a ChemiDoc XRS scanner. The labels directly above each lane denote the yeast strain.
IP=immunoprecipitate, Nonsp. IgG = nonspecific rabbit IgG.

a.

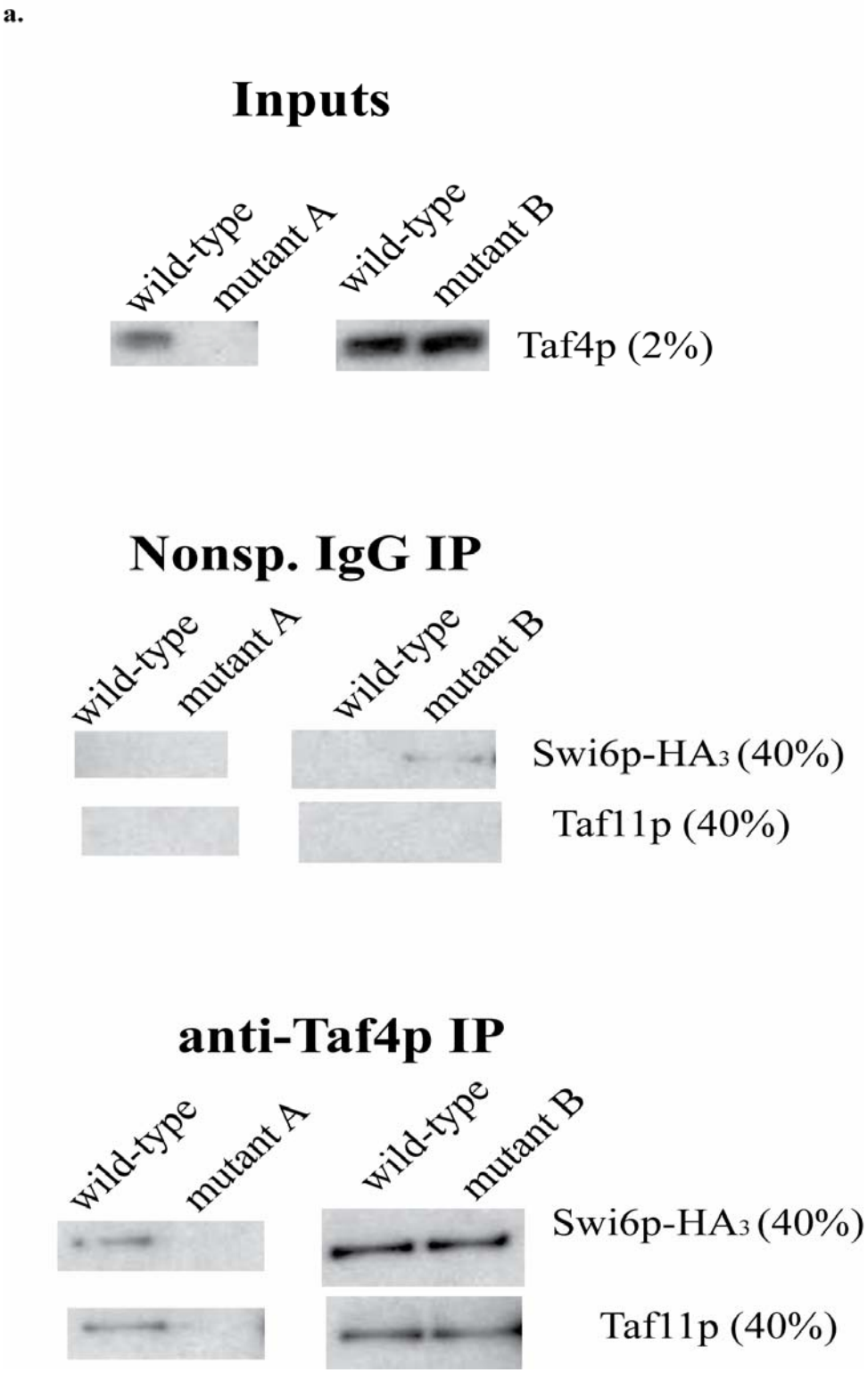

Figure III-3.

b.

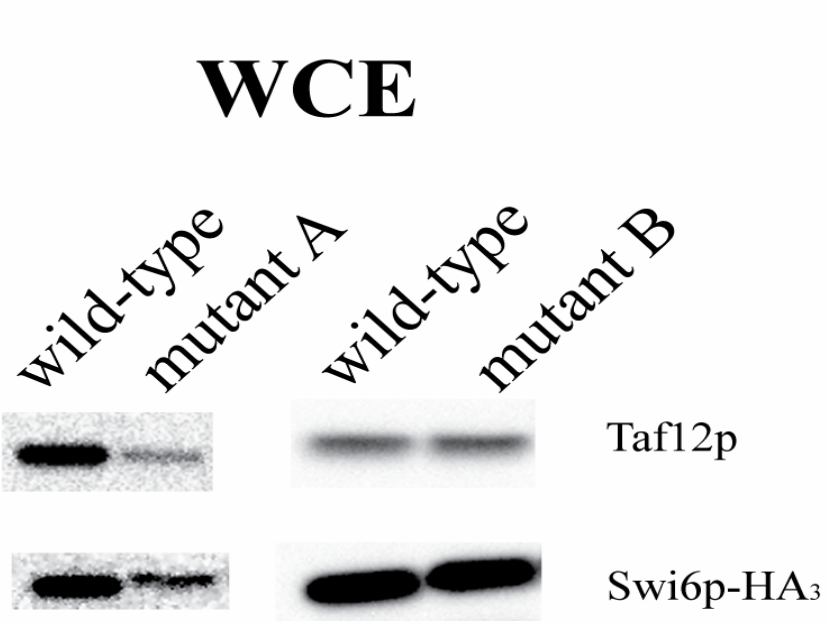

c.

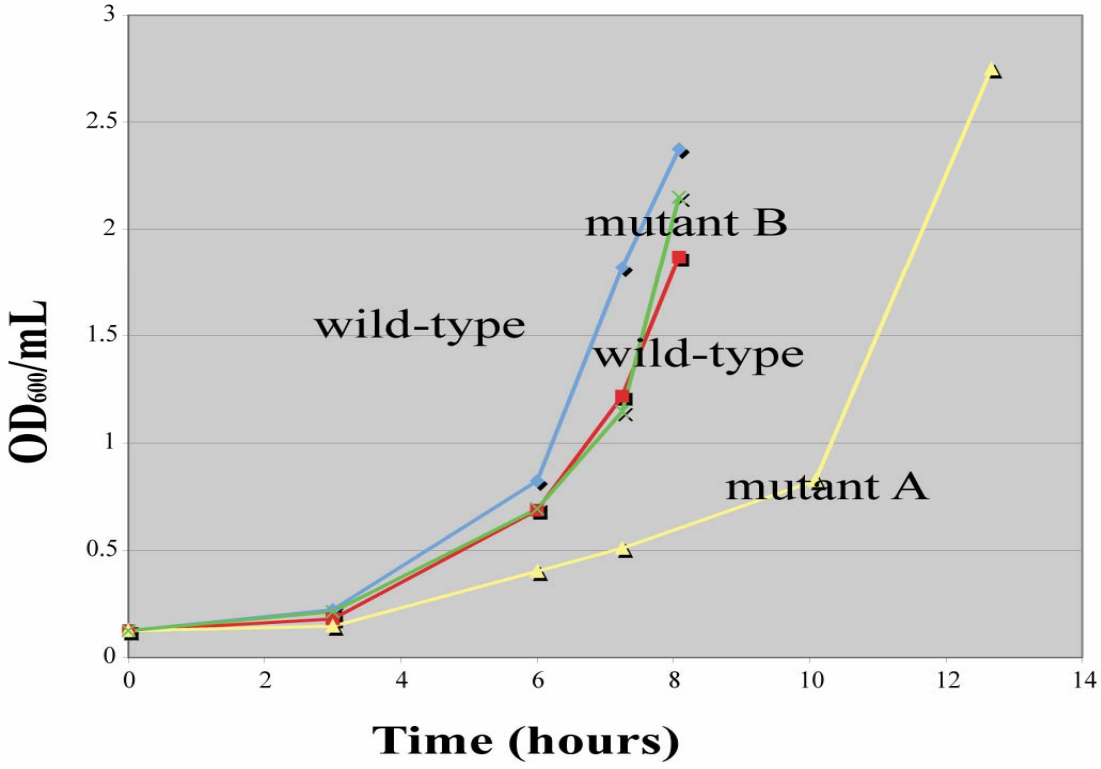

Figure III-3.

Figure III-3. A *taf9W133stop* mutant was isolated that showed reduced protein expression levels and slower growth relative to wild-type.
In **a.** and **b**., the protein signals in the inputs and immunoprecipitates had been detected directly with a ChemiDoc XRS scanner. The labels directly above each lane denote the yeast strain.
a. Yeast WCE was immunoprecipitated with polyclonal anti-Taf4p antibodies, and the immunoprecipitate was analyzed by SDS-PAGE and immunoblot. A *taf9W133stop* mutant (mutant A) was isolated that showed reduced levels of Swi6p-HA_3 and Taf11p in an anti-Taf4p immunoprecipitate, and reduced levels of Taf4p in the input. The number (in %) to the side of each input indicates the percentage of total protein subjected to immunoprecipitation, whereas the numbers (in %) to the side of each immunoprecipitate indicates the percentage of the volume of LDS-solubilized immunoprecipitate that was subjected to immunoblot analysis. The labels directly above each lane denote the yeast strain. The proteins that were probed for in the immunoprecipitate are indicated to the right of each data panel. IP=immunoprecipitate, Nonsp. IgG = nonspecific rabbit IgG.
b. Expression levels of Taf12p and Swi6p-HA_3 were also reduced in the inputs of mutant A relative to wild-type. In each lane, 22 μg of WCE had been analyzed (based on concentrations determined by Bradford assay).
c. The *taf9W133stop* isolate, mutant A, showed a slower growth at the permissive temperature (30°C) compared to a possible revertant of the *taf9W133stop* mutation (mutant B) and two wild-type clones.

Table III-2. Summary of phenotypes observed in *taf9W133stop* mutant clones.

mutant type	interaction between Swi6p and $Taf_{II}s$	expression levels of Swi6p, Taf12p and Taf4p	growth rate
A	reduced	reduced	slower than wild-type
B	intact	wild-type	like wild-type
C	reduced	wild-type	like wild-type

tested this hypothesis by monitoring the growth of multiple *taf9W133stop* clones in liquid culture at the permissive temperature. I measured the growth rate of four wild-type clones from two wild-type glycerol stocks, the lab stock and my own stock derived from the lab stock (two clones per glycerol stock). I also measured the growth rate of twenty *taf9W133stop* clones from two *taf9W133stop* glycerol stocks, the lab stock and my own stock derived from the lab stock. I performed this experiment in this way because I had used my glycerol stocks exclusively to grow yeast that were used in the anti-Taf12p immunoprecipitations, and I had used both the lab glycerol stocks and my own glycerol stocks to grow yeast that were used in the anti-Taf4p immunoprecipitations. I would like to point out that the mutant A phenotype had been observed in yeast grown from the lab *taf9W133stop* glycerol stock, whereas the mutant B and C phenotypes had been observed in yeast grown from my *taf9W133stop* stock.

I monitored the growth of each culture by measuring OD_{600} until the rate of change in OD_{600} plateaued for that culture. Analysis of the growth curves led to several striking observations (Figure III-4). First, there was very little variation in the growth curves of the four wild-type clones. Second, nine of the *taf9W133stop* clones grew at the same rate as the wild-type clones, and again, there was very little variation in the growth curves of these clones. I noted that all nine of these clones were from my *taf9W133stop* stock. Third, eleven of the *taf9W133stop* clones showed significantly slower growth than wild-type. I noted that one of these clones were from my *taf9W133stop* stock whereas the rest were from the lab *taf9W133stop* stock. Fourth, there was a broad variation in the growth curves of these slow-growing eleven clones. Taken together, these observations indicate that the *taf9W133stop* mutants do revert to wild-type growth at a high rate. Only

one out of ten clones from my *taf9W133stop* stock grew slowly whereas the rest showed growth similar to wild-type. My *taf9W133stop* stock had been created from a logarithmically growing yeast culture that had been inoculated with a single colony from the lab *taf9W133stop* stock. This means that, in my *taf9W133stop* stock, nine out of ten colonies had reverted to wild-type growth. The broad variation in the growth curves of the mutant clones from the lab *taf9W133stop* stock suggests that a proportion of the cells in some cultures had reverted to wild-type growth or that the cells had acquired mutations that only partly restored wild-type growth. Thus, the variation in the growth curves may reflect different percentages and/or extents of reversion in each culture.

As noted above, the expression of some Taf_{II}s and Swi6p was reduced in the slow-growing mutant clone. To test whether this observation was specific to only these proteins, I analyzed the total protein in the WCEs of wild-type yeast and in *taf9W133stop* mutant clones A and B. The concentrations of each WCE were determined by Bradford assay, with BSA as a standard. The concentration of WCE, as determined by Bradford, was virtually the same for wild-type and mutants A and B (average of two wild-type clones was 1.905 μg/μL, mutant A was 1.91 μg/μL, and mutant B was1.90 μg/μL).

Next, I performed SDS-PAGE analysis of equal volumes of each WCE. The resulting gels were stained with either Coomassie R-250 or Sypro Ruby, and the stained gels were scanned with a regular light scanner or an FX laser scanner, respectively (Figure III-5). Quantitation of the total protein in the Sypro Ruby-stained gel showed that the total protein in mutant A WCE was reduced from wild-type by 33%, whereas the total protein in mutant B WCE was increased from wild-type by 2%. .

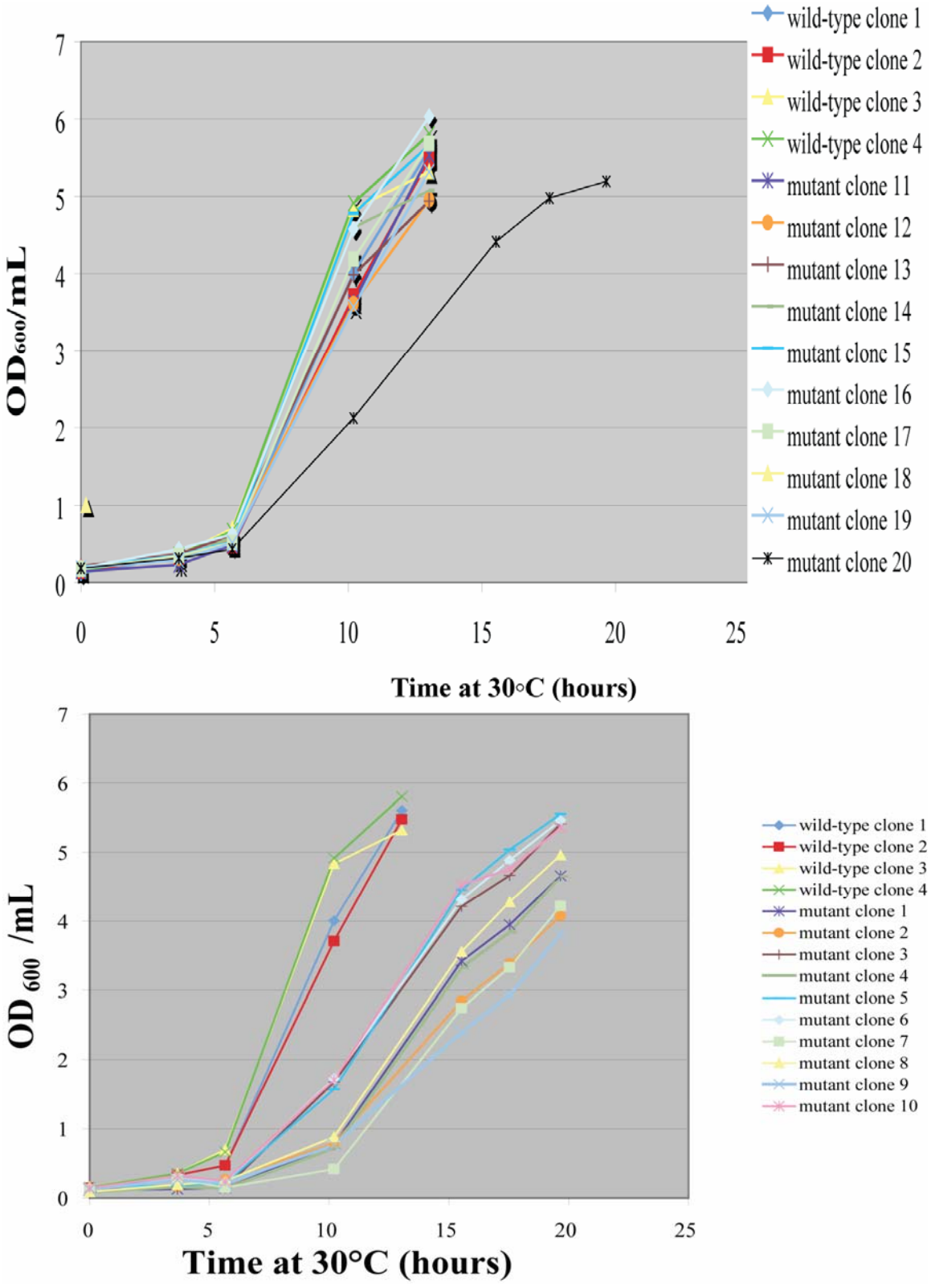
OD600/mL
Time at 30◦C (hours)
wild-type clone 1
wild-type clone 2
wild-type clone 3
wild-type clone 4
mutant clone 11
mutant clone 12
mutant clone 13
mutant clone 14
mutant clone 15
mutant clone 16
mutant clone 17
mutant clone 18
mutant clone 19
mutant clone 20
OD 600 /mL
Time at 30°C (hours)
wild-type clone 1
wild-type clone 2
wild-type clone 3
wild-type clone 4
mutant clone 1
mutant clone 2
mutant clone 3
mutant clone 4
mutant clone 5
mutant clone 6
mutant clone 7
mutant clone 8
mutant clone 9
mutant clone 10

Figure III-4.

Figure III-4. Growth curve analysis of *taf9W133stop* clones from two glycerol stocks. (Top) Nine of ten *taf9W133stop* clones from one glycerol stock grew like wild-type. (Bottom) All ten *taf9W133stop* clones from another glycerol stock grew slower than wild-type. Data for the same four wild-type clones are shown in both graphs.

a.

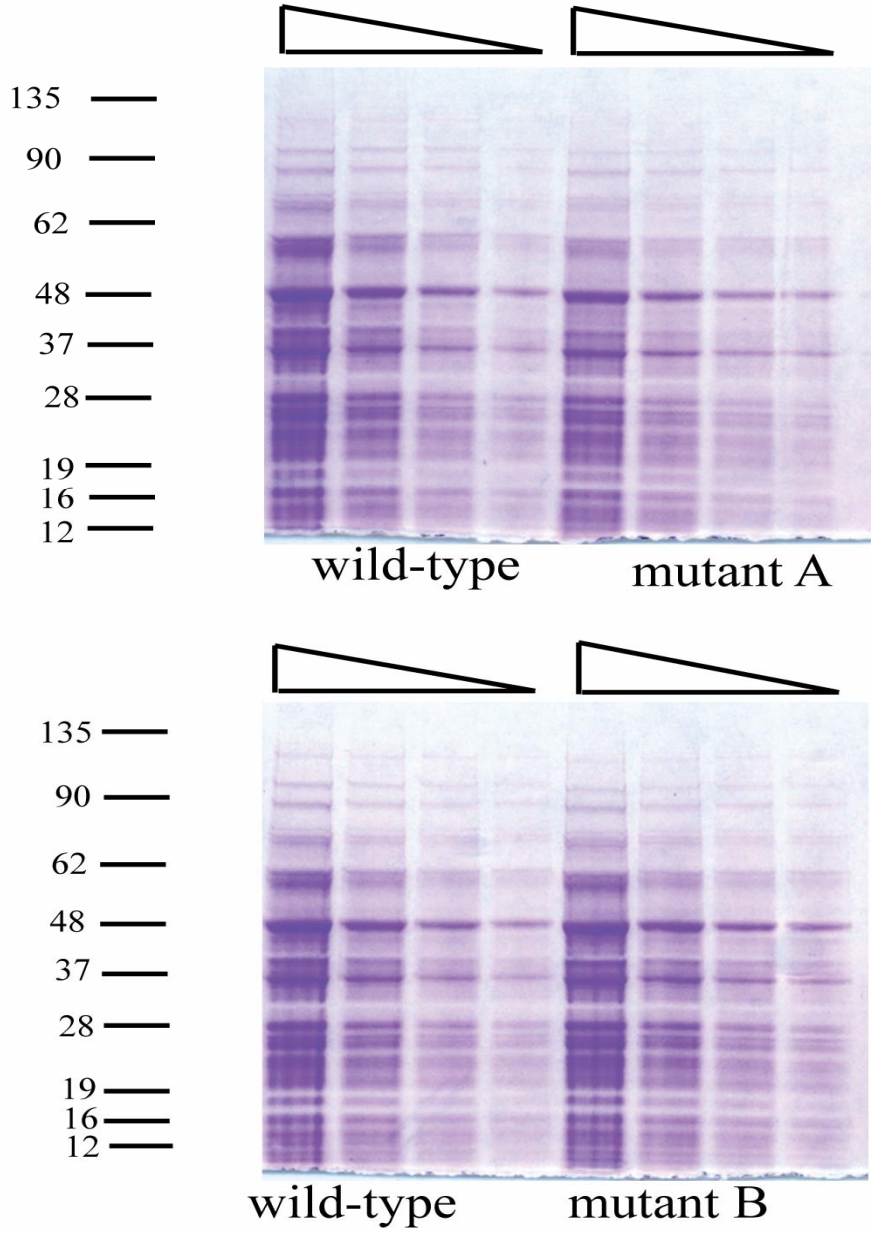

Figure III-5.

b.

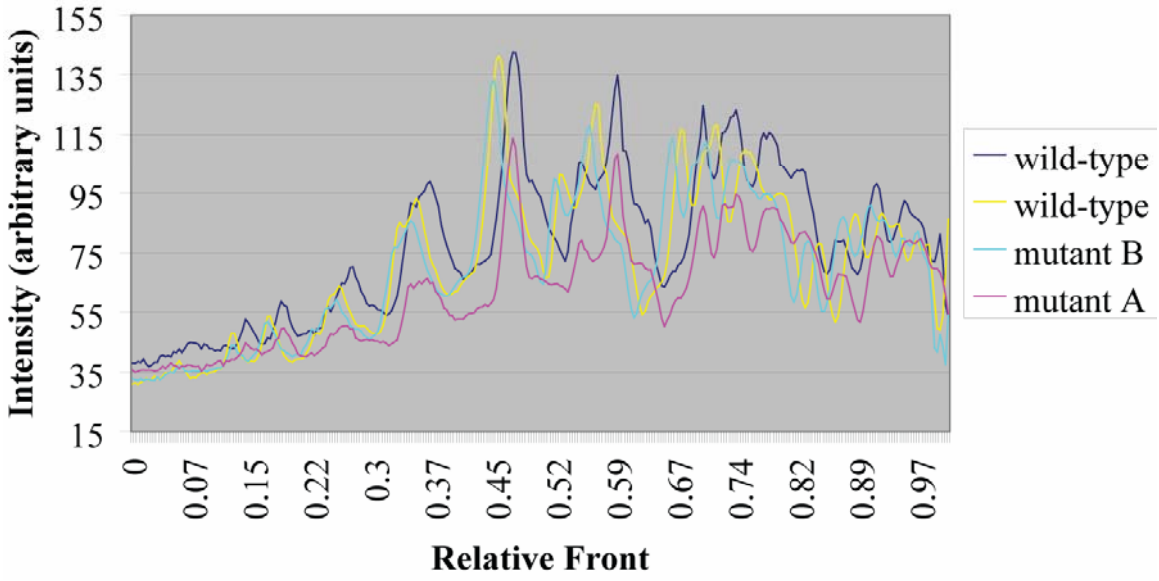

Figure III-5.

c.

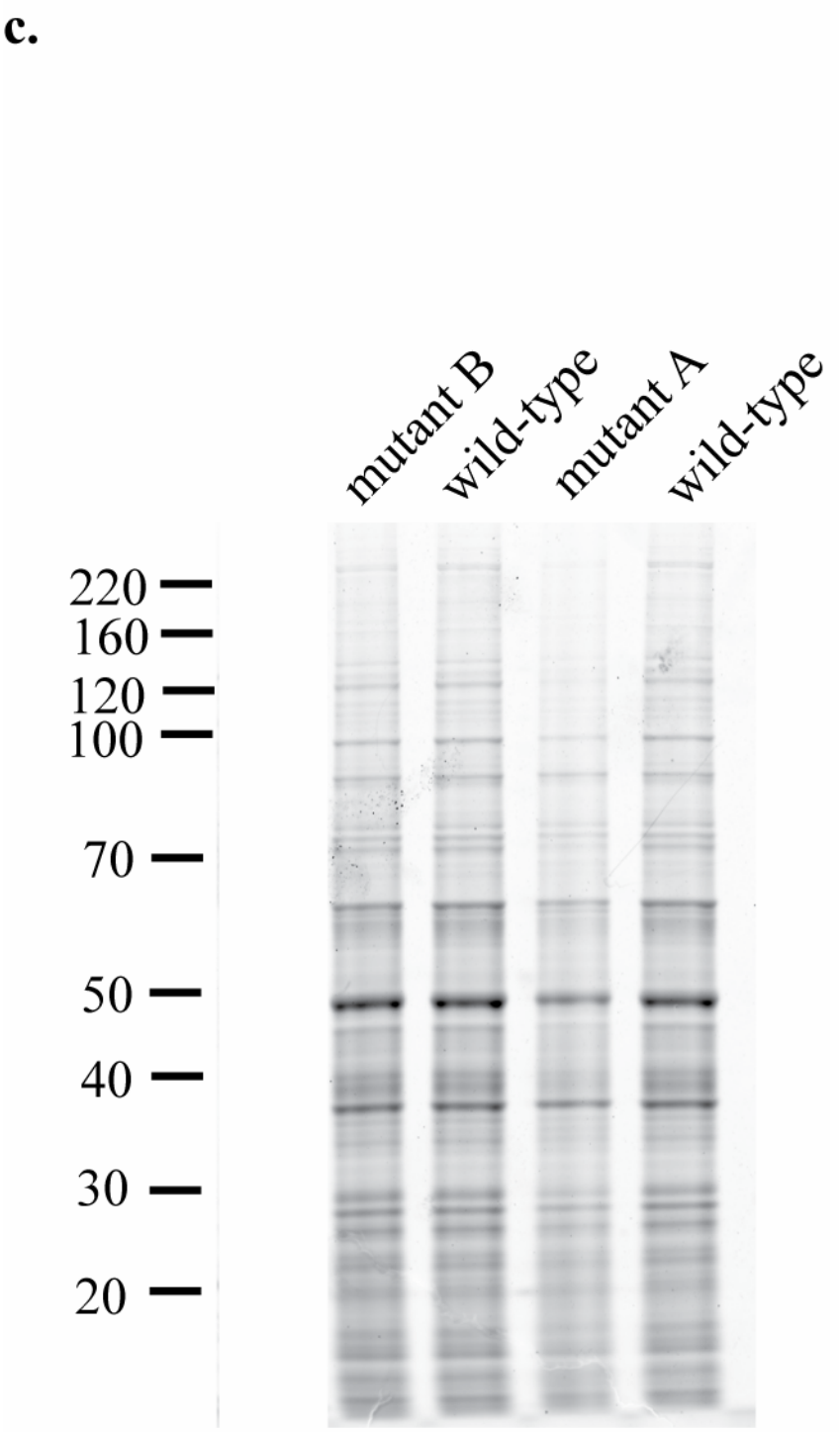

Figure III-5.

Figure III-5. There was a global reduction of protein levels in the slow-growing *taf9W133stop* isolate, mutant A.
a. Shown is a Coomassie stain of WCEs from two wild-type clones and *taf9W133stop* mutants A and B. For each clone, four lanes of WCE of decreasing amounts of protein, from left to right, were loaded. For each clone, the following volumes of LDS-solubilized WCE were loaded (left to right): 10 μL, 5 μL, 2.5 μL, and 1.3 μL.
b. A plot of **a.**, comparing the levels of intensity in the lanes in which 10 μL of protein had been loaded. "Relative front" refers to equivalent positions in each lane analyzed.
c. Sypro Ruby stained gel of WCEs from two wild-type clones and *taf9W133stop* mutants, A and B. In each lane, 1 μL of LDS-solubilized WCE was loaded.
In **a.** and **c.**, the numbers to the left of each gel are the MWs, in kDa.

It is not unusual that protein concentrations determined by Bradford and by gel analysis of the same sample are not equivalent. Previous work in the literature has shown that the Bradford assay is sensitive to differences in overall concentration of positive charges in the proteins being measured (32). Therefore, it is possible that, although the protein expression levels in *taf9W133stop* clone A was reduced, the concentration determined by Bradford assay is similar to wild-type due to changes in the overall charge of cellular protein.

Differences in the quantities of protein released during preparation of the WCE are unlikely as all yeast were beaten with glass beads until the lysis efficiency was over 95% (see **Materials and Methods**). Furthermore, wild-type and all *taf9W133stop* yeast were of the same size and morphology, so that harvesting equivalent OD_{600} of wild-type and *taf9W133stop* yeast was equivalent to harvesting equivalent numbers of cells of wild-type and *taf9W133stop* yeast.

Of course, there are other, more rigorous ways in which levels of overall protein expression in a cell can be measured. For example, one such method is measuring the concentration of DNA in WCE. DNA concentration would be expected to be the same in both a wild-type and mutant yeast cell. Therefore, DNA concentration in wild-type and mutant WCEs would be the same if the same number of cells was harvested, and the extent of cell breakage and release of intracellular contents were the same for wild-type and mutant yeast. Therefore, if levels of protein expression inside a mutant cell are really decreased relative to wild-type, then the difference in protein concentration of the mutant WCE should persist even after normalizing for DNA concentration. However, due to time constraints, I am unable to perform these analyses.

In summary, I have shown that Swi6p interacts with Taf12p and Taf4p in wild-type WCE. I had repeated an observation made by Steven Sanders, that the interaction between Taf12p and Swi6p was reduced in yeast harboring a *taf9W133stop* mutation. I isolated a slow-growing *taf9W133stop* clone, mutant A, that showed reduced interaction between Taf4p and Swi6p, but also showed reduced expression of Taf4p and Swi6p in the WCE. In addition, Taf12p expression was reduced in the WCE as well. Overall, I found that protein expression was reduced globally in this mutant. In addition, I found that *taf9W133stop* yeast revert to wild-type growth at a high frequency during logarithmic growth. The initial interpretation of Sanders' data had been that the *taf9W133stop* mutation lowered the affinity of TFIID for Swi6p. Analysis of my data also leads me to speculate that the *taf9W133stop* mutation somehow affects levels of protein synthesis as well.

Co-immunoprecipitation of Swi6p and Taf9p from yeast WCE

I had initially hypothesized that Taf9p serves as a coactivator for Swi6p. One of the first questions I attempted to answer was whether Taf9p interacted with Swi6p *in vivo*. To answer this question, I performed immunoprecipitations in yeast WCE. The lack of suitable polyclonal anti-Taf9p antibodies for immunoprecipitation precluded me from performing anti-Taf9p immunoprecipitations directly in wild-type yeast; therefore, I carried out immunoprecipitations in yeast that expressed Taf9p-HA_3 using 12CA5 monoclonal antibodies (12CA5 antibodies specifically recognize the HA epitope).

The immunoprecipitation efficiency of 12CA5 with respect to Taf9p-HA_3 was 49%, regardless of salt concentration, 150mM or 300mM NaCl (Figure III-6a and Figure III-6b). However, Swi6p did not co-immunoprecipitate under these conditions at either

salt concentration (Figure III-6a and III-6b). As a positive control, Taf8p was probed in these immunoprecipitates, and it was found that Taf8p did co-immunoprecipitate with Taf9p-HA_3 under these conditions, regardless of salt concentration.

Furthermore, as discussed in the preceding section, Swi6p co-immunoprecipitated with Taf12p in reactions in which the immunoprecipitation efficiency of the polyclonal anti-Taf12p antibodies, with respect to Taf12p, was 38%. Since the immunoprecipitation efficiency of Taf9p-HA_3 was even greater (at 49%) in these experiments, the inability of Swi6p to co-immunoprecipitate with Taf9p-HA_3 was not likely due to insufficient capture of antigen.

The inability of Swi6p to co-immunoprecipitate with Taf9p-HA_3 was also not likely due to degradation of Swi6p because Swi6p was detected, at comparable levels, in the 12CA5 immunoprecipitates from both wild-type and Taf9p-HA_3 strains (Figure III-6c).

In summary, I found that Swi6p did not co-immunoprecipitate with Taf9p- HA_3 under conditions in which another Taf_{II}, Taf8p, could co-immunoprecipitate with Taf9p-HA_3. The inability to co-immunoprecipitate is not likely due to low immunoprecipitation efficiency, since Swi6p co-immunoprecipitated with Taf12p in immunoprecipitations where the efficiency of the anti-Taf12p antibody was lower than the efficiency of 12CA5 (see **Swi6p interaction with Taf_{II}s in *taf9W133stop* yeast**). Also, the inability to co-immunoprecipitate is unlikely due to degradation of Swi6p, as Swi6p was detected, at comparable levels, in 12CA5 immunoprecipitates of both wild-type and Taf9p-HA_3 yeast.

As discussed in **Chapter I**, the *taf9W133stop* mutation results in the truncation of Taf9p at the C terminus. The inability of Swi6p to co-immunoprecipitate with Taf_{II}s in

taf9W133stop yeast suggests that the C terminus of Taf9p is important in mediating interaction between TFIID and Swi6p. The inability of Swi6p to co-immunoprecipitate with Taf9p-HA_3 indirectly supports the notion that the C terminus of Taf9p is important for mediating interaction between Swi6p and Taf9p-HA_3 because it is possible that an HA tag at the C terminus of Taf9p-HA_3 blocks the interaction between Swi6p and TFIID. If this is the case, then Swi6p should be able to co-immunoprecipitate with Taf9p that has been tagged at the N terminus only.

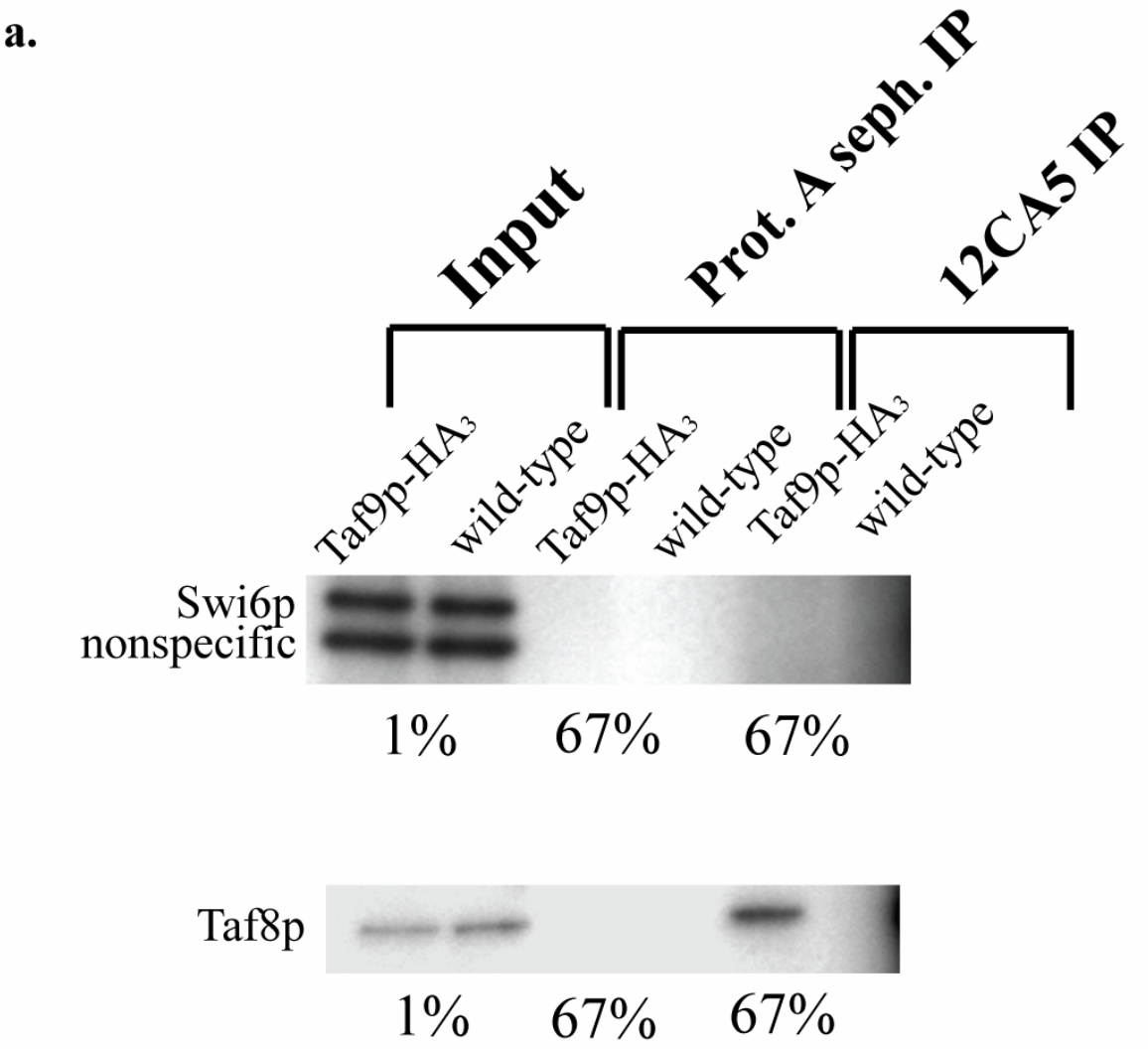
a.
Input
Prot. A seph. IP
12CA5 IP
Taf9p-HA3
wild-type
Taf9p-HA3
wild-type
Taf9p-HA3
wild-type
Swi6p
nonspecific
1%
67%
67%
Taf8p
1%
67%
67%

Figure III-6.

b.

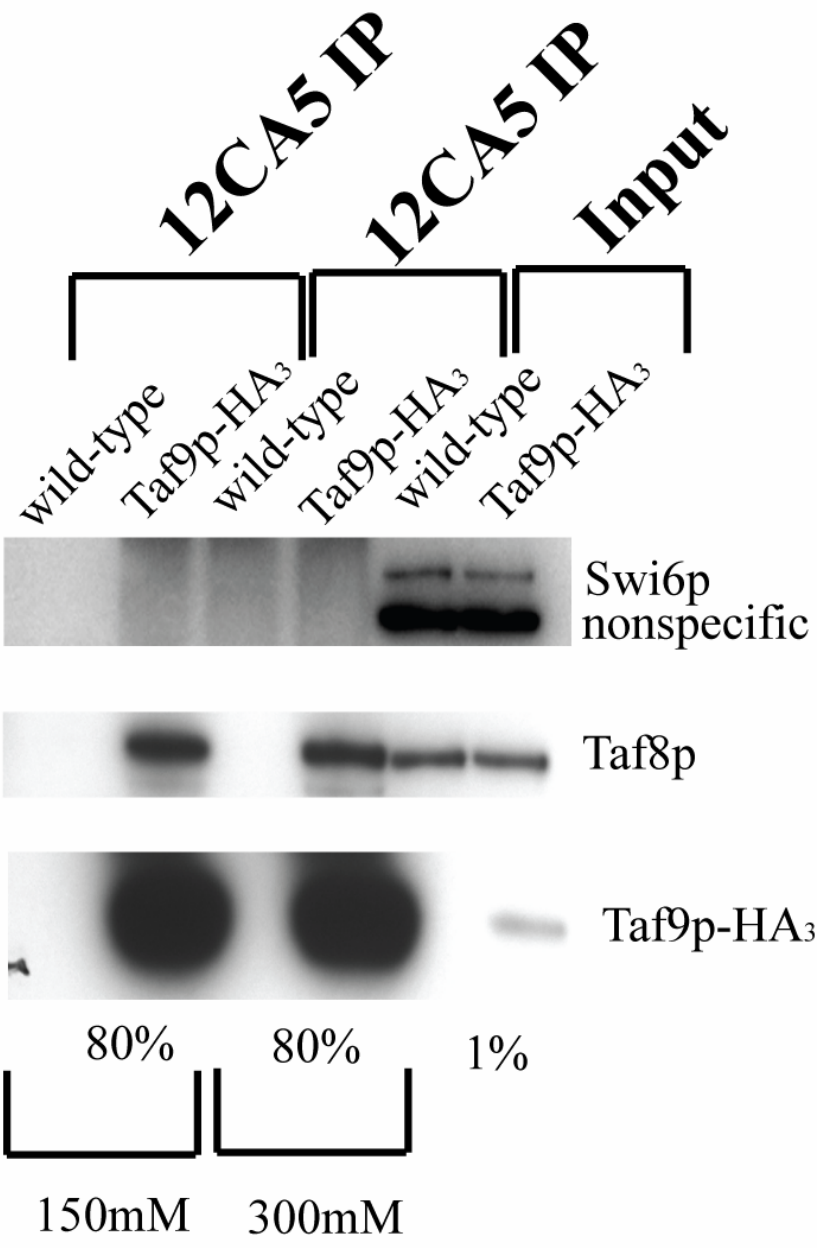

Figure III-6.

c.

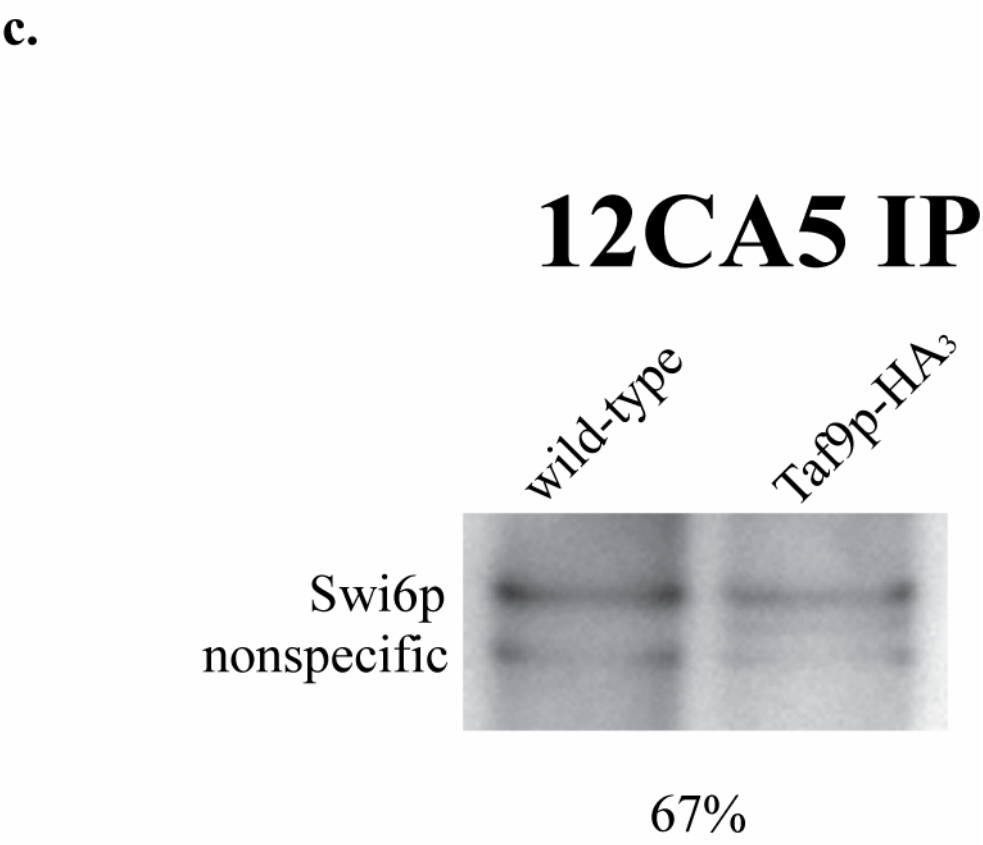

Figure III-6.

Figure III-6. Swi6p does not co-immunoprecipitate with Taf9p-HA$_3$. Pre-cleared yeast WCE was immunoprecipitated with 12CA5 monoclonal antibodies, and the immunoprecipitate was analyzed by SDS-PAGE and immunoblot. The number beneath inputs indicates the percentage of total protein subjected to immunoprecipitation, whereas the numbers beneath the immunoprecipitate indicates the percentage of the volume of LDS-solubilized immunoprecipitate that was subjected to immunoblot analysis. The labels directly above each lane denote the yeast strain. The proteins that were probed for in the immunoprecipitate are indicated either to the right or left of each data panel. IP=immunoprecipitate.

a. Shown are immunoprecipitates and inputs probed with anti-Swi6p or stripped and re-probed with anti-Taf8p. The immunoprecipitates depicted in this panel were in 300mM NaCl.

b. Shown are immunoprecipitates and inputs probed with anti-Swi6p or stripped and re-probed with either anti-Taf8p or anti-HA HRP. The immunoprecipitations depicted in this panel were performed in either 150mM or 300mM NaCl. "150mM" and "300mM" refer to NaCl concentrations.

c. Swi6p did not degrade over the course of the 12CA5 immunoprecipitation. Shown is an immunoblot of 67% of an immunoprecipitate.

Discussion

During the course of performing the anti-Taf12p and anti-Taf4p immunoprecipitations, I observed three types of *taf9W133stop* phenotypes. These are summarized in Table III-2.

The *taf9W133stop* mutant varied in terms of interaction between Swi6p and the Taf_{II}s, expression levels of cellular protein, and growth rate. I propose the following model (Figure III-7). The *taf9W133stop* mutation has such pleiotropic effects in the cell because Taf9p is important for mediating transcriptional activation by at least two transcription factors, Rap1p and the Swi6p-containing complex, SBF. Rap1p mediates transcription of ribosomal protein genes. Therefore, the reduction in cellular protein may be due to a defect in transcription of ribosomal protein genes. SBF, on the other hand, mediates transcription of genes that are important for regulating the cell cycle. Therefore, the longer cell cycle may be due to a defect in transcription of these genes. The slow growth may be due to both the reduction in cellular protein and to reduced expression of genes that regulate the cell cycle. During the course of logarithmic growth, some *taf9W133stop* clones acquire mutations that restore wild-type growth and that restore wild-type levels of protein expression. Some of these acquired mutations also restore interaction between SBF and Taf12p and Taf4p, whereas other mutations restore wild-type growth and wild-type levels of protein expression but do not restore interaction between Swi6p and these Taf_{II}s. Both recent work performed by others in our laboratory and work done by me support this model.

First, recent work in our laboratory has shown that TFIID serves as a coactivator for Rap1p at ribosomal protein genes, and that transcription of a ribosomal protein gene,

RPS5, is downregulated in a *taf9* temperature sensitive mutant (33). Therefore, it is possible that the *taf9W133stop* mutation impairs the ability of Taf9p, and hence TFIID, to serve as coactivator for Rap1p.

Second, my own data suggests that TFIID may serve as a coactivator for SBF at the promoters of cell-cycle regulated genes. I have found that the Swi6p-containing complex, SBF, mediates direct interaction with a subset of Taf_{II}s (Taf12p, Taf5p, and Taf4p). Furthermore, there is evidence that one of these Taf_{II}s, Taf12p, regulates the expression of several cell-cycle regulated genes (discussed in **Chapter II**). Previous work and my own data had shown that the ability of Swi6p to co-immunoprecipitate with Taf_{II}s is reduced in the *taf9W133stop* mutant. By cryo EM, SBF interacts with a domain of TFIID that contains all the directly interacting Taf_{II}s (Taf12p, Taf4p, and Taf5p) and Taf9p.

Interestingly, Rap1p also interacts directly with Taf12p, Taf4p, and Taf5p. Furthermore, it was found that transcription of *RPS5* was also regulated by Taf12p, Taf4p, and Taf5p. Finally, as for SBF, it was found that Rap1p interacts with domains of TFIID that contain all the directly interacting Taf_{II}s (Taf12p, Taf4p, and Taf5p) and Taf9p (unpublished communications with collaborator, Patrick Schultz).

However, I did not detect any direct interaction between SBF and Taf9p. Interestingly, no direct interaction was detected between Taf9p and Rap1p either. How can Taf9p play a role in regulating transcription of genes mediated by Rap1p and SBF if it does not directly interact with them? One can envision multiple mechanisms by which Taf9p may indirectly serve as a coactivator for Rap1p and SBF, none of which are mutually exclusive. First, Taf9p may stabilize interaction between Rap1p and SBF with Taf12p, Taf4p, and Taf5p. Second, Taf9p may mediate a conformational change in

TFIID such that the binding surfaces of these Taf_{II}s are exposed in the intact TFIID complex, thus enabling TFIID to engage Rap1p and SBF. Indeed, it has been proposed that Taf9p interacts with a Taf12p-Taf4p heterotetramer (34). Finally, in the case of SBF, it is also possible that Taf9p may interact with the other component of SBF, Swi4p, in a manner that does not depend on Swi6p. Such an interaction could have escaped detection in the Far Western assay (Figure II-15b and **Discussion** in **Chapter II**).

Previous work in the literature shows that TFIID is involved in the transcriptional regulation of two fundamental cellular processes: ribosome biogenesis and cell cycle regulation. The work done by me and others in this laboratory suggests that TFIID performs this role by acting as a coactivator for two transcription factors, Rap1p and SBF, that regulate transcription of genes required for these processes. Furthermore, our work suggests that TFIID interacts with Rap1p and SBF through the same set of Taf_{II}s (Taf12p, Taf4p, and Taf5p). In addition, Taf9p may modulate the interaction between TFIID and SBF. The observations that global levels of protein expression is reduced in some *taf9W133stop* mutant clones and that transcription of *RPS5* is downregulated in a *taf9* ts mutant suggest that Taf9p may also modulate interaction between TFIID and Rap1p as well. It is striking that TFIID employs similar mechanisms to interact with two distinct transcription factors, but on reflection, not unusual. In eukaryotes, the activities of TOR kinase links cellular protein synthesis and cell cycle regulation (35). In a similar way, TFIID may be an example of another link that coordinates two cellular processes that are essential to cell survival.

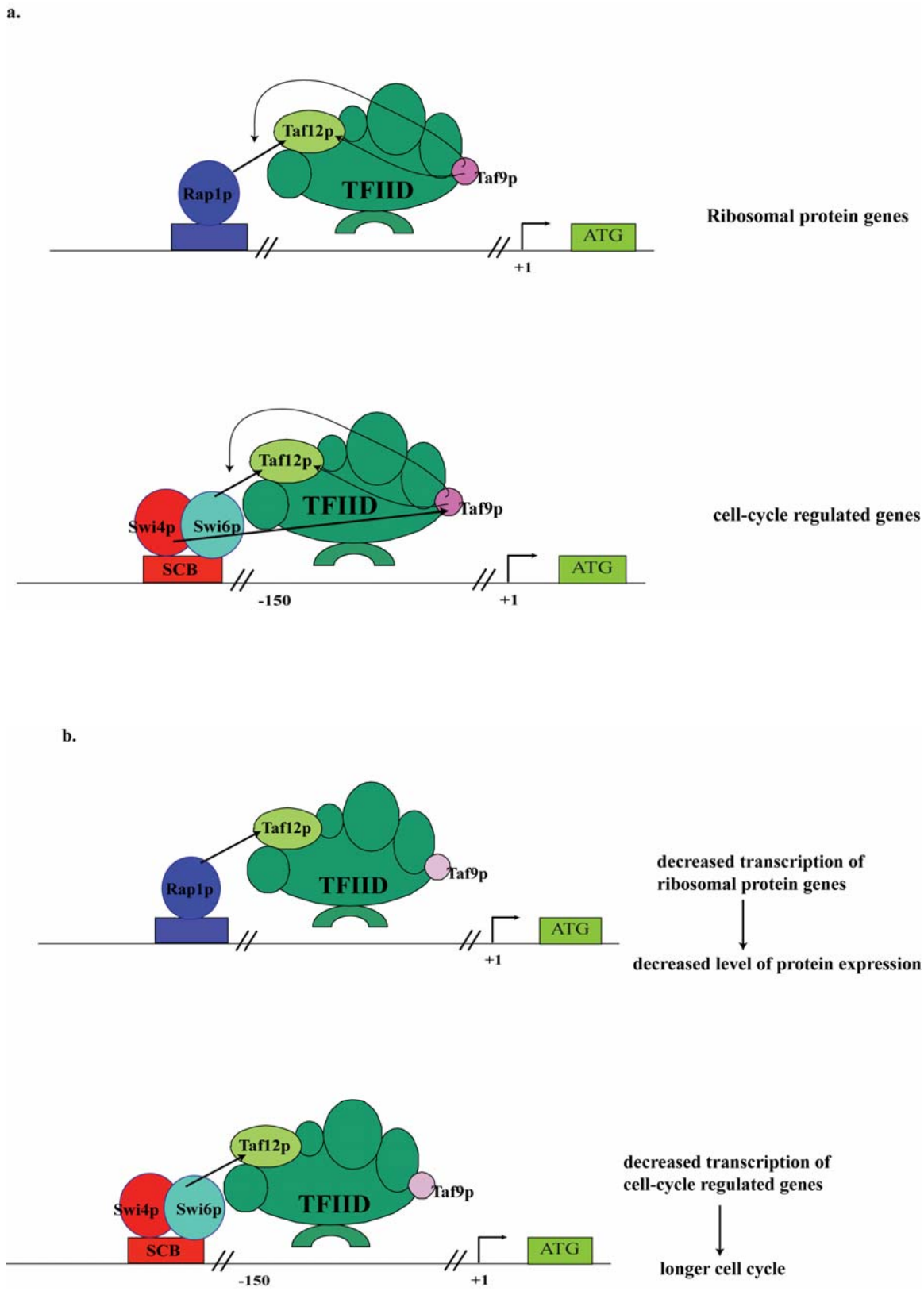
a.
Taf12p
Taf9p
TFIID
Rap1p
ATG
+1
Ribosomal protein genes
Taf12p
TFIID
Taf9p
Swi4p
Swi6p
SCB
ATG
-150
+1
cell-cycle regulated genes
b.
Taf12p
Taf9p
TFIID
Rap1p
ATG
+1
decreased transcription of
ribosomal protein genes
decreased level of protein expression
Taf12p
Taf9p
TFIID
Swi4p
Swi6p
SCB
ATG
-150
+1
decreased transcription of
cell-cycle regulated genes
longer cell cycle

Figure III-7.

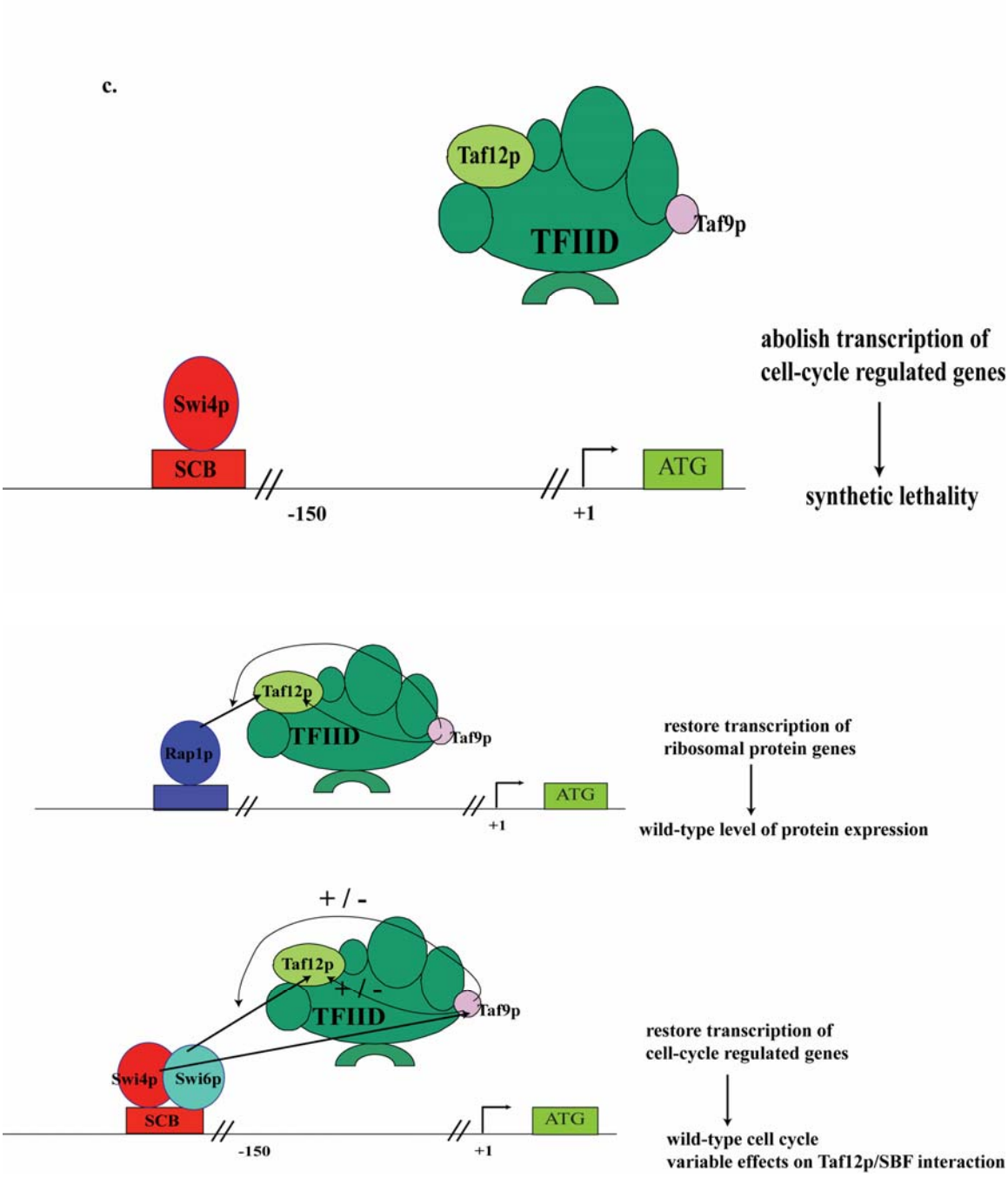
c.
Taf12p
TFIID
Taf9p
abolish transcription of
cell-cycle regulated genes
Swi4p
SCB
ATG
-150
+1
synthetic lethality
Taf12p
TFIID
Taf9p
Rap1p
ATG
+1
restore transcription of
ribosomal protein genes
wild-type level of protein expression
+ / -
Taf12p
+ / -
TFIID
Taf9p
Swi4p
Swi6p
SCB
ATG
-150
+1
restore transcription of
cell-cycle regulated genes
wild-type cell cycle
variable effects on Taf12p/SBF interaction

Figure III-7.

Figure III-7. The *taf9W133stop* mutation may affect both the transcription of ribosomal protein genes and cell-cycle regulated genes.

a. Taf9p (dark pink sphere) may play a role in transcription mediated by Rap1p and SBF indirectly, through stabilizing interaction between both transcription factors and other Taf_{II}s, or by altering conformation of the interacting Taf_{II}s. In the case of SBF, Taf9p may also mediate direct interaction with Swi4p.

b. Mutant Taf9p (light pink sphere) is unable to participate in mediating transcription by Rap1p and SBF. As a consequence of the inability of the mutant Taf9p to participate in transcription by Rap1p, the levels of expression of ribosomal protein genes is decreased, which results in reduced global levels of protein synthesis. As a consequence of the inability of the mutant Taf9p to participate in transcription by SBF, the levels of expression of genes that regulate the cell cycle are reduced, which results in a longer cell cycle. The combination of a longer cell cycle and reduced level of protein synthesis leads to slow growth. However, TFIID still drives transcription, albeit to a lesser extent, because of the direct interactions between other Taf_{II}s and both transcription factors.

c. In the absence of Swi6p, TFIID is no longer able to drive transcription of cell-cycle regulated genes. The lack of expression of genes that are required for the G_1/S transition results in the uniform arrest of yeast in G_1.

d. Compensating mutations in other genes restore TFIID's ability to drive transcription mediated by Rap1p even in the presence of mutant Taf9p. These compensations restore wild-type levels of expression of ribosomal protein genes, which in turn leads to wild-type levels of protein synthesis. These compensating mutations also restore wild-type growth. However, in the case of SBF, these mutations may or may not restore interaction between the other Taf_{II}s and Swi6p, which explains why Swi6p co-immunoprecipitates with Taf12p and Taf4p in some yeast clones but not in others. However, the restoration of interaction between Ta9p and Swi4p makes up for this deficit.

REFERENCES

1. Burley S.K., Roeder R.G. Biochemistry and structural biology of transcription factor IID (TFIID). *Annu. Rev. Biochem*., 1996, **65**: 769-799

2. Tora L. A unified nomenclature for TATA box binding protein (TBP)-associated factors (TAFs) involved in RNA polymerase II transcription. *Genes Dev*., 2002, **16**: 673-675

3. Yatherajam G., Zhang L., Kraemer S.M., Stargell L.A. Protein-protein interaction map for yeast TFIID. *Nucleic Acids Res.*, 2003, **31**: 1252-1260

4. Leurent C., Sanders S., Ruhlmann C., Mallouh V., Weil P.A., Kirschner D. B., Tora L., Schultz P. Mapping histone fold Tafs within yeast TFIID. *EMBO J*., 2002, **21**: 3424-3433

5. Chen J-L., Attardi L.D., Verrijzer C.P., Yokomori K., Tjian R. Assembly of recombinant TFIID reveals different coactivator requirements for distinct transcriptional activators. *Cell*, 1994, **79**: 93-105

6. Klemm R.D., Goodrich J.A., Zhou S., Tjian R. Molecular cloning and expression of the 32-kDa subunit of human TFIID reveals interactions with VP16 and TFIIB that mediate trancriptional activation. *PNAS*, 1995, **92**: 5788-5792

7. Thut C.J., Chen J.-L., Klemm R., Tjian R. p53 transcriptional activation mediated by coactivators $Taf_{II}40$ and $Taf_{II}60$. *Science*, 1995, **267**:100-103

8. Gill G., Pascal E., Tseng Z.H., Tjian R. A glutamine-rich hydrophobic patch in transcription factor Sp1 contacts the $dTAF_{II}110$ component of the Drosophila TFIID complex and mediates transcriptional activation. *PNAS*, 1994, **91**: 192-196

9. Shen W-C., Green M.R. Yeast $Taf_{II}145$ functions as a core promoter selectivity factor, not a general coactivator. *Cell*, 1997, **90**: 615-624

10. Walker S.S., Shen W.-C., Reese J.C., Apone L.M., Green M.R. Yeast $Taf_{II}145$ required for transcription of G1/S cyclin genes and regulated by the cellular growth state. *Cell*, 1997, **90**: 607-614

11. Green M.R. TBP-associated factors (TAF_{II}s): multiple, selective transcriptional mediators in common complexes. *Trends Biochem. Sci.*, 2000, **25**: 59-63

12. Sanders S.L., Jennings J., Canutescu A., Link A. J., Weil P.A. Proteomics of the eukaryotic transcription machinery: identification of proteins associated with components of yeast TFIID by multidimensional mass spectrometry. *MCB*, 2002, **22**: 4723-4738

13. Breeden L., Nasmyth K. Cell cycle control of the yeast *HO* gene: cis- and trans-acting regulators. *Cell*, 1987, **48**: 389-397

14. Breeden L.L. Periodic transcription: A cycle within a cycle. *Current Biology*, 2003, **13**: R31-R38

15. Iyer V.R., Horak C.E., Scafe C.S., Botstein D., Snyder M., Brown P.O. Genomic binding sites of the yeast cell-cycle transcription factors SBF and MBF. *Nature*, 2001, **409**: 533-538

16. Sidorova, J., Breeden L. Analysis of the SWI4/SWI6 protein complex, which directs G_1/S-specific transcription in *Saccharomyces cerevisiae*. *MCB*, 1993, **13**: 1069-1077

17. Nasmyth K., Dirick L. The role of SWI4 and SWI6 in the activity of G1 cyclins in yeast. *Cell*, 1991, **66**: 995-1013

18. Macpherson N., Measday V., Moore L., Andrews B. A yeast *taf17* mutant requires the *Swi6* transcriptional activator for viability and shows defects in cell cycle-regulated transcription. *Genetics*, 2000, **154**: 1561-1576

19. Sedgwick S.G., Taylor I.A., Adam A.C., Spanos A., Howell S. Morgan B.A., Treiber M.K., Kanuga N., Banks G.R., Foord R., Smerdon S.J. Structural and functional architecture of the yeast cell-cycle transcription factor Swi6. *J. Mol. Biol*., 1998, **281**: 763-775

20. Foord R., Taylor I.A., Sedgwick S.G., Smerdon S.J. X-ray structural analysis of the yeast cell cycle regulator Swi6 reveals variations of the ankyrin fold and has implications for Swi6 function. *Nature Structural Biology*, 1999, **6**: 157-165

21. Siegmund R.F., Nasmyth K.A. The Saccharomyces cerevisiae start-specific transcription factor Swi4 interacts through the ankyrin repeats with the mitotic Clb2/Cdc28 kinase and through its conserved carboxy terminus with Swi6. *MCB*, 1996, **16**: 2647-2655

22. Baetz K., Moffat J., Haynes J., Chang M., Andrews B. Transcriptional coregulation by the cell integrity mitogen-activated protein kinase Slt2 and the cell cycle regulator Swi4. *MCB*, 2001, **21**: 6515-6528

23. Dirick L, Moll T., Auer H., Nasmyth K. A central role for *SWI6* in modulating cell cycle Start-specific transcription in yeast. *Nature*, 1992, **357**: 508-513

24. Hess D., Winston F. Evidence that *Spt10 and Spt21 of Saccharomyces cerevisiae* play distinct roles *in vivo* and functionally interact with MCB-binding factor, SCB-Binding factor and Snf1. *Genetics*, 2005, **170**: 87-94

25. Queralt E., Igual J.C. Cell cycle activation of the Swi6p transcription factor is linked to nucleocytoplasmic shuttling. *MCB*, 2003, **23**: 3126-31240

26. Walker S.S, Reese J.C., Apone L.M., Green M.R. Transcription activation in cells lacking Taf_{II}s. *Nature*, 1996, **383**: 185-188

27. Hisatake K., Hasegawa S., Takada R., Nakatani Y., Horikoshi M., Roeder R.G. The p250 subunit of native TATA-box binding factor TFIID is the cell-cycle regulatory protein CCG1. *Nature*, 1993, **362**: 179-181

28. Suzuki-Yagawa Y., Guermah M., Roeder R.G. The ts13 mutation in the $TAF_{II}250$ subunit (CCG1) of TFIID directly affects transcription of D-type cyclin genes in cells arrested in G_1 at the nonpermissive temperature. *MCB*, 1997, **17**: 3284-3294

29. Hamard P.-J., Dalbies-Tran R., Hauss C., Davidson I., Kedinger C., Chatton B. A functional interaction between ATF7 and TAF12 that is modulated by TAF4. *Oncogene*, 2005, **24**: 3472-3483

30. Natarajan K., Jackson B.M., Rhee E., Hinnebusch A. G. yTafII61 has a general role in RNA polymerase II transcription and is required by Gcn4p to recruit the SAGA coactivator complex. *Molecular Cell*, 1998, **2**: 683-692

31. de Bruin R. A. M., Kalashnikova T. I., Chahwan C., McDonald W.H., Wohlschlegel J., Yates III J., Russell P., Wittenberg C. Constraining G1-specific transcription to late G1 phase: the MBF-associated corepressor Nrm1 acts via negative feedback. *Mol. Cell*, 2006, **23**: 483-496

32. Tal M., Silberstein A., Nusser E. Why does Coomassie Brilliant Blue R ineract differently with different proteins? *JBC*, 1980, **260**:9976-9980

33. Garbett K. A., Tripathi M.K., Cenkci B., Layer J.H., Weil P.A. Yeast TFIID serves as a coactivator for Rap1p by direct protein-protein interaction. *MCB*, 2007, **27**: 297-311

34. Selleck W., Howley R., Fang Q., Podolny V., Fried M.G., Buratowski S., Tan S. A histone fold TAF octamer within the yeast TFIID transcriptional coactivator. *Nat. Struct. Biol.*, 2001, **8**: 695-700

35. Arsham A.M., Neufeld T.P. Thinking globally and acting locally with TOR. *Current Opinion in Cell Biology*, 2006, **18**: 589-597